Release Date
JUN 24 1958

CONFIDENTIAL

CLASSIFICATION CANCELLED
Authority NASA PUBLICATIONS
ANNOUNCEMENTS NO. 11
Date 1/21/60 By S

Copy 1
RM L58D18

NACA RM L58D18

NACA

RESEARCH MEMORANDUM

AERODYNAMIC CHARACTERISTICS OF SEVERAL JET-SPOILER CONTROLS ON A 45° SWEPTBACK WING AT MACH NUMBERS OF 1.61 AND 2.01

By Douglas R. Lord

Langley Aeronautical Laboratory
Langley Field, Va.

CLASSIFIED DOCUMENT

This material contains information affecting the National Defense of the United States within the meaning of the espionage laws, Title 18, U.S.C., Secs. 793 and 794, the transmission or revelation of which in any manner to an unauthorized person is prohibited by law.

NATIONAL ADVISORY COMMITTEE FOR AERONAUTICS

WASHINGTON

June 24, 1958

NACA FILE COPY
Loan expires on last date stamped on back cover.
PLEASE RETURN TO
DIVISION OF RESEARCH INFORMATION
NATIONAL ADVISORY COMMITTEE
FOR AERONAUTICS
Washington 25, D. C.

CONFIDENTIAL

CLASSIFICATION CANCELLED
Authority NASA PUBLICATIONS
ANNOUNCEMENTS NO.
Date By

NATIONAL ADVISORY COMMITTEE FOR AERONAUTICS

RESEARCH MEMORANDUM

AERODYNAMIC CHARACTERISTICS OF SEVERAL JET-SPOILER CONTROLS ON A 45° SWEPTBACK WING AT MACH NUMBERS OF 1.61 AND 2.01

By Douglas R. Lord

SUMMARY

An investigation has been made in the Langley 4- by 4-foot supersonic pressure tunnel at Mach numbers of 1.61 and 2.01 to determine the aerodynamic characteristics of several jet-spoiler controls on a wing having a 45° sweepback of the quarter-chord line, an aspect ratio of 3.5, a taper ratio of 0.3, and an NACA 65A005 airfoil section. The model was equipped with various arrangements of jet holes located along the 70-percent-chord line and extending from 13 to 78 percent of the wing semispan. Tests were made at a Reynolds number of 2.8×10^6 (based on the mean aerodynamic chord of the wing) and covered a range of angles of attack from -12° to 15° for a range of ratios of jet total pressure to stream static pressure from the jet-off condition to a maximum of 24.1.

The test results indicated that the jet-spoiler effectiveness increased with increasing angle of attack and correlated well with the momentum of the jet flow. For a constant momentum, the effectiveness of the jet spoiler increased as the jet hole angle was inclined forward or as the spoiler was moved outboard. The wing aerodynamic drag appeared to be more favorable for the jet-spoiler control than for conventional spoilers, but the air-flow requirements may be prohibitive for practical application of jet-spoiler controls at supersonic speeds.

INTRODUCTION

Considerable interest is being manifested in spoiler-type controls for use in obtaining lateral control on high-speed aircraft. Many investigations have been made of solid spoilers and spoiler-slot-deflector controls, and several investigations have been made (refs. 1 to 11) of jet spoilers in which compressed air, obtained either from

stream ram or from other sources, is exhausted normal to the wing surface. In addition to the jet-reaction effect, the latter control has been shown to change the lift over the wing in a manner similar to that produced by a solid spoiler. The supersonic tests have thus far been limited to an angle of attack of 0° and the use of stream ram air.

In order to investigate the control effectiveness and drag of jet spoilers at supersonic speeds for a range of angles of attack while using some other source of air, such as would be available from a jet engine, a series of tests has been conducted in the Langley 4- by 4-foot supersonic pressure tunnel of several jet-spoiler configurations on a wing having a 45° sweepback of the quarter-chord line. The purpose of this report is to present the results of these tests and to compare the effectiveness of the jet spoilers with the effectiveness of other types of controls.

The semispan wing model was tested in the presence of a half-fuselage model at angles of attack from -12° to 15°. Jet-spoiler variables included jet-pressure ratio, hole angle, hole size, span, and spanwise location. The tests were conducted at Mach numbers of 1.61 and 2.01 for a Reynolds number of 2.8×10^{6}, based on the wing mean aerodynamic chord of 10.65 inches.

SYMBOLS

C_L semispan wing lift coefficient, $\frac{\text{Lift}}{qS}$

C_D semispan wing drag coefficient, $\frac{\text{Drag}}{qS}$

C_m semispan wing pitching-moment coefficient referred to $0.25\bar{c}$, $\frac{\text{Pitching moment}}{qS\bar{c}}$

$C_{l,gross}$ semispan wing rolling-moment coefficient, $\frac{\text{Rolling moment}}{2qSb}$

C_l incremental rolling-moment coefficient produced by control

C_μ momentum coefficient, $\frac{wV_j}{gqS}$ (note that this coefficient is based on the semispan wing area)

$\frac{b}{2}$ wing semispan

b_j control span

c wing local chord

$\bar{c}$ wing mean aerodynamic chord

D_j diameter of jet-spoiler holes

g acceleration of gravity, ft/sec^2

h height of fixed spoiler above wing surface

K_l rolling-moment magnification factor, ratio of rolling moment produced by the control C_l to rolling moment computed for the control reactive force alone

M stream Mach number

p stream static pressure

$p_{t,j}$ total pressure in plenum chamber

q stream dynamic pressure, lb/ft^2

w weight flow rate of air used in jet control, lb/sec

S semispan wing area, ft^2

V_j jet velocity associated with isentropic expansion to the critical pressure ratio at the jet exit, ft/sec

y_i perpendicular distance from plane of symmetry to inboard end of control

y_o perpendicular distance from plane of symmetry to outboard end of control

$\bar{y}$ perpendicular distance from plane of symmetry to centroid of control

α wing angle of attack

δ_d/δ_s ratio of deflector to spoiler projection on spoiler-slot-deflector configuration

δ_j streamwise angle between center line of jet holes and wing surface

Δ prefix indicating increment due to control

TEST APPARATUS AND MODEL

Wind Tunnel

This investigation was conducted in the Langley 4-by 4-foot supersonic pressure tunnel, which is a rectangular, closed-throat, single-return type of wind tunnel with provisions for the control of the pressure, temperature, and humidity of the enclosed air. Flexible nozzle walls were adjusted to give the desired test-section Mach numbers of 1.61 and 2.01. During the tests the dewpoint was kept below -20° F at atmospheric pressure, so that the effects of water condensation in the supersonic nozzle were negligible.

Model and Model Mounting

The model used in these tests consisted of a semispan wing and a half-fuselage as shown in figure 1. The wing was made of steel and had a 45° sweepback of the quarter-chord line, an aspect ratio of 3.5, a taper ratio of 0.3, and NACA 65A005 airfoil sections parallel to the air stream. Jet-spoiler controls were constructed by milling out a portion of the upper surface of the wing from the wing root to about the 80-percent-semispan station to form a plenum chamber. Interchangeable cover plates were then constructed, each having 73 holes of 0.055-inch diameter located along the wing 70-percent-chord line at 3/16-inch spacings, with the holes drilled at angles of 50°, 70°, 90°, and 110° to the surface measured in the streamwise direction. (See fig. 1.) The hole size and number were modified during the tests as described in a later section. In addition to the jet spoilers, one fixed spoiler was constructed of steel and had the same span and location as the row of jets but had a height equal to 5 percent of the wing mean aerodynamic chord.

The fuselage, which was constructed of aluminum alloy, had an ogival nose with a fineness ratio of 2.5, a cylindrical center portion, and a boattailed afterbody with a base diameter of 50 percent of the maximum body diameter. (See fig. 1.)

The semispan wing was mounted on a balance which was located in the turntable of a boundary-layer bypass plate installed vertically about 10 inches from the tunnel sidewall. The half-fuselage was mounted on

the turntable independently of the wing, with 0.010-inch clearance between the wing and the fuselage.

TESTS

The forces and moments on the wing were measured in the presence of the fuselage by the four-component balance. High-pressure air was obtained from a dry air supply outside the tunnel and delivered to the wing plenum chamber by means of a 1-inch-diameter feeder tube. This tube was approximately 24 inches in length and floated in rubber "O" rings at either end so that the forces transmitted around the balance would be negligible. The feeder tube was shielded from the airstream between the bypass plate and the tunnel wall by a fairing.

The angle of attack of the model was changed manually by rotating the turntable in the bypass plate on which the model was mounted, and the angle of attack was measured by a vernier scale located outside the tunnel. The total pressure of the air in the jet plenum chamber was measured by an external gage connected to two 0.055-inch-diameter tubes inserted in the plenum chamber.

A complete description of the spoiler geometry for each of the eleven test configurations is presented in table I. The four basic configurations (configurations 1 to 4), were tested at both Mach numbers (1.61 and 2.01), and several modifications were made to the orifice geometry for additional tests at $M = 1.61$ (configurations 5 to 11). These modifications were made by enlarging the holes of the configuration for $\delta_j = 90^\circ$, first to 0.0760-inch diameter and then to 0.0935-inch diameter, and sealing various spanwise groups of holes on the configuration for $\delta_j = 50^\circ$.

The wing angle-of-attack range was from -12° to 15°. A valve in the 2-inch high-pressure air line ahead of the 1-inch feeder tube was used to control the pressure in the jet plenum chamber from a minimum with the valve closed to a maximum of 40 pounds per square inch absolute. The tests were made at tunnel stagnation pressures of 11.5 and 13.2 pounds per square inch absolute at Mach numbers of 1.61 and 2.01, respectively, corresponding to a Reynolds number based on the wing mean aerodynamic chord of 2.8×10^6.

In order to insure a turbulent boundary layer over the wing during the tests, 1/8-inch-wide strips of No. 60 carborundum grains were attached to the wing upper and lower surfaces at a distance of 3/4 inch from the leading edge. Configuration 1 was also tested without transition strips, and the data showed negligible changes.

PRECISION OF DATA

The mean Mach numbers in the region occupied by the model were estimated from calibration to be 1.61 and 2.01, with local variations smaller than ±0.02. There was no evidence of significant flow angularity.

The angle of attack of the wing root could be set within ±0.05°; however, the wing twist due to aeroelastic effects is estimated to be as much as 0.75° at the wing tip for the largest angles of attack used. The estimated accuracies of the balance measurements and other pertinent quantities are as follows:

C_L	±0.02
C_D	±0.002
C_m	±0.002
$C_{l,gross}$	±0.001
$p_{t,j/p}$	±0.1

Note that the accuracy of the lift coefficient is very poor for this balance. Most of the data, however, indicate the balance to be more reliable than is indicated from these values, which were determined primarily from balance calibrations. It should be remembered that throughout these tests the incremental forces and moments due to the jet spoiler were small with respect to the gross forces and moments and, therefore, the accuracy of the incremental coefficients is very poor.

RESULTS AND DISCUSSION

Basic Wing Characteristics

The variations of wing lift, drag, pitching-moment, and gross rolling-moment coefficients with angle of attack for the basic wing with the jet spoiler inoperative are shown in figure 2. These variations are presented in order to illustrate the magnitude of the coefficients at the two Mach numbers and because the ensuing analysis of the spoiler characteristics relies on the incremental coefficients due to the spoilers.

In general, the curves of the various wing coefficients with angle of attack (fig. 2) are smooth, and the effect of increasing the Mach number from 1.61 to 2.01 is to decrease the slopes of the curves. The changes in slopes of the lift, pitching-moment, and rolling-moment curves are slightly greater than the inverse ratio of $\sqrt{M^2 - 1}$. The values of the

coefficients are identical to those obtained on another model having the same geometry, reported in reference 12, except for the drag coefficients, which are somewhat greater herein. The faired values taken from the curves of figure 2 were subtracted from the measured values with the spoilers operative in order to obtain the incremental coefficients due to the spoilers.

Jet-Spoiler Effectiveness and Drag

The basic plots of the incremental wing lift, drag, pitching-moment, and rolling-moment coefficients due to the various jet-spoiler controls are presented in figures 3 to 6. The coefficients are plotted against jet pressure ratio for a constant angle of attack. In general, all of the jet-spoiler configurations produced negative lift, positive pitching moment, and positive rolling moment at all angles of attack, as would be expected both from the spoiling action and from the reactive force of the jet spoiler. The one exception to this generality is for the $\alpha = -12^{\circ}$ condition at $M = 1.61$ where the jet spoilers produced zero or negative pitching moment and rolling moment. This exception is probably caused by detachment of the leading-edge shock for this angle and Mach number. The action of the jet spoilers generally caused reductions in drag coefficient at the positive angles of attack and increases in drag coefficient at the negative angles of attack. This variation is primarily caused by the lift-spoiling action of the jet spoilers as attested by the fact that the jet reactive force alone for the $\delta_j = 50^{\circ}$ configurations should increase the drag even at $\alpha = 15^{\circ}$ because of the angle of the jets with respect to the drag axis (see fig. 4(a)).

As the angle of attack is increased, the slopes of the lift and drag curves (figs. 3 and 4) generally become more negative, whereas the slopes of the pitching-moment and rolling-moment curves (figs. 5 and 6) become more positive. The increasing effectiveness with increasing angle of attack is probably the result of the decreased pressure on the upper surface of the wing which effectively increases the height of the jet spoiler. The slopes of the lift and drag curves become more positive and the slopes of the pitching-moment and rolling-moment curves become more negative as the jet pressure ratio is increased and as the Mach number is increased from 1.61 to 2.01. These changes are again associated with the effective increase in jet-spoiler height. Also, in general, the curves tend to become more nearly linear as jet pressure ratio and Mach number are increased.

Previous results for jet spoilers have shown that for a given jet angle the effectiveness can usually be correlated with the momentum coefficient of the jet flow (refs. 3, 5, and 6). The computed momentum coefficients are plotted in figure 7 for the jet-spoiler configurations

as a function of jet-pressure ratio. In figure 8 the effectiveness and drag coefficients for three of the configurations tested herein are plotted against the momentum coefficient for three test angles of attack. The configurations chosen were those having $\frac{2b_j}{b} = 0.65$ and $\delta_j = 90^\circ$, but the hole size varied from 0.0550-inch to 0.0935-inch diameter. These curves show excellent correlation on the basis of C_μ and also illustrate the increasing effectiveness and decreasing drag as the angle of attack is increased. The increasing effectiveness with angle of attack is in agreement with previous results found at transonic speeds in reference 6.

In reference 3 it was shown that in low-speed tests of a jet spoiler on a two-dimensional airfoil, considerable increase in effectiveness could be obtained by inclining the angle of the jet holes forward. Comparisons of the effectiveness and drag produced by the configurations tested herein having various jet-hole angles at Mach numbers of 1.61 and 2.01 are presented in figures 9 and 10, respectively. The variations are presented against angle of attack for a hole diameter of 0.0550 inch and constant jet-pressure ratio of 12.0 (and hence constant momentum). From the curves of figures 9 and 10 it is evident that effectiveness of the jet spoiler does increase as δ_j decreases; however, the drag increases. The change in drag is associated primarily with the inclination of the jet-reactive-force axis with the drag axis.

In order to compare the performance of various spanwise locations of the spoilers, the effectiveness and drag of the spoilers having $\frac{2b_j}{b} = 0.330$ (configurations 6 to 8) are shown in figure 11 for a constant jet pressure ratio of 12.0 (and constant momentum). There is very little change in lift or drag due to spanwise movement of the spoiler; however, both the pitching moment and rolling moment tend to increase with movement outboard. Since, to a first approximation, the pitching or rolling moment created by the jet spoiler should be a direct function of its location and momentum, an attempt was made to correlate the rolling-moment coefficient for the five configurations for which $\delta_j = 50^\circ$ with a factor for spanwise location $\left(\frac{2\bar{y}}{b}\right)$ times momentum coefficient (C_μ). These curves, presented in figure 12, indicate that the correlation is fairly good, particularly at $\alpha = 0^\circ$ and $\alpha = 6^\circ$.

Jet-Spoiler Reaction Magnification

In order to compare the efficiency of the various spoiler configurations in producing rolling moment, the rolling-moment magnification

factor is plotted against angle of attack in figure 13. The thrust of the jets was computed by using the method shown in reference 5. For computing the thrust at various angles of attack the wing upper-surface pressure measured at the jet-spoiler station with the jet inoperative was used instead of the free-stream static pressure called for in the method of reference 5. The computed values used in figure 13 are believed to be fairly accurate because similar computations checked very closely calibrations made in the tunnel with the wind off. In these calibrations, the tunnel was evacuated to a low pressure equal to the static pressure at the test Mach number, and the forces and moments due to operation of the jet were determined.

The variations of the rolling-moment magnification factor with angle of attack show an increase in efficiency as the jet hole angle is decreased (figs. 13(a) and 13(b)). Decreasing the hole diameter from 0.0935 inch to 0.0760 inch (fig. 13(c)) causes negligible changes in the rolling-moment magnification factor; however, further decreasing the hole diameter to 0.0550 inch results in an increased efficiency, particularly at the positive angles of attack. It should be remembered that decreasing the hole size for a constant pressure ratio causes a reduction in momentum requirement, and the increased efficiency is, therefore, directly related to the nonlinear variation of the rolling-moment coefficient with momentum coefficient at angles of attack (fig. 8(b)). The rolling-moment magnification factor generally increases as the spoiler is moved inboard, as shown by the curves in figure 13(d); however, these curves should be used only qualitatively since the incremental coefficients used in the computation are small and the inaccuracies become significant. In general the magnification factors at the positive angles of attack indicated that the spoiler controls give better roll control than would be provided by a pure reaction control located at the wing tip. The lift and pitching-moment magnifications, although not presented, are similar to those shown in figure 13 for the rolling moment.

Jet-Spoiler Drag and Momentum Comparison

Since the primary use of a jet spoiler is for roll control, a comparison of the drag coefficients and momentum coefficients required for various configurations to produce given rolling-moment coefficients are shown in figure 14. It should be mentioned that an inboard half-span trailing-edge control of 25-percent chord has been shown to produce a rolling-moment coefficient of 0.002 with an aileron deflection of 4° on a similar semispan wing at $M = 1.9$ (ref. 13). The curves of figures 14(a) and 14(b) indicate that, for a rolling-moment coefficient of 0.002, the momentum requirements for the jet-spoiler control decrease but the drag increases as the hole angle is decreased. Therefore,

although the forward inclination of the jet holes is good from the effectiveness standpoint, the unfavorable drag effect must be considered. The curves of figure 14(c) indicate that, for rolling-moment coefficients of 0.002 and 0.004, both the drag and momentum are relatively unaffected by changes in hole size, as might be expected from the momentum correlation previously shown. There is some indication, however, that the smaller holes are slightly more favorable from the momentum standpoint.

Comparison of Jet Spoiler With Other Controls

In figure 15, the variations of the incremental wing coefficients with angle of attack are presented for the fixed spoiler ($h = 0.05\bar{c}$) as compared with those for the largest jet spoiler tested herein (configuration 10) at a jet pressure ratio of 12.0. At $\alpha = 0^{\circ}$, the lift and pitching-moment coefficients for the two controls are comparable, but the fixed spoiler gives considerably more rolling moment than does the jet spoiler. Since it would be anticipated that the lift and rolling-moment comparison for the two controls would be similar, the inaccuracy of the lift measurements is probably responsible for the nearness of the lift results. At the highest angles of attack, the jet spoiler produces more negative lift and more positive rolling moment than does the fixed spoiler. These changes are caused by the decreasing effectiveness with increasing angle of attack for the fixed spoiler and the increasing effectiveness with increasing angle of attack for the jet spoiler. The decreasing effectiveness with increasing angle of attack for the fixed spoiler is caused by the increase in local Mach number and is similar to the variation shown for the spoiler alone in reference 12. Throughout the angle-of-attack range the drag characteristics for the jet spoiler are considerably better and are negative over much of the angle range.

In order to compare the jet spoiler and the fixed spoiler tested herein with a flap-type spoiler and a spoiler-slot-deflector of equal span on the same wing (ref. 12), the incremental wing aerodynamic drag coefficient required for each of the spoilers to provide the rolling moment obtained with the fixed spoiler are plotted against angle of attack in figure 16. The variations for the three solid spoilers are very nearly alike, whereas the jet spoiler exhibits considerably less drag over most of the angle-of-attack range. This comparison does not consider the losses in thrust that would be imposed on an aircraft in order to provide the air flow for the jet spoiler or the actuating power for the solid spoilers. If these losses were taken into account, the advantage of the jet spoiler from the drag standpoint would be considerably less.

In order to get an approximation of the practicability of using engine bleed air for a jet-spoiler roll control, some computations were made by using available information on the Pratt & Whitney J75 turbojet engine. The aircraft was assumed to have a wing span of 34 feet and to be operating at altitudes between 45,000 and 60,000 feet at a Mach number of 1.61 with the engine at the cruising condition. At these conditions, enough bleed air could be obtained from the engine compressor to produce a momentum coefficient of 0.0021. The bleed air was limited to 5.5 percent of the total engine air flow. According to the results presented herein, this momentum coefficient of 0.0021 would provide a rolling-moment coefficient of 0.0010 at $\alpha = 0^{\circ}$ and 0.0027 at $\alpha = 12^{\circ}$. Unpublished results of tests on a conventional inboard half-span trailing-edge aileron indicate that these rolling-moment coefficients would be comparable to aileron deflections of only $\pm 2.0^{\circ}$ and $\pm 2.5^{\circ}$ at angles of attack of 0° and 12°, respectively.

CONCLUSIONS

An investigation has been made at Mach numbers of 1.61 and 2.01 to determine the aerodynamic characteristics of several jet-spoiler controls on a 45° sweptback wing. The conclusions indicated are as follows:

1. The jet-spoiler effectiveness and drag for a given jet hole angle is a direct function of the momentum of the jet flow.

2. For a constant momentum, the effectiveness of the jet spoiler increases as the jet hole angle is inclined forward or as the spoiler is moved outboard.

3. The effectiveness of the jet spoilers increases with increasing angle of attack, and the drag increments are generally negative in the positive angle-of-attack range.

4. Despite the favorable wing aerodynamic drag characteristics of the jet spoilers as compared with those for the conventional spoilers, it appears questionable whether sufficient air can be obtained to make them practical at supersonic speeds when using conventional methods of obtaining air.

Langley Aeronautical Laboratory,
National Advisory Committee for Aeronautics,
Langley Field, Va., April 3, 1958.

REFERENCES

1. Lowry, John G., and Turner, Thomas R.: Low-Speed Wind-Tunnel Investigation of a Jet Control on a 35° Swept Wing. NACA RM L53I09a, 1953.

2. Attinello, John S.: An Air-Jet Spoiler NAVAER Rep. DR-1579, Bur. Aero., Aug. 1953.

3. Ballentine, Donald C., and Barnard, George A.: Two-Dimensional Wind-Tunnel Tests of a Jet-Type Spoiler on an NACA 64A010 Airfoil Section Equipped With High-Lift Devices. Aero. Rep. 862, David W. Taylor Model Basin, Navy Dept., June 1954.

4. Schult, Eugene D.: A Free-Flight Investigation at High Subsonic and Low Supersonic Speeds of the Rolling Effectiveness and Drag of Three Spoiler Controls Having Potentially Low Actuating-Force Requirements. NACA RM L55G11a, 1955.

5. Turner, Thomas R., and Vogler, Raymond D.: Wind-Tunnel Investigation at Transonic Speeds of a Jet Control on an 80° Delta-Wing Missile. NACA RM L55H22, 1955.

6. Vogler, Raymond D., and Turner, Thomas R.: Wind-Tunnel Investigation at Transonic Speeds of a Jet Control on a 35° Swept Wing - Transonic-Bump Method. NACA RM L55K09, 1956.

7. Vogler, Raymond D.: Wind-Tunnel Investigation at High Subsonic Speeds of Jet, Spoiler, and Aileron Controls on a 1/16-Scale Model of the Douglas D-558-II Research Airplane. NACA RM L56E25, 1956.

8. Schult, Eugene D.: Free-Flight Investigation at Mach Numbers Between 0.5 and 1.7 of the Zero-Lift Rolling Effectiveness and Drag of Various Surface, Spoiler, and Jet Controls on an 80° Delta-Wing Missile. NACA RM L56H29, 1956.

9. Schult, Eugene D.: Some Characteristics of Roll Controls Having Possible Application to Fin-Stabilized Ammunition. NACA RM L57A04, 1957.

10. Kehlet, Alan B.: Free-Flight Investigation of Comparative Zero-Lift Rolling Effectiveness of a Leading-Edge and a Trailing-Edge Air-Jet Spoiler on an Unswept Wing. NACA RM L57F10, 1957.

11. Schult, Eugene D.: Free-Flight Roll Performance of a Steady-Flow Jet-Spoiler Control on an 80° Delta-Wing Missile Between Mach Numbers of 0.6 and 1.8. NACA RM L57J28, 1958.

12. Lord, Douglas R., and Moring, Robert: Aerodynamic Characteristics of a Spoiler-Slot-Deflector Control on a 45° Sweptback Wing at Mach Numbers of 1.61 and 2.01. NACA RM L57E16a, 1957.

13. Jacobsen, Carl R.: Effects on Control Effectiveness of Systematically Varying the Size and Location of Trailing-Edge Flaps on a 45° Sweptback Wing at a Mach Number of 1.9. NACA RM L51I26, 1951.

TABLE I

CONFIGURATIONS TESTED

Configuration	δ_j, deg	D_j, in.	$\frac{2b_j}{b}$	$\frac{2y_i}{b}$	$\frac{2y_o}{b}$	M
1	50	0.0550	0.65	0.13	0.78	1.61 and 2.01
2	70	.0550	.65	.13	.78	1.61 and 2.01
3	90	.0550	.65	.13	.78	1.61 and 2.01
4	110	.0550	.65	.13	.78	1.61 and 2.01
5	90	.0760	.65	.13	.78	1.61
6	50	.0550	.33	.45	.78	1.61
7	50	.0550	.33	.29	.62	1.61
8	50	.0550	.32	.13	.45	1.61
9	(a)	(a)	.65	.13	.78	1.61
10	90	.0935	.65	.13	.78	1.61
11	50	.0550	.17	.45	.62	1.61

[a]Configuration 9 was a fixed spoiler, perpendicular to the surface and 0.533 inch in height.

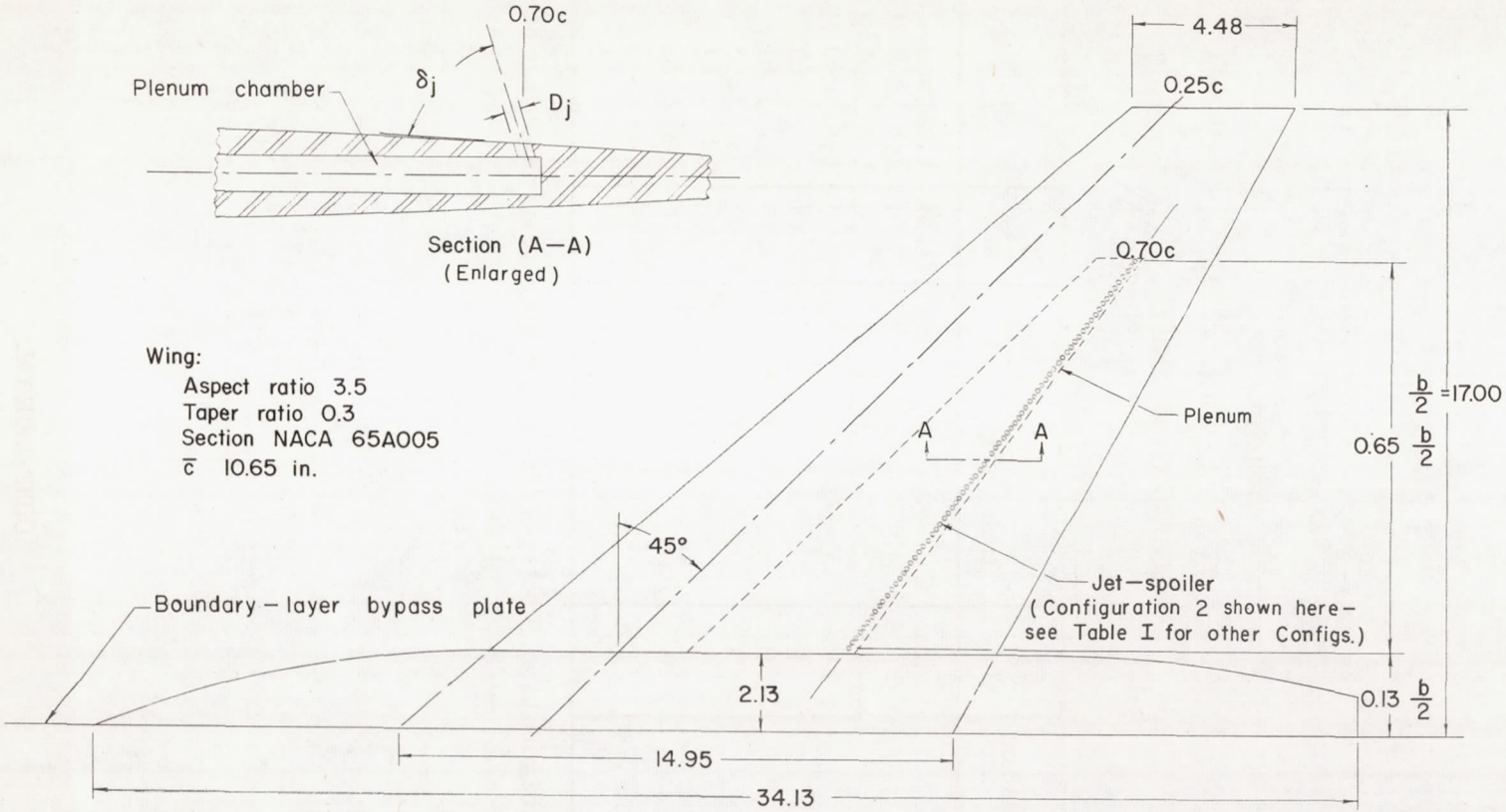

Figure 1.- Sketch of semispan wing-fuselage model. All dimensions are in inches.

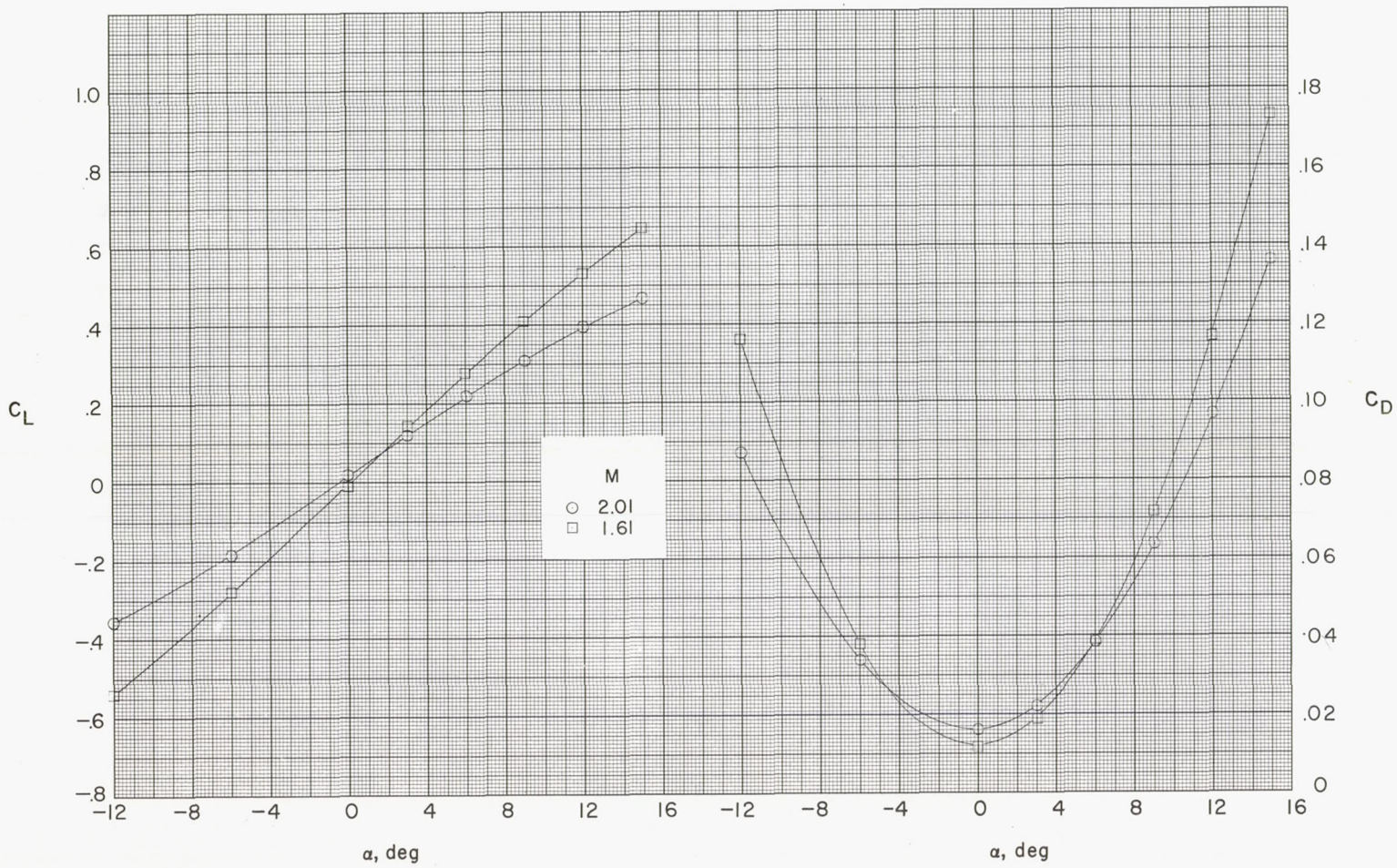

(a) C_L and C_D.

Figure 2.- Variation of basic wing lift, drag, pitching-moment, and gross rolling-moment coefficients with angle of attack. Jet spoiler inoperative.

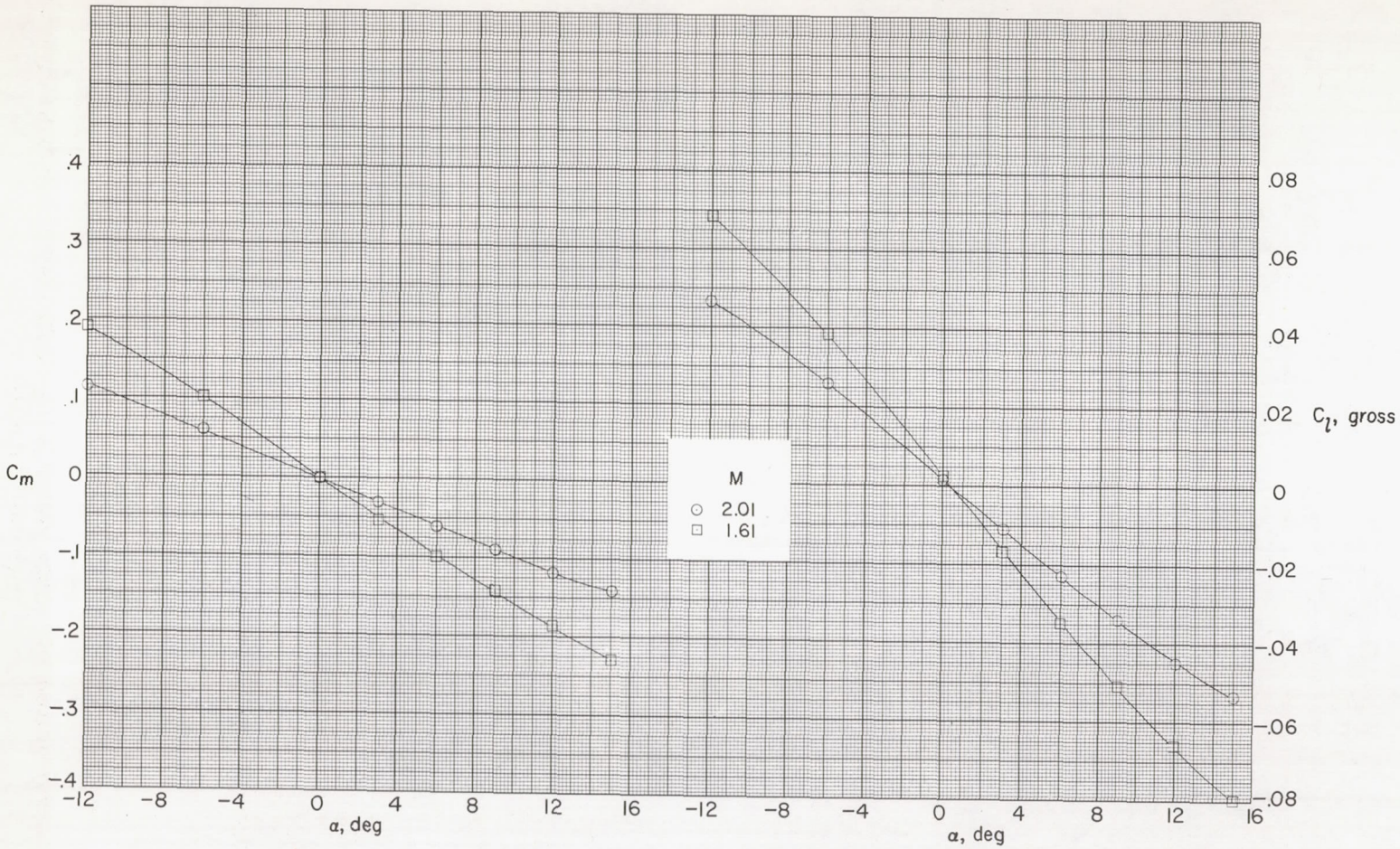

(b) C_m and $C_{l,gross}$.

Figure 2.- Concluded.

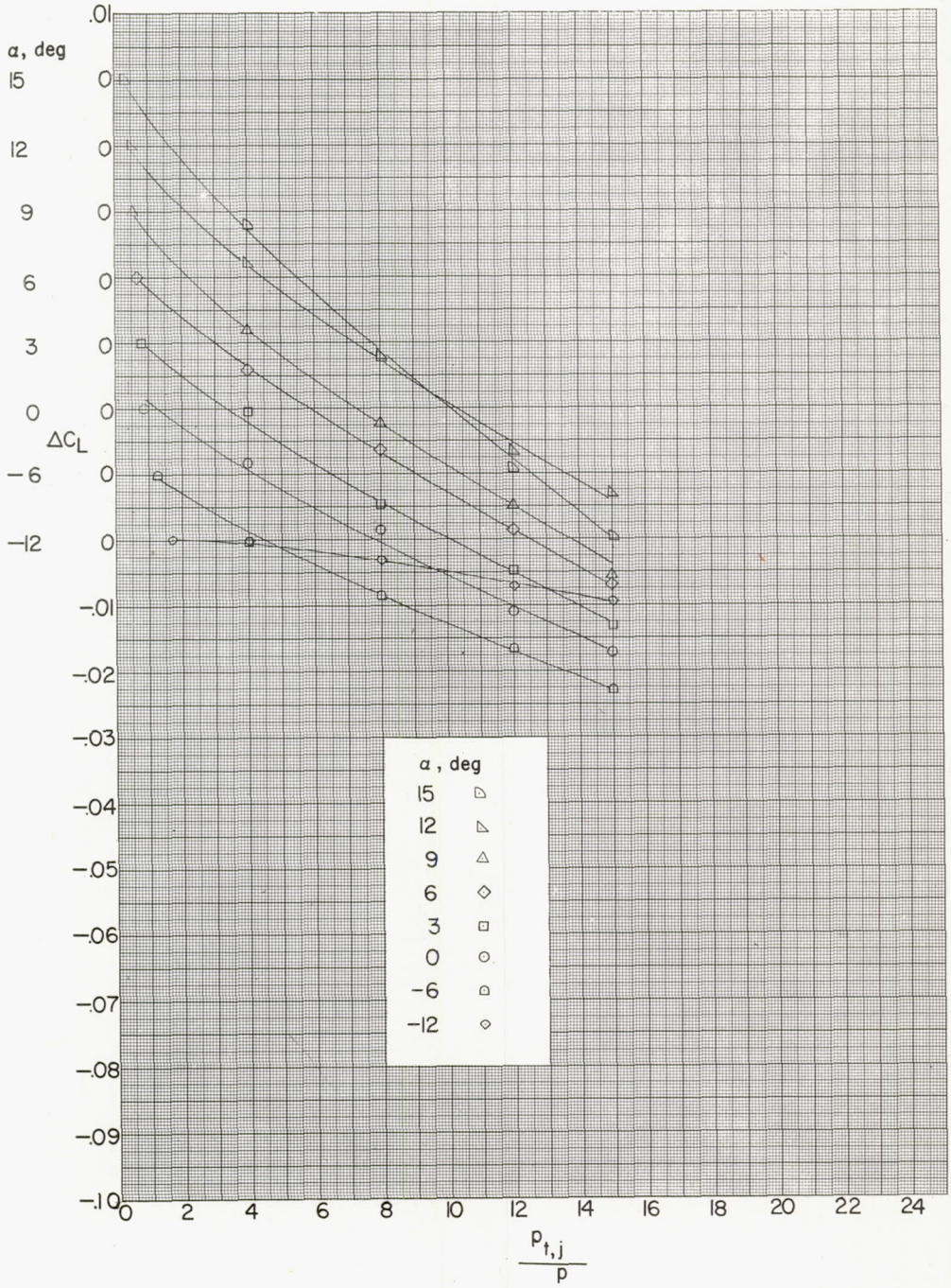

(a) Configuration 1; M = 1.61.

Figure 3.- Variation of incremental wing-lift coefficient with jet pressure ratio.

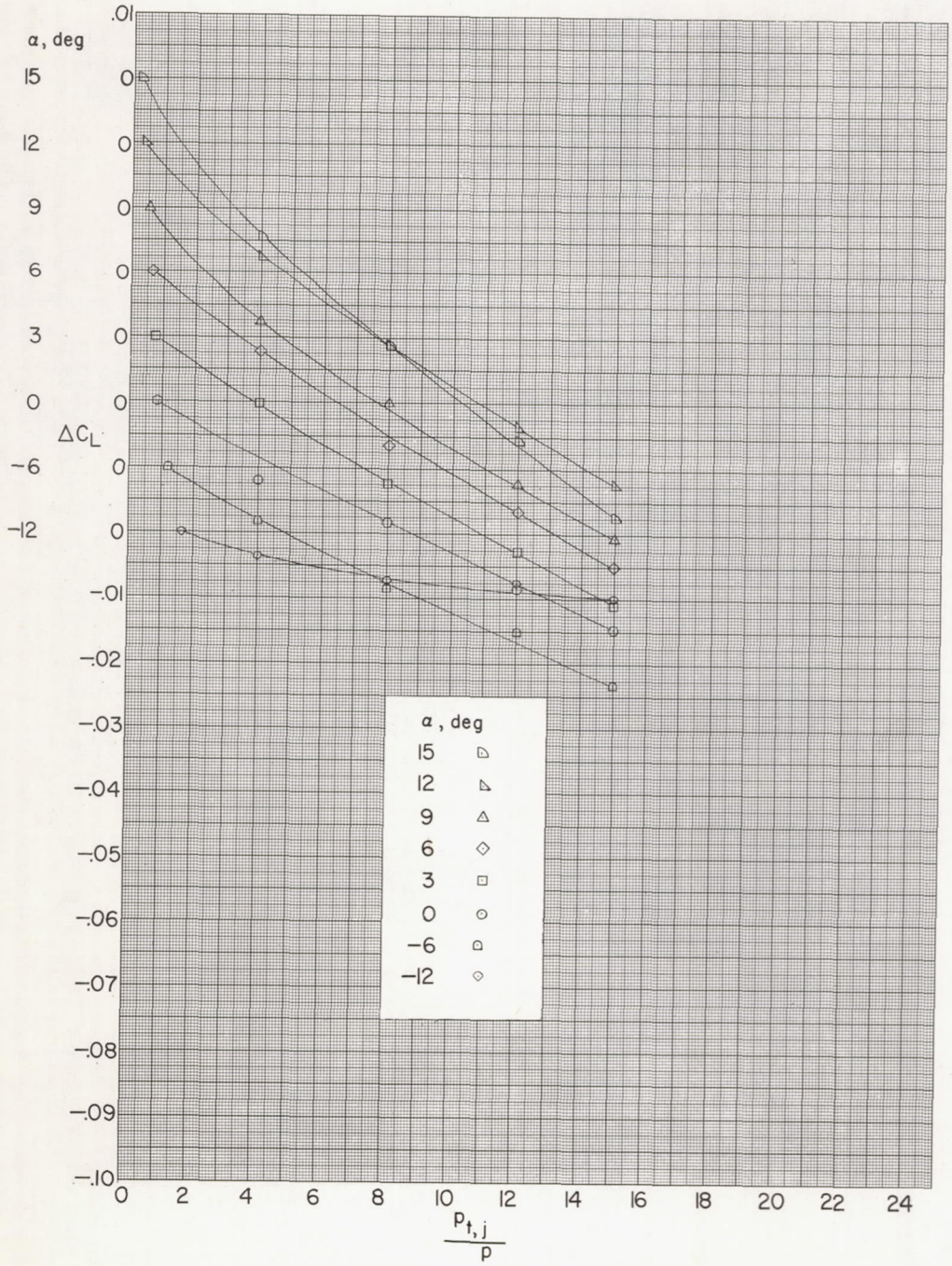

(b) Configuration 2; M = 1.61.

Figure 3.- Continued.

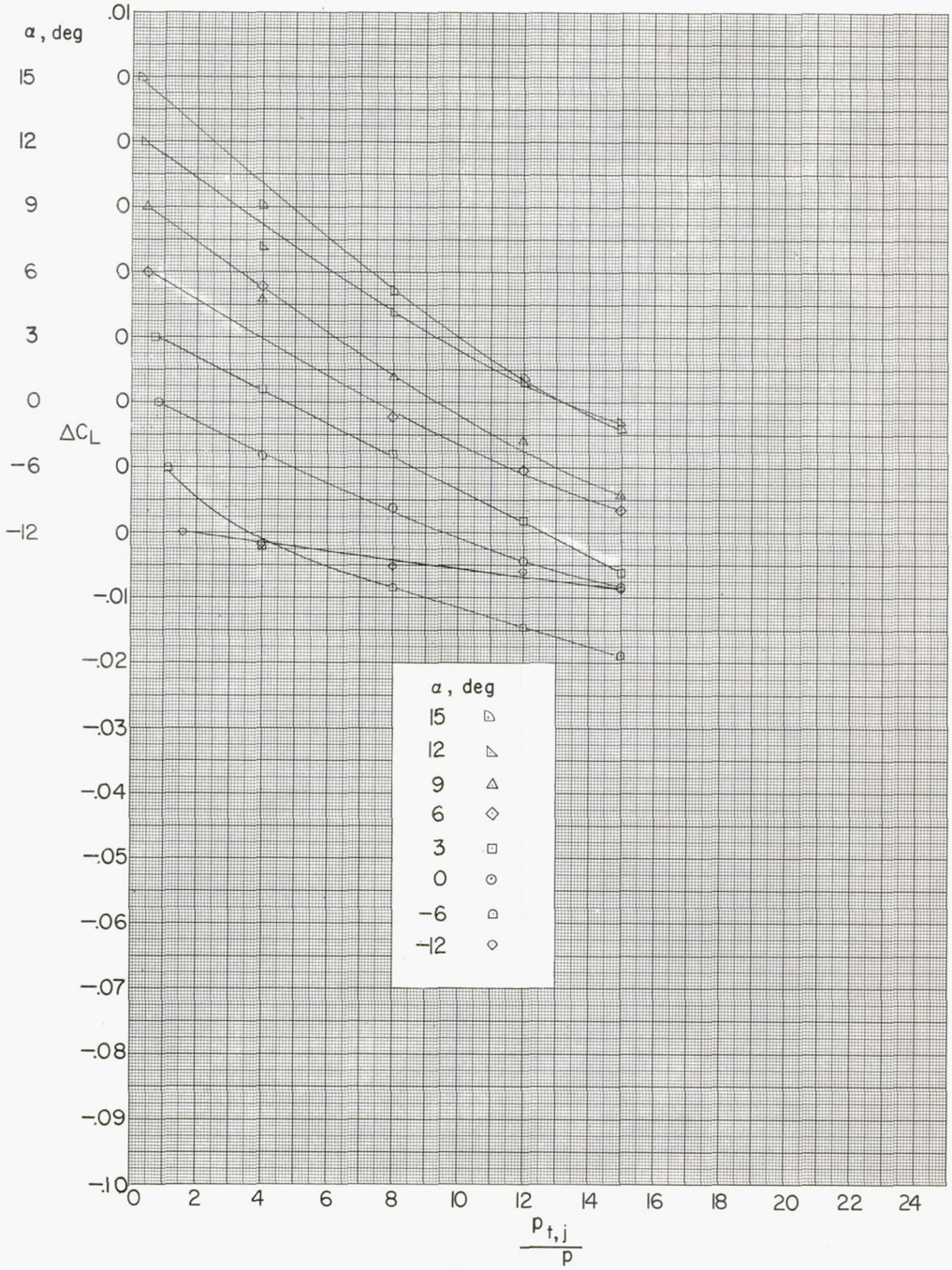

(c) Configuration 3; M = 1.61.

Figure 3.- Continued.

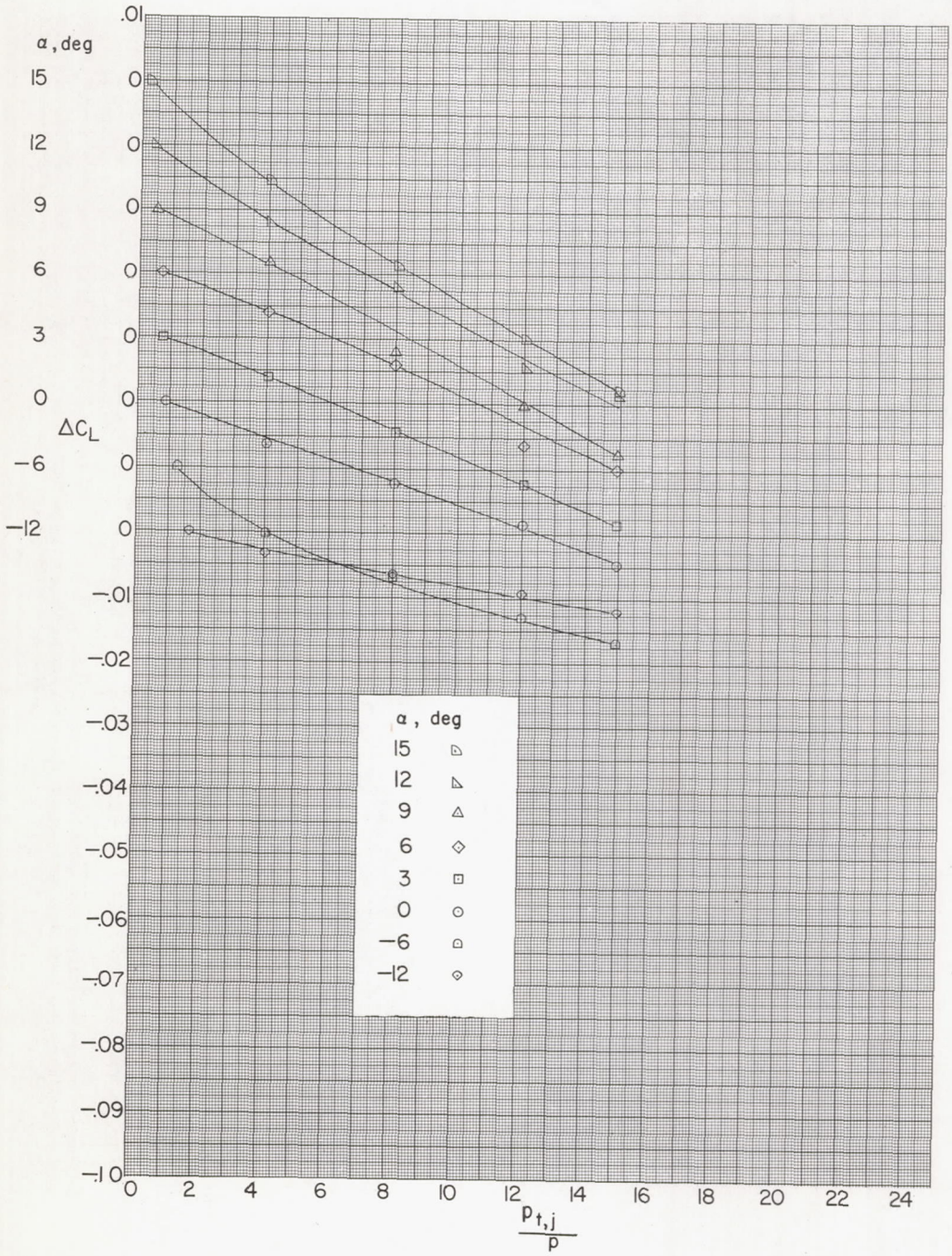

(d) Configuration 4; M = 1.61.

Figure 3.- Continued.

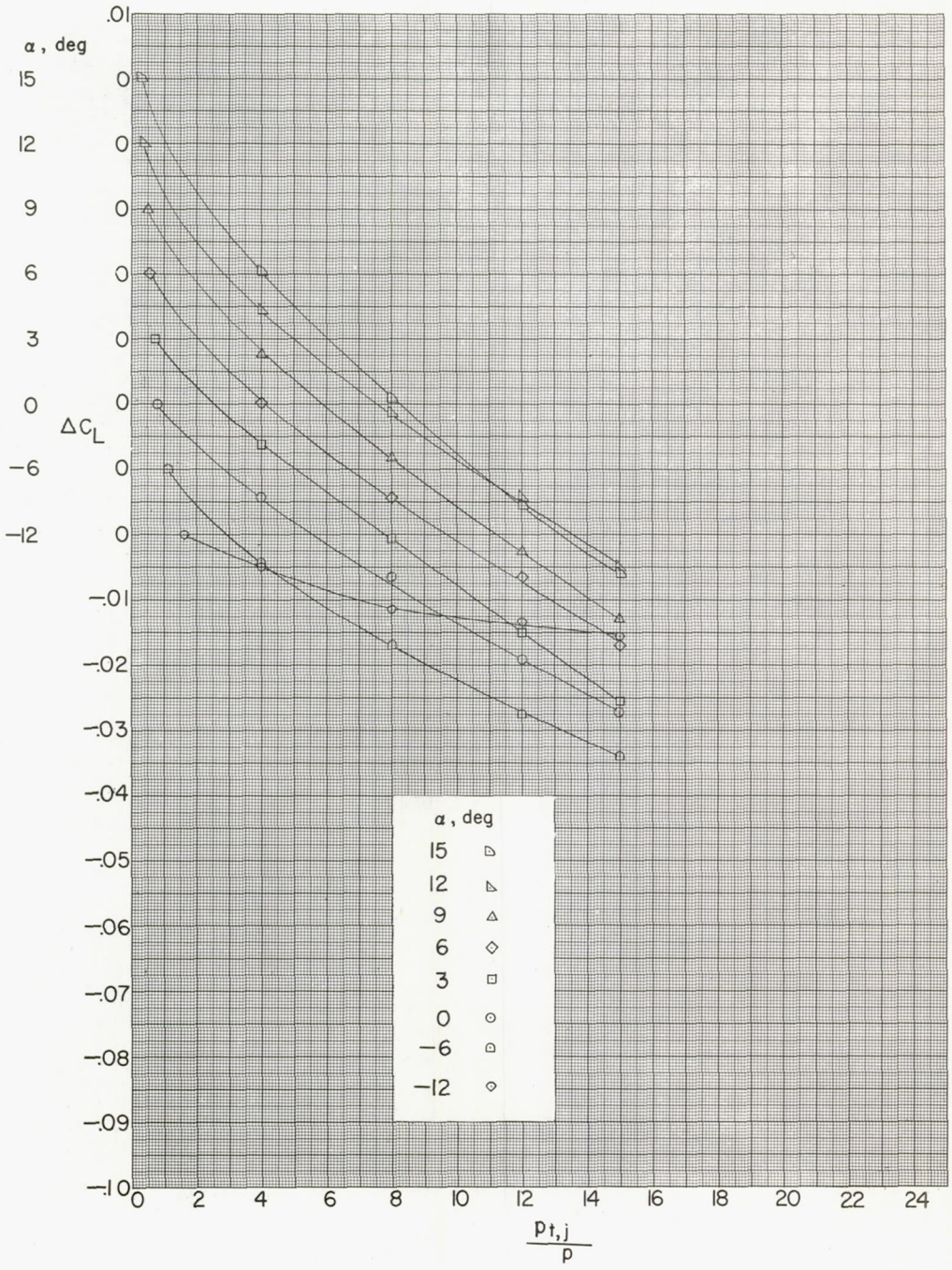

(e) Configuration 5; M = 1.61.

Figure 3.- Continued.

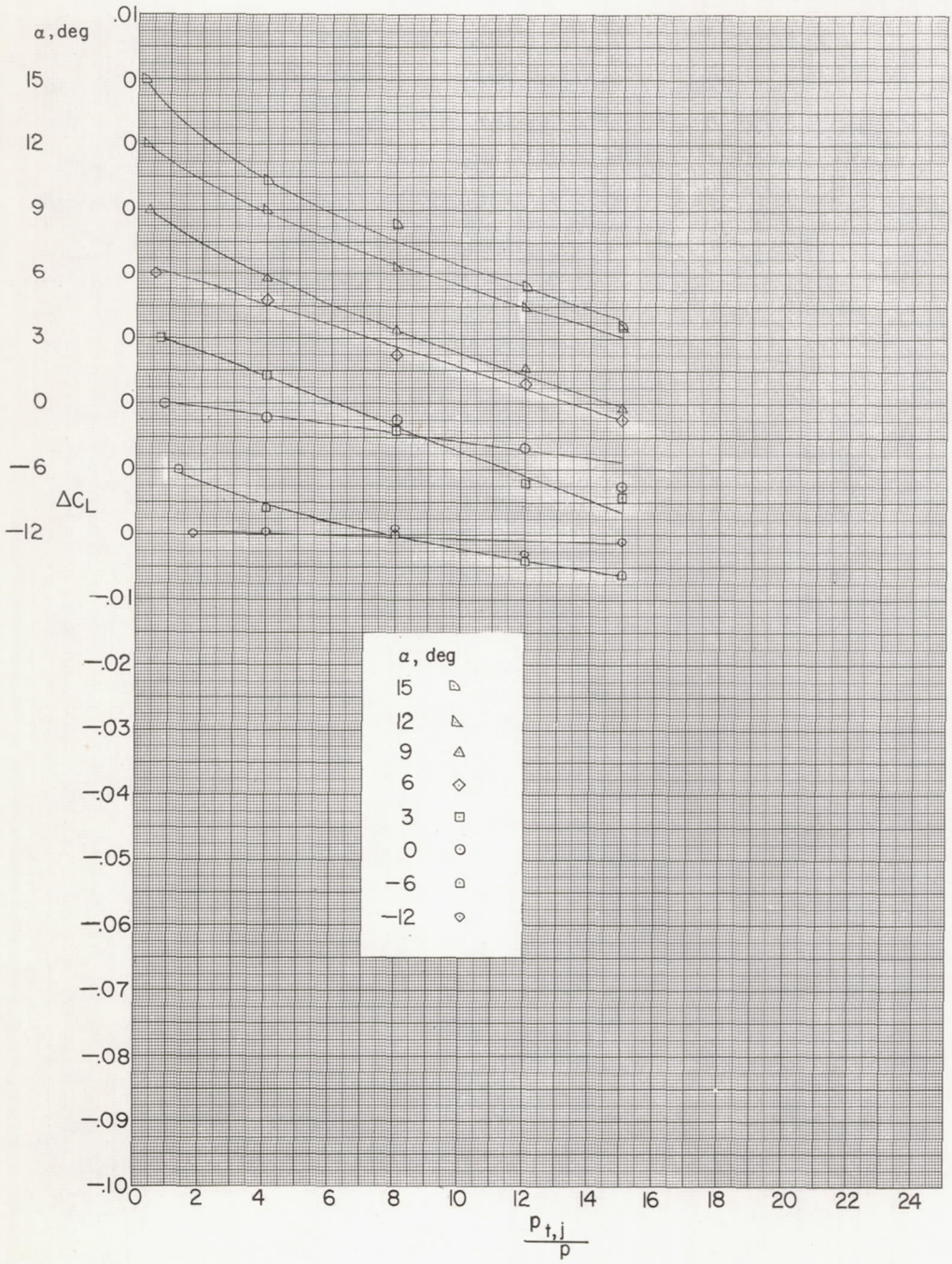

(f) Configuration 6; M = 1.61.

Figure 3.- Continued.

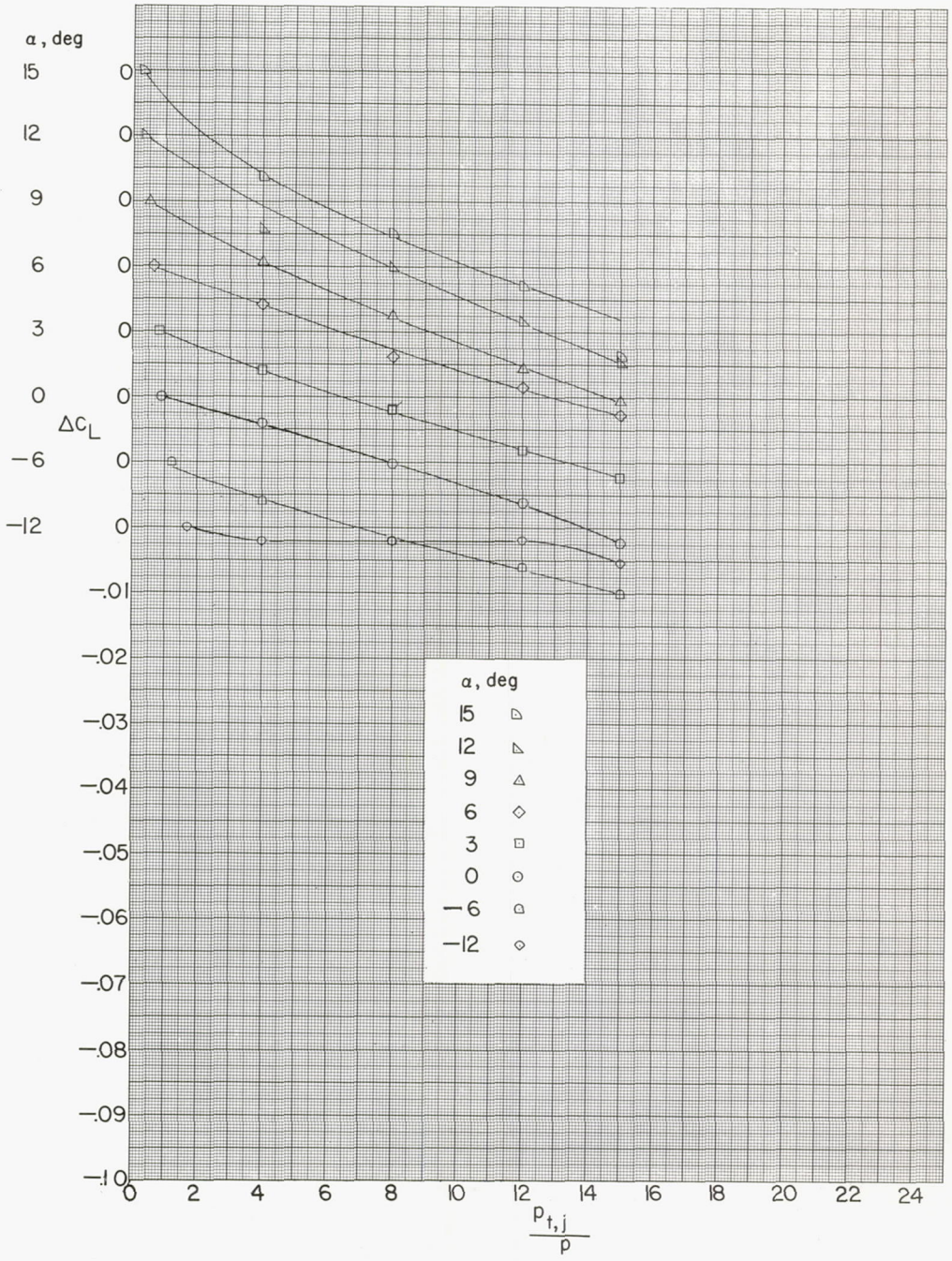

(g) Configuration 7; M = 1.61.

Figure 3.- Continued.

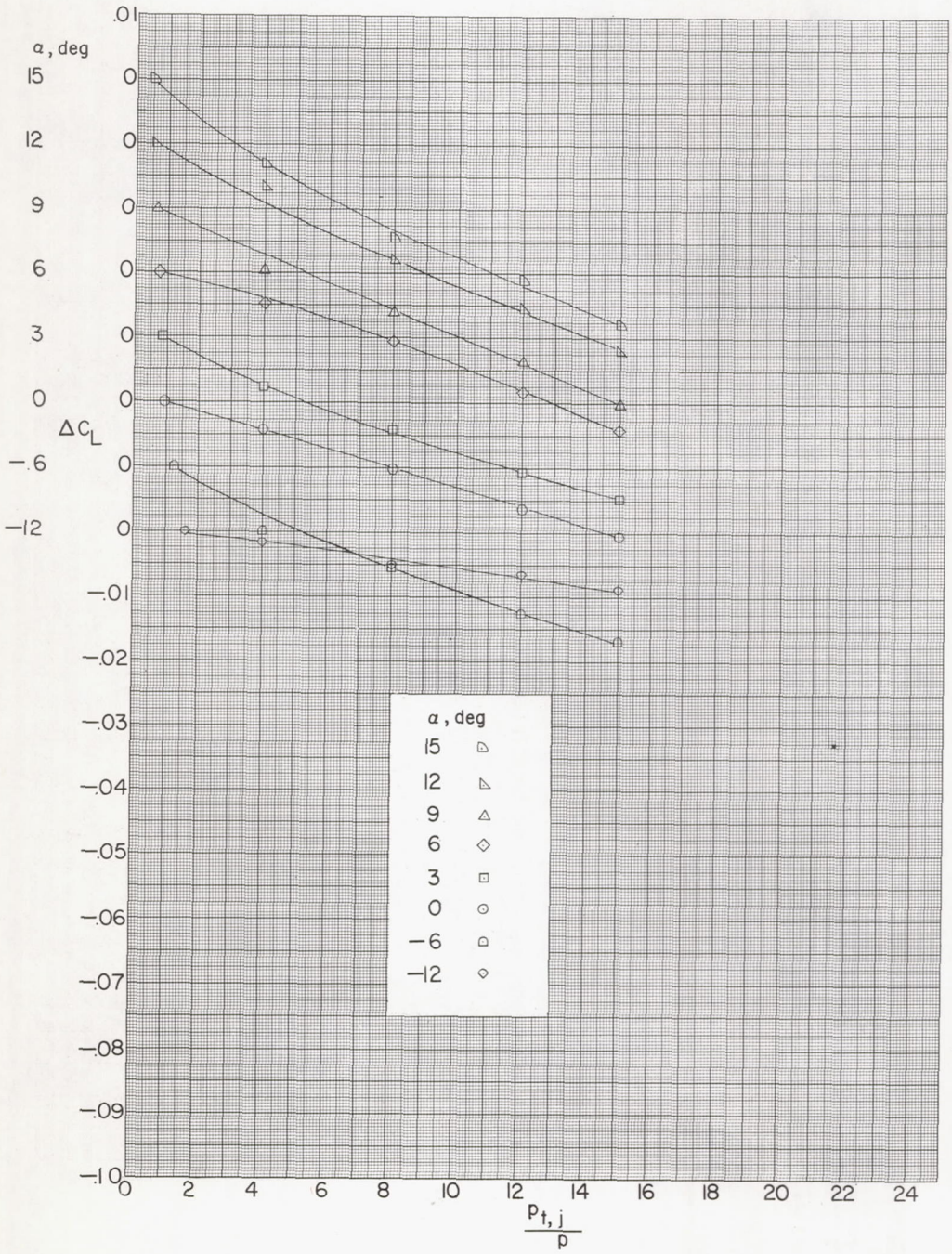

(h) Configuration 8; M = 1.61.

Figure 3.- Continued.

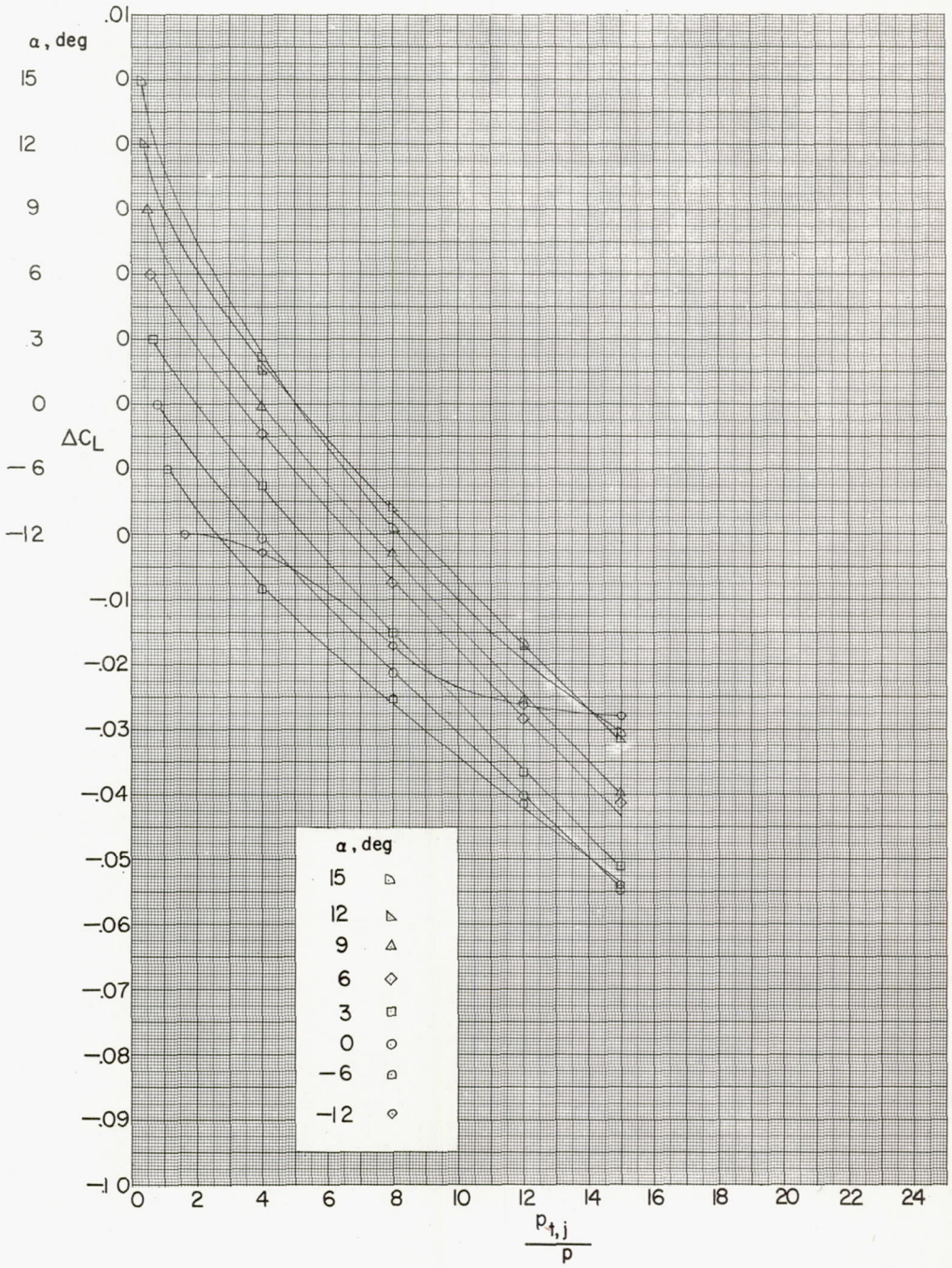

(i) Configuration 10; M = 1.61.

Figure 3.- Continued.

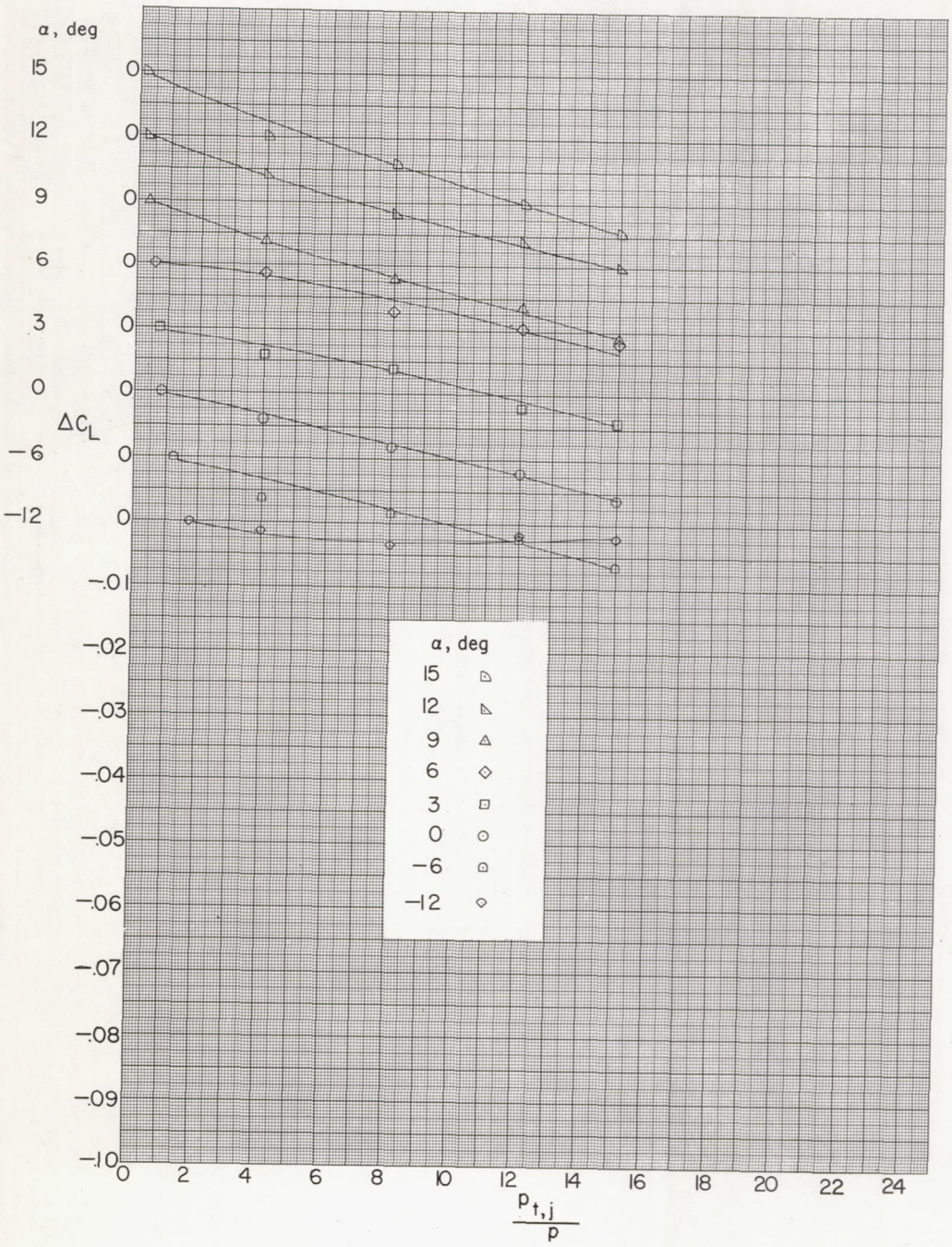

(j) Configuration 11; M = 1.61.

Figure 3.- Continued.

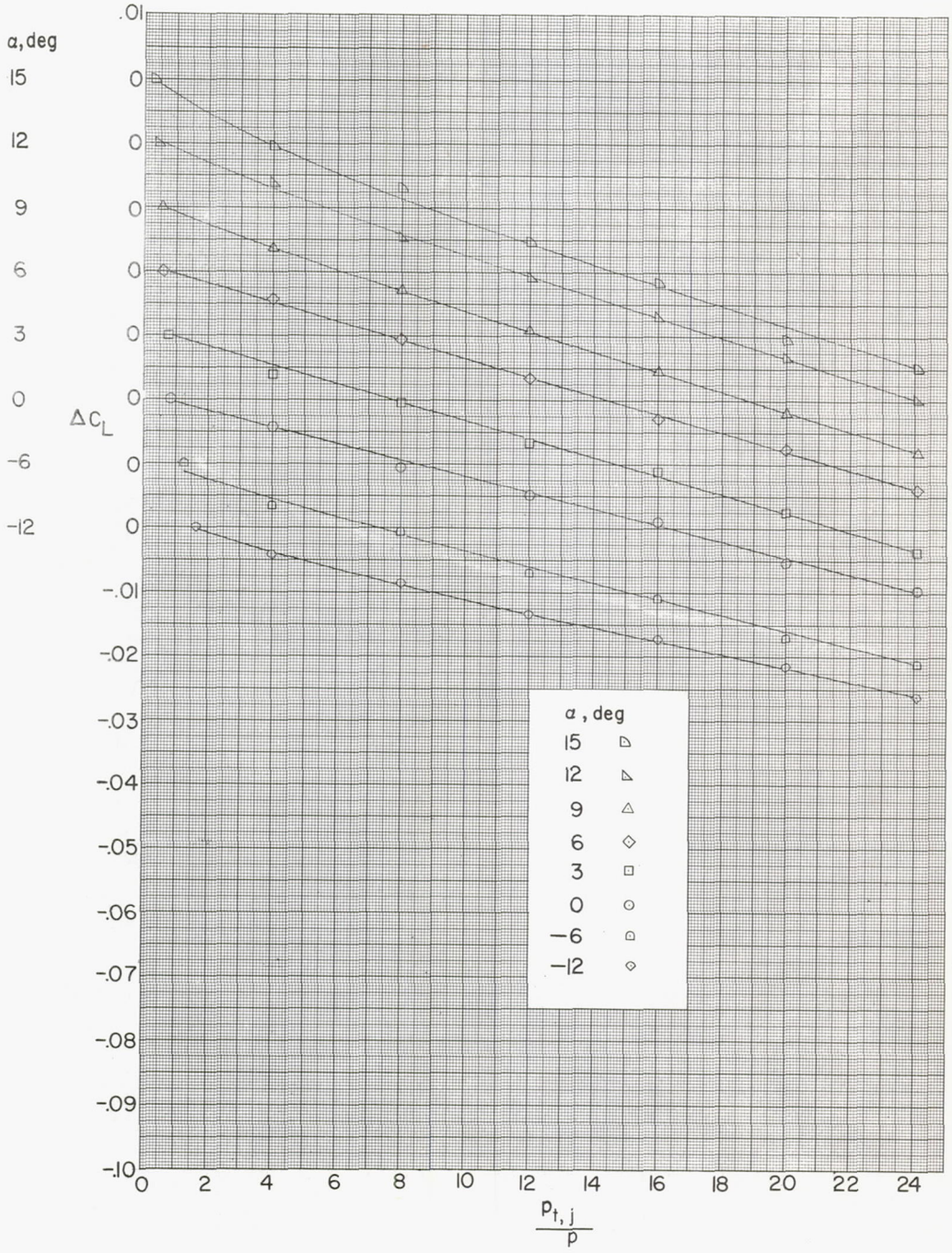

(k) Configuration 1; M = 2.01.

Figure 3.- Continued.

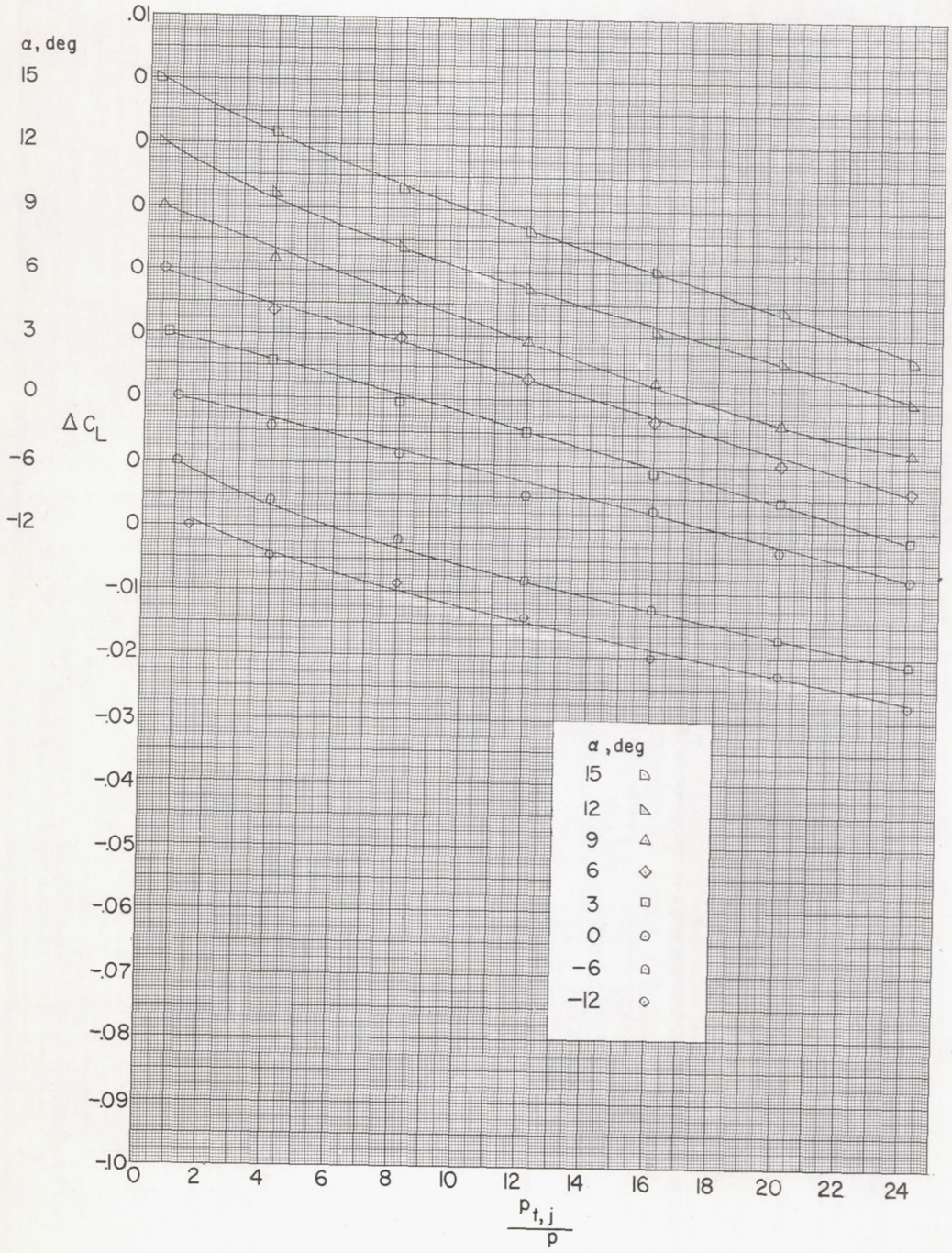

(l) Configuration 2; M = 2.01.

Figure 3.- Continued.

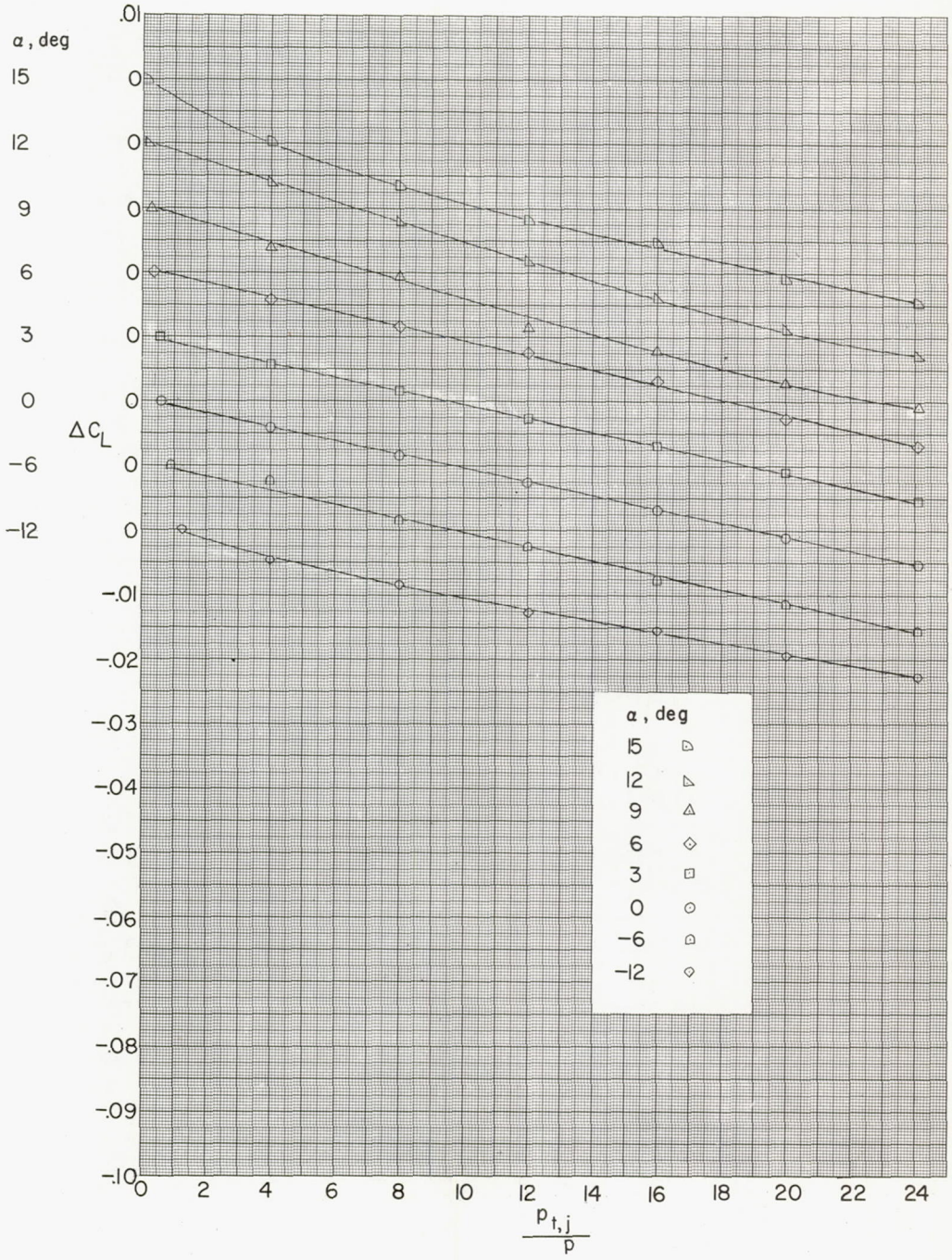

(m) Configuration 3; M = 2.01.

Figure 3.- Continued.

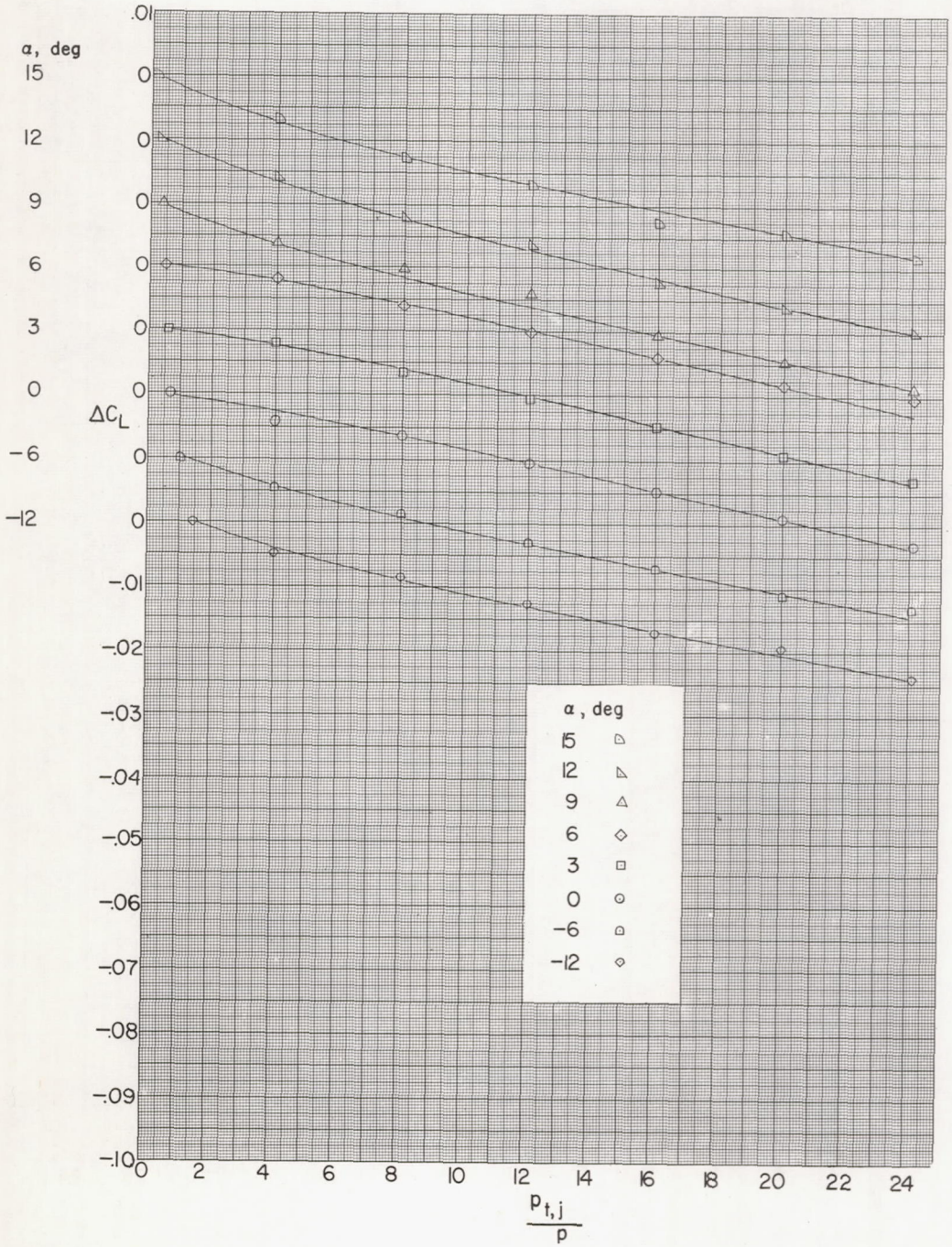

(n) Configuration 4; M = 2.01.

Figure 3.- Concluded.

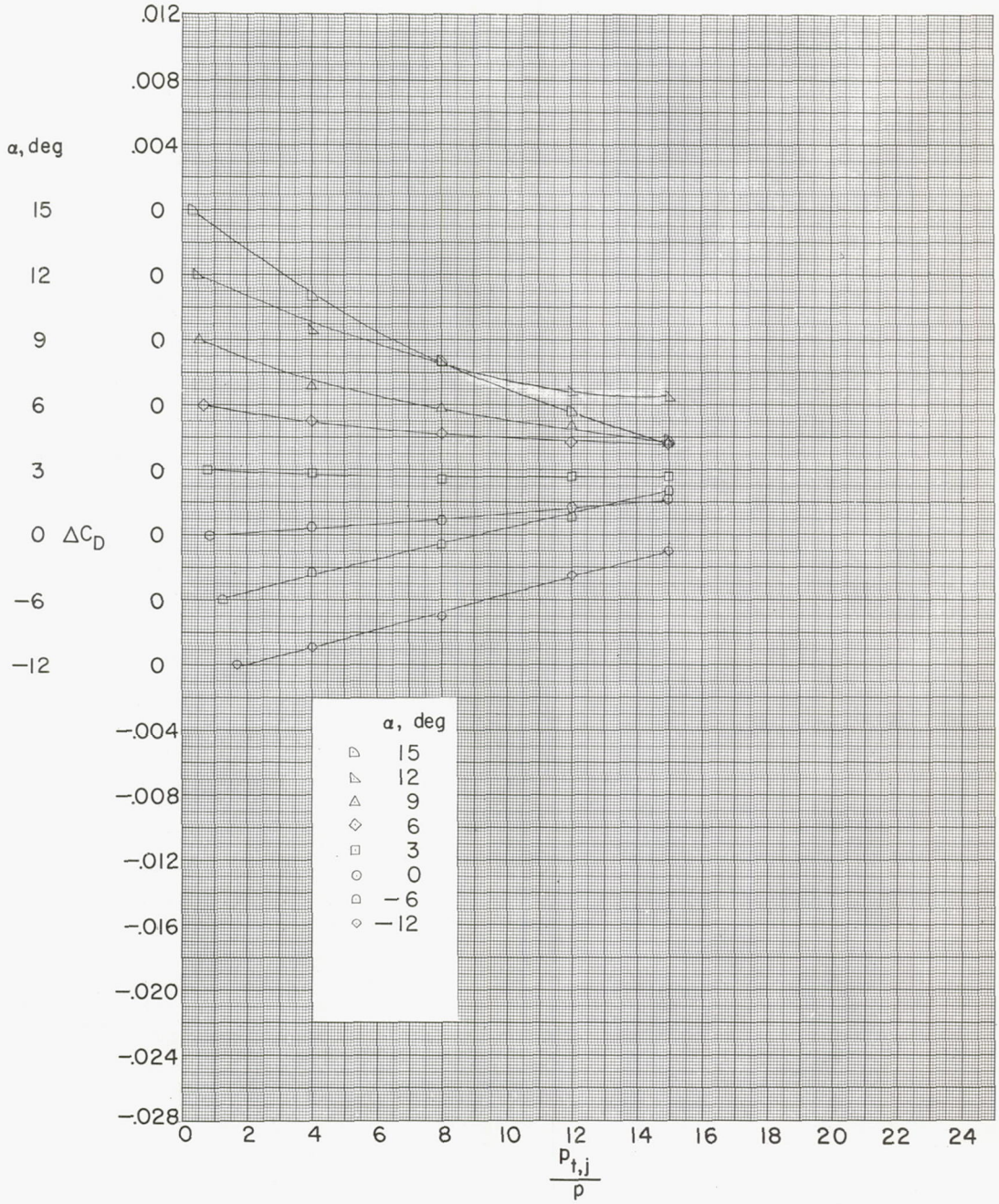

(a) Configuration 1; M = 1.61.

Figure 4.- Variation of incremental wing drag coefficient with jet pressure ratio.

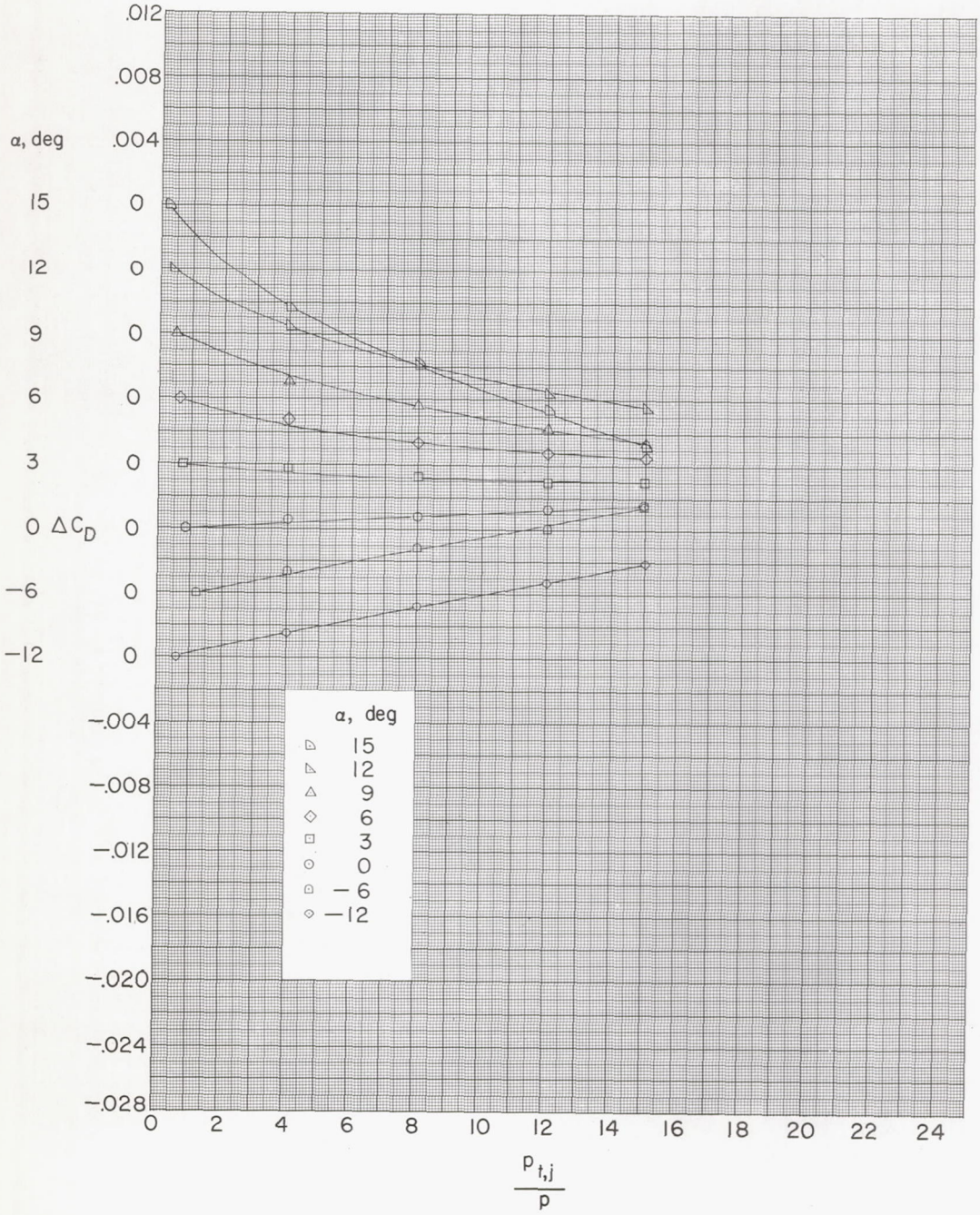

(b) Configuration 2; M = 1.61.

Figure 4.- Continued.

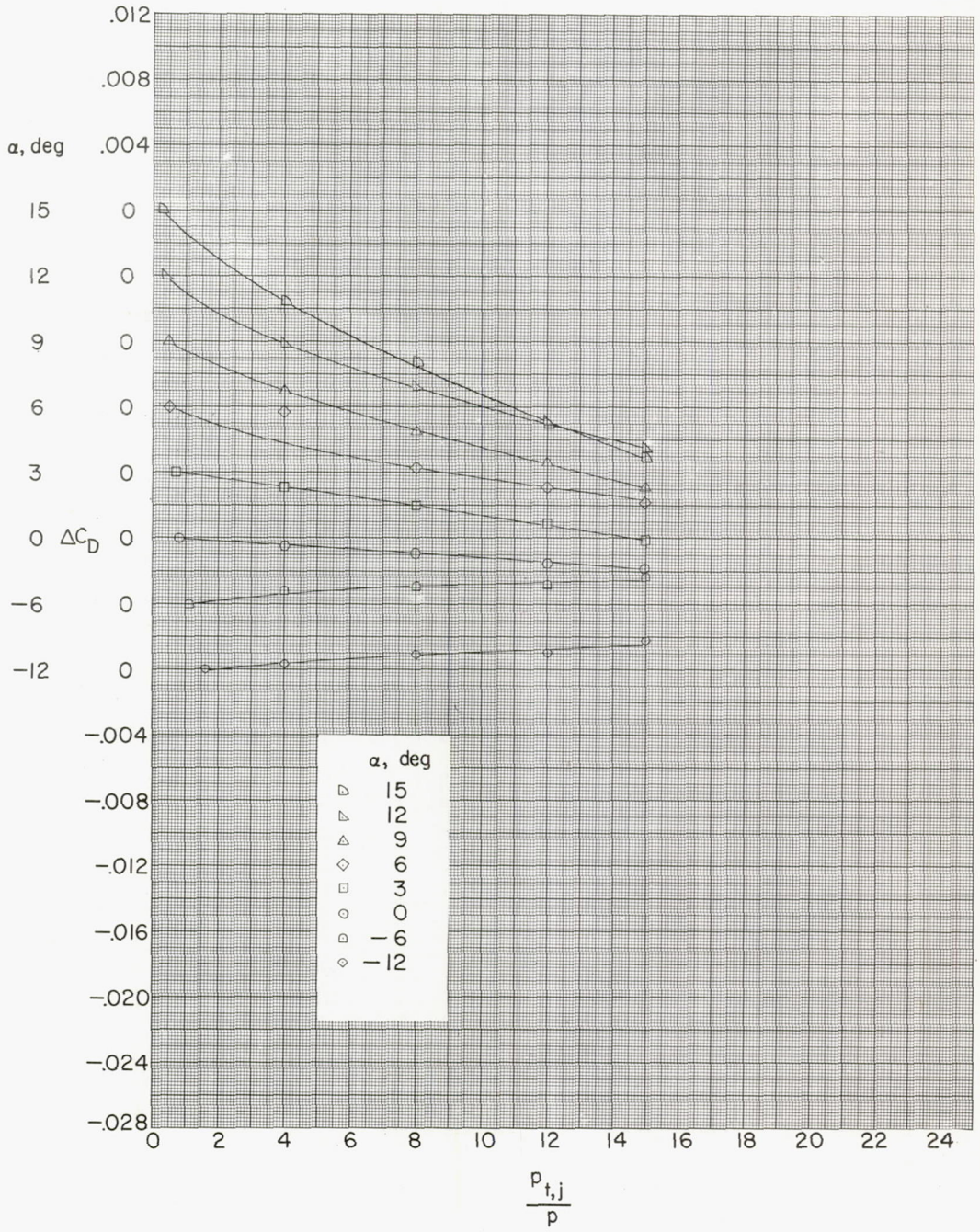

(c) Configuration 3; M = 1.61.

Figure 4.- Continued.

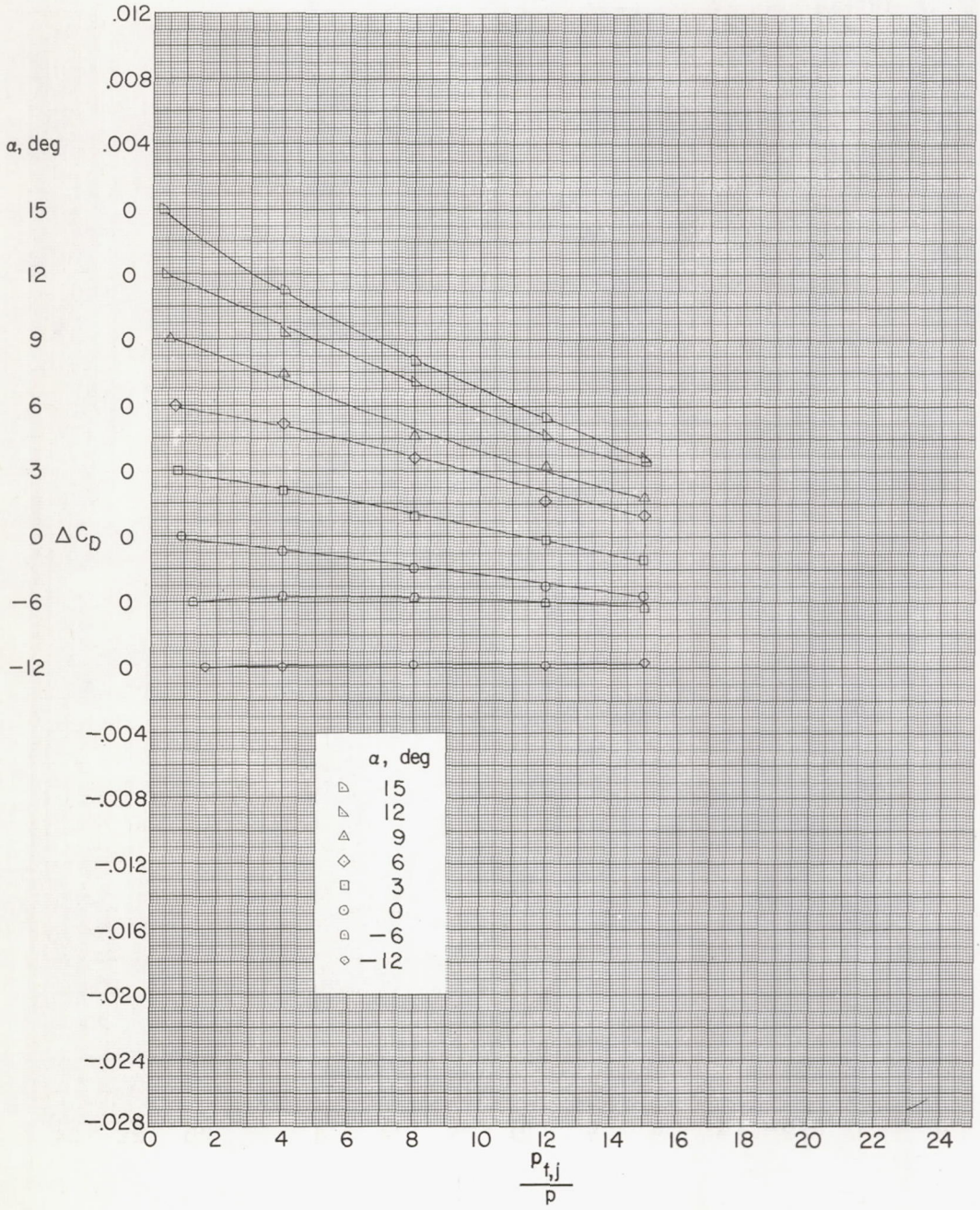

(d) Configuration 4; M = 1.61.

Figure 4.- Continued.

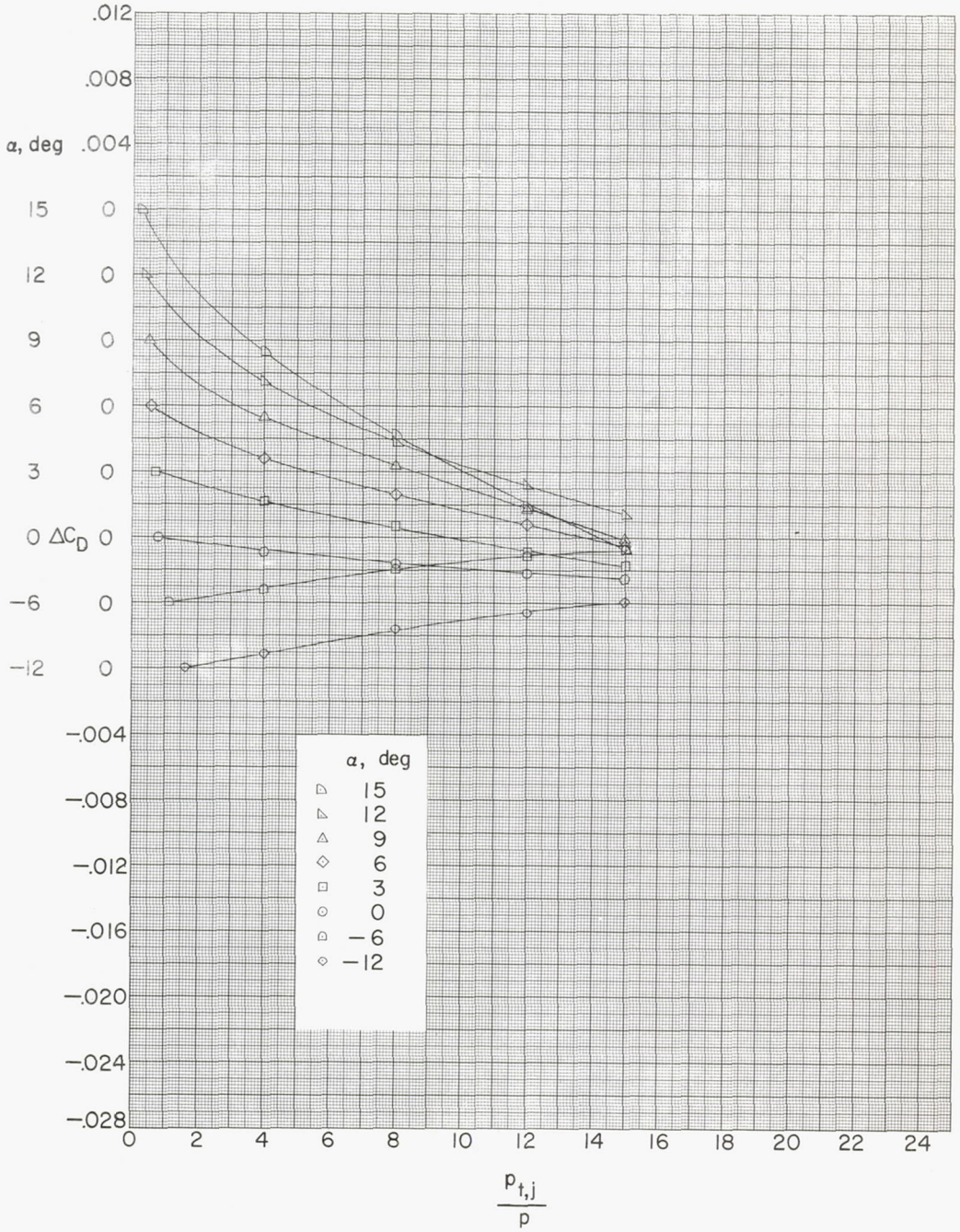

(e) Configuration 5; M = 1.61.

Figure 4.- Continued.

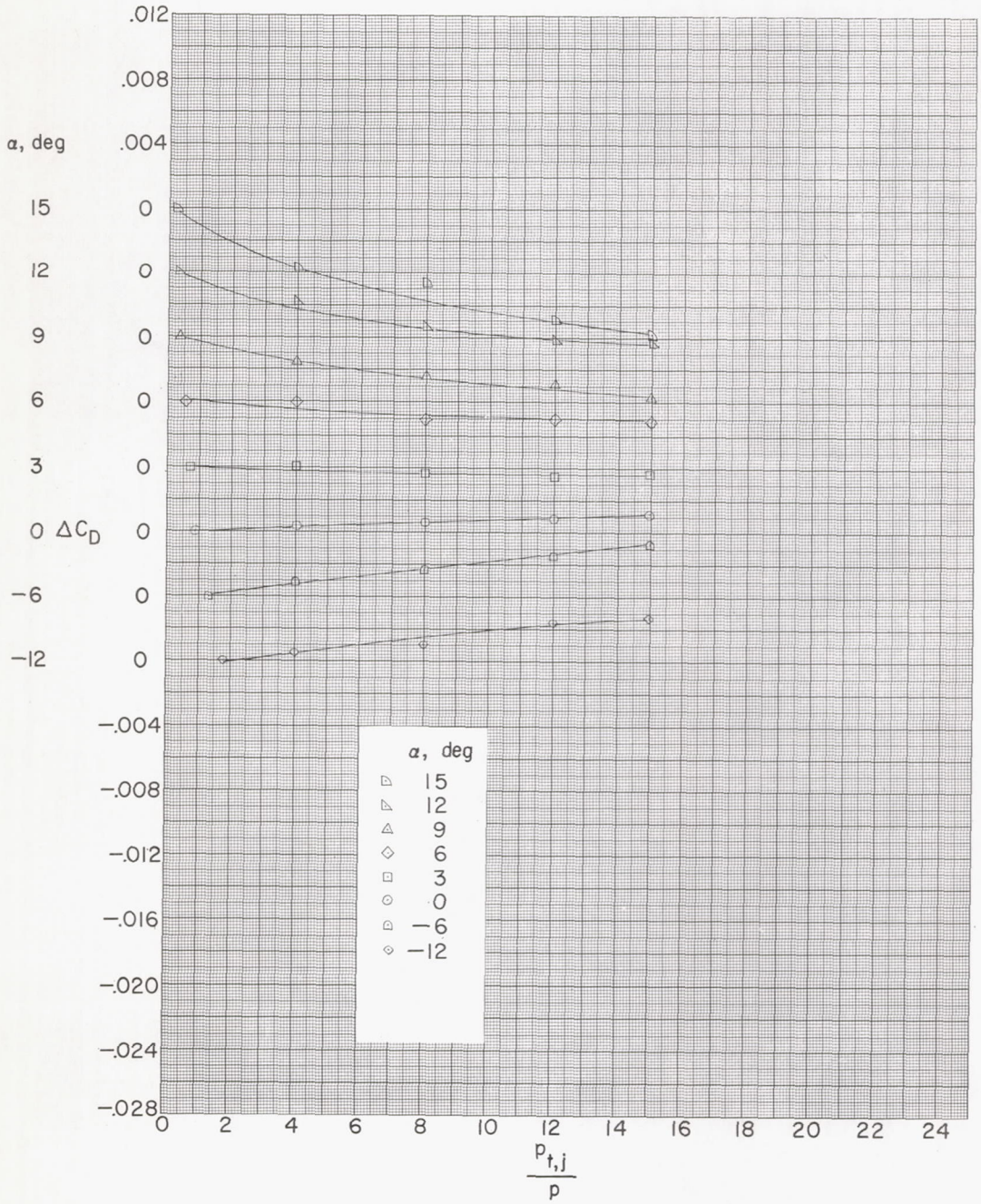

(f) Configuration 6; M = 1.61.

Figure 4.- Continued.

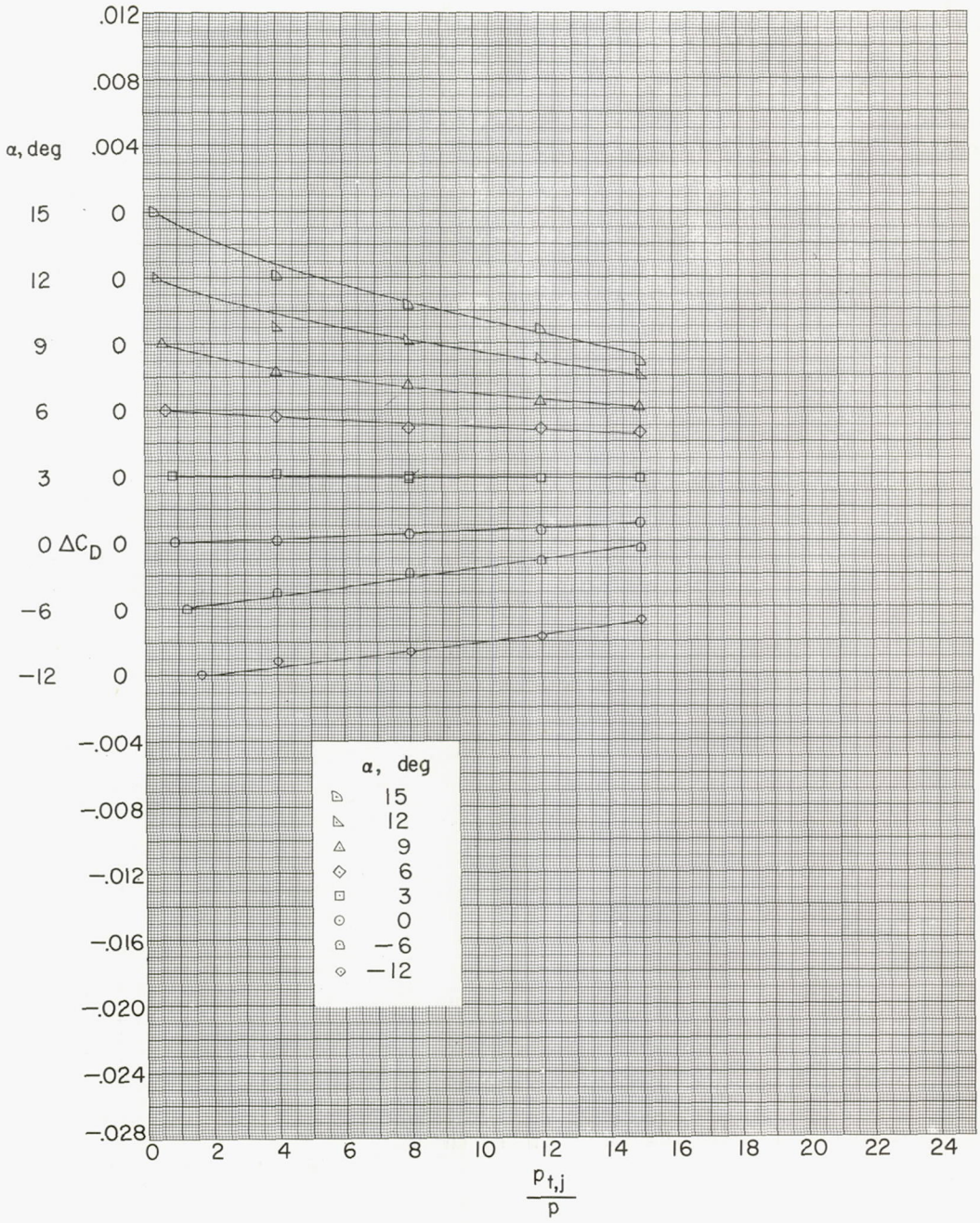

(g) Configuration 7; M = 1.61.

Figure 4.- Continued.

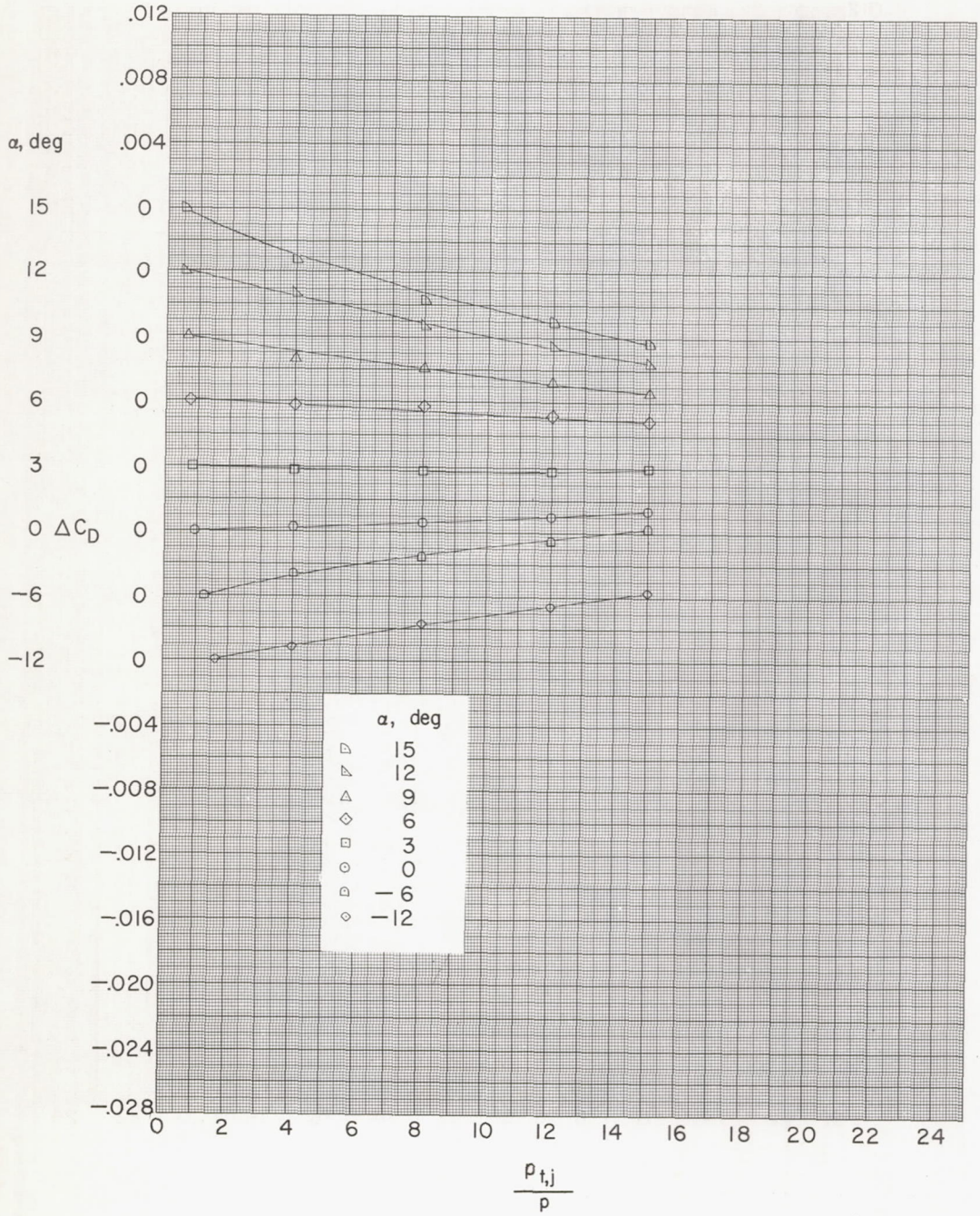

(h) Configuration 8; M = 1.61.

Figure 4.- Continued.

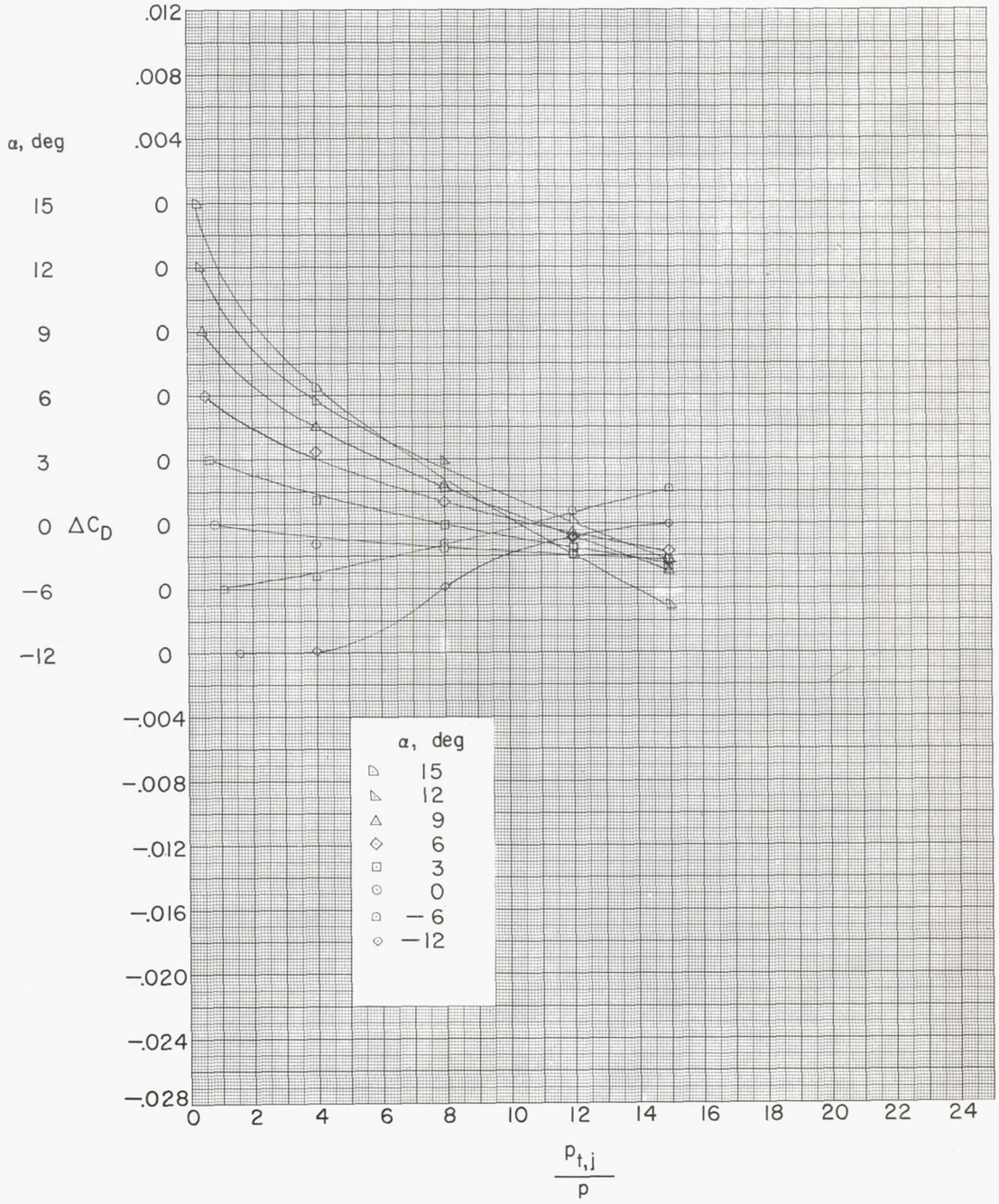

(i) Configuration 10; M = 1.61.

Figure 4.- Continued.

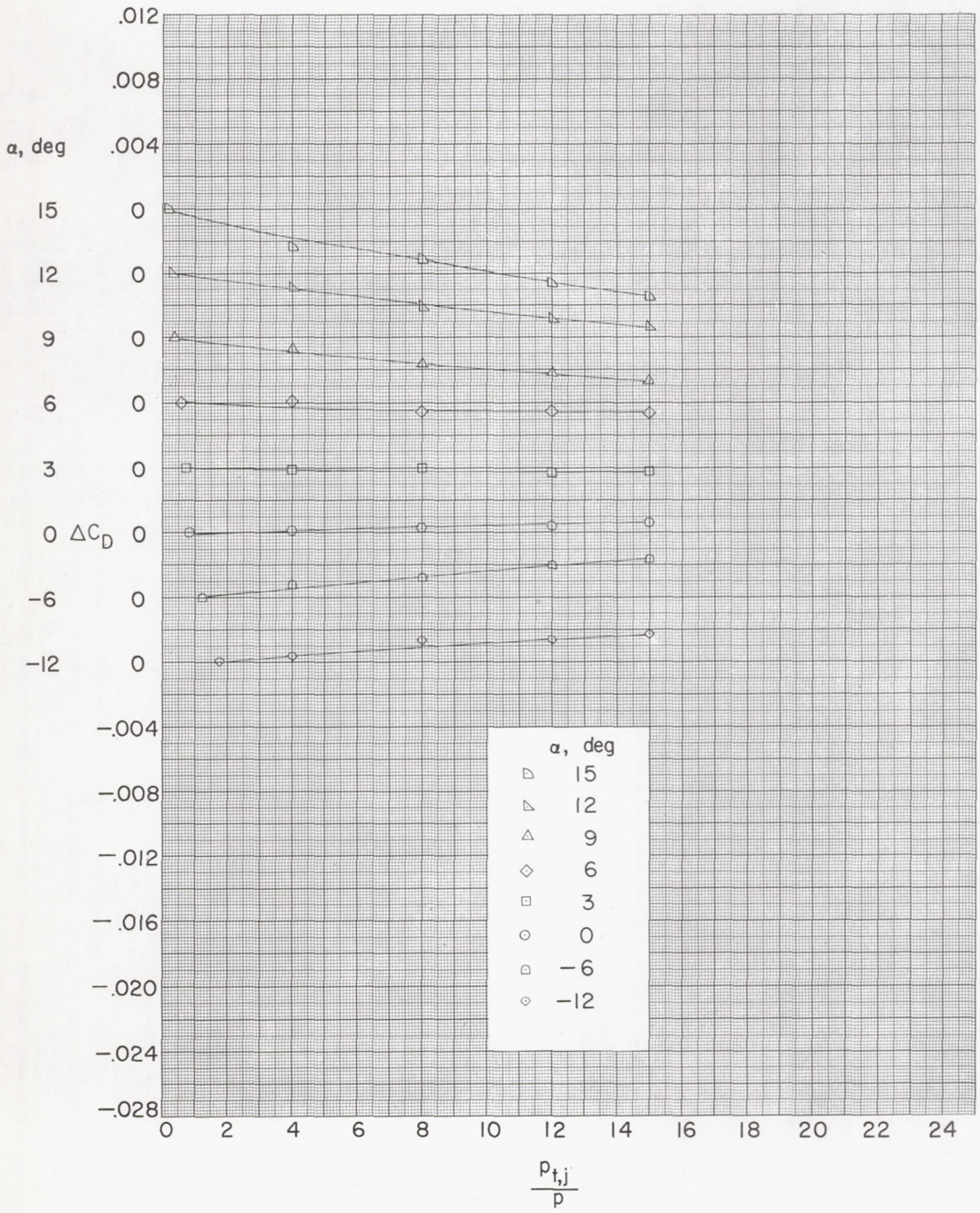

(j) Configuration 11; M = 1.61.

Figure 4.- Continued.

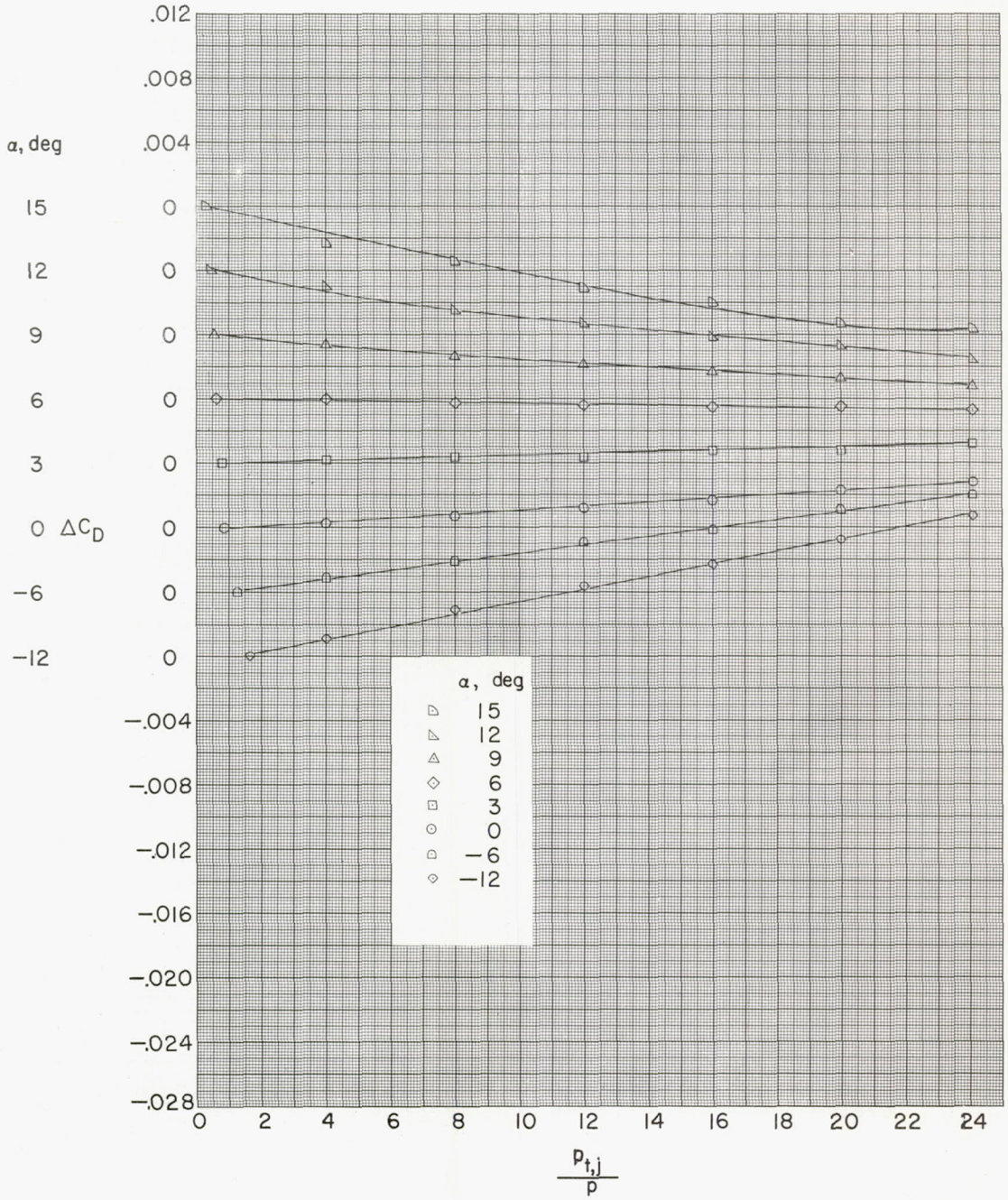

(k) Configuration 1; M = 2.01.

Figure 4.- Continued.

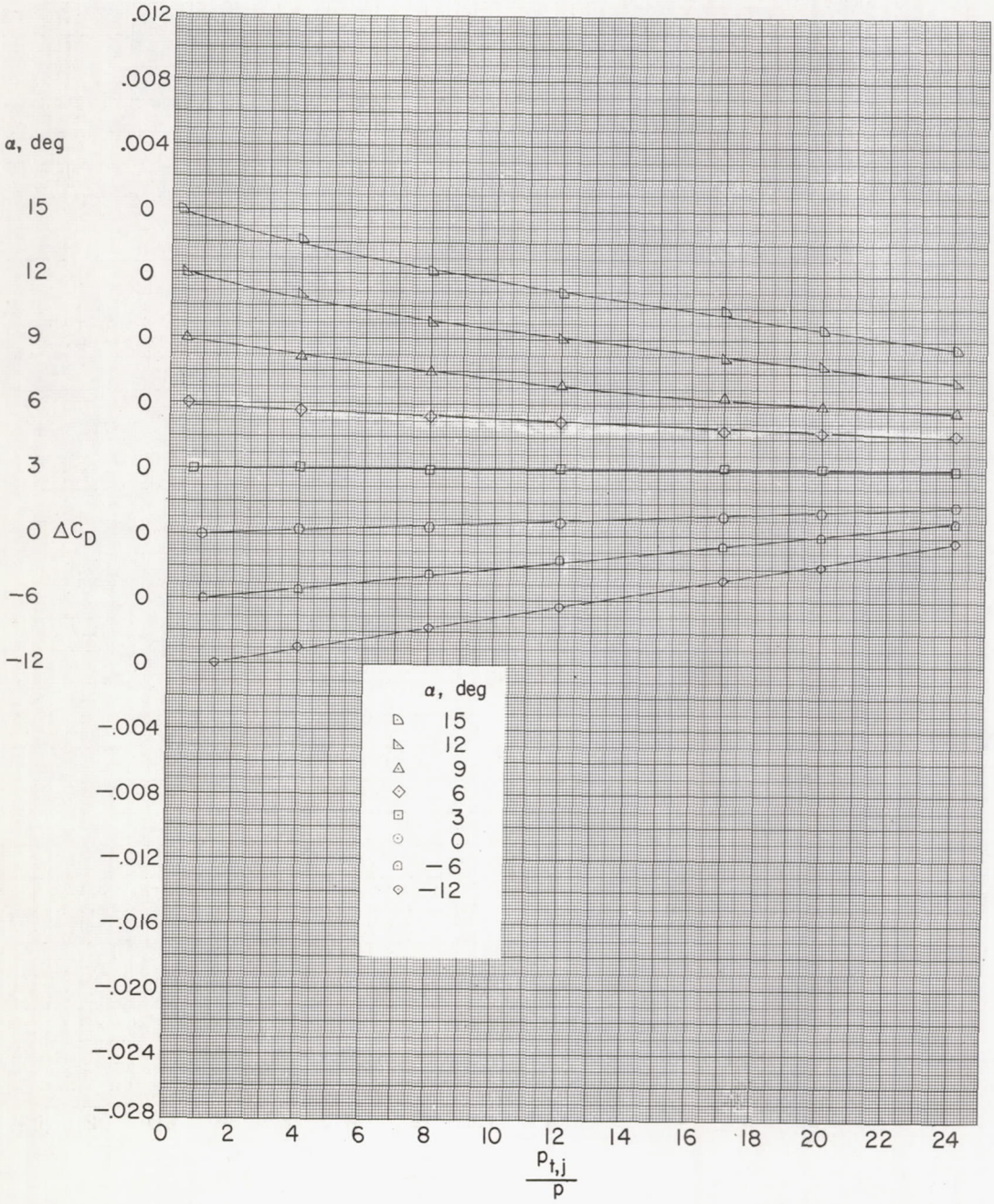

(l) Configuration 2; M = 2.01.

Figure 4.- Continued.

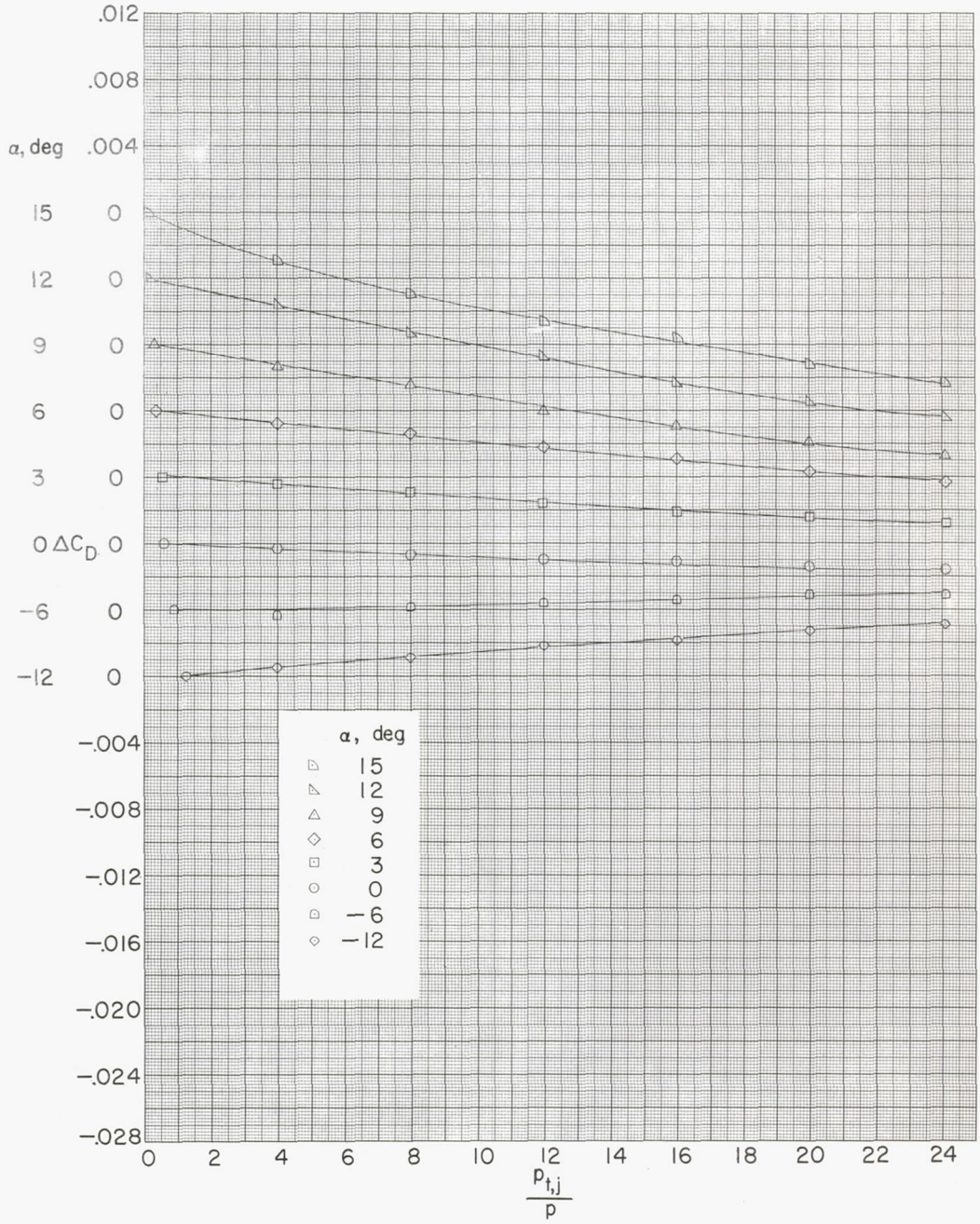

(m) Configuration 3; M = 2.01.

Figure 4.- Continued.

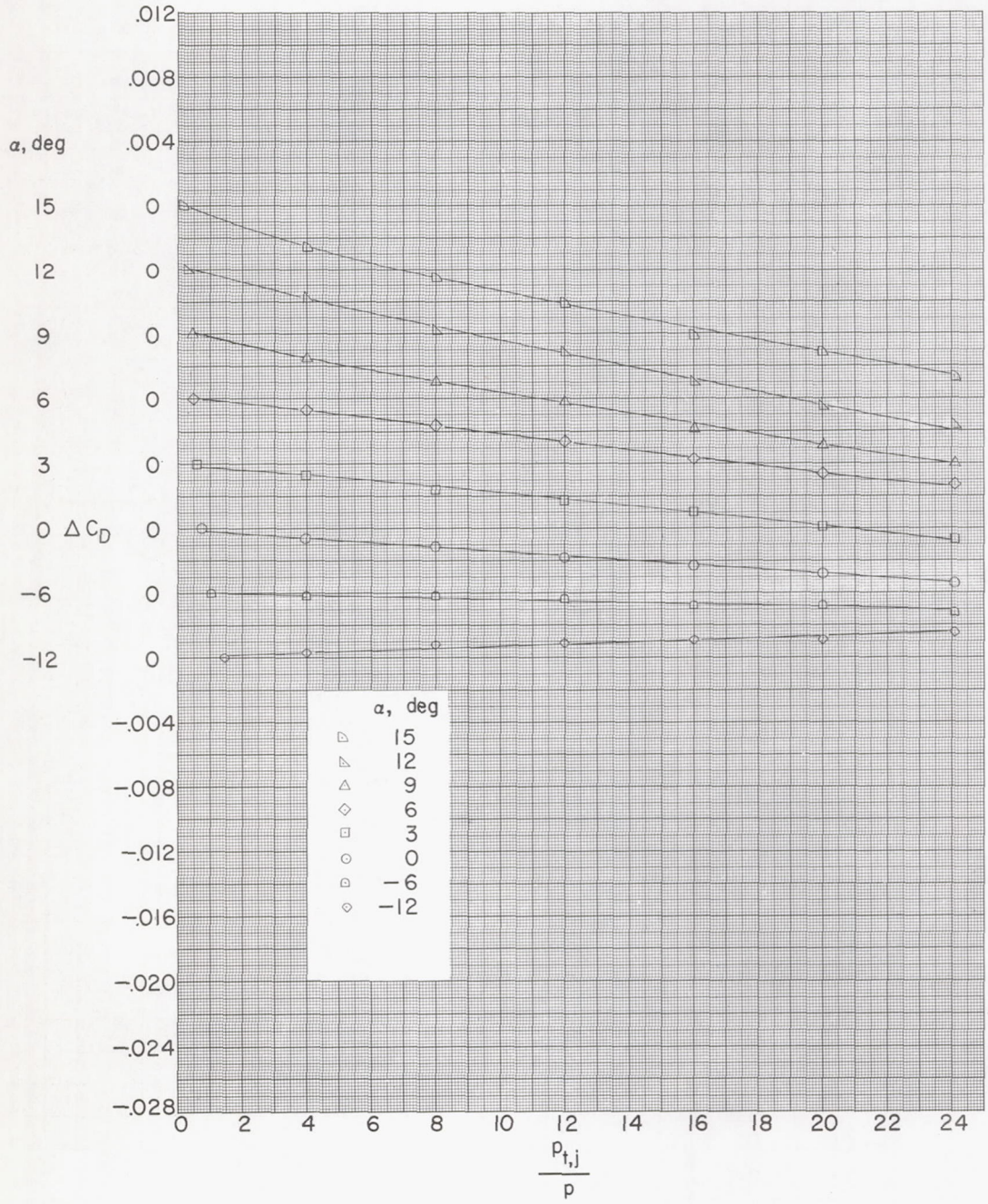

(n) Configuration 4; M = 2.01.

Figure 4.- Concluded.

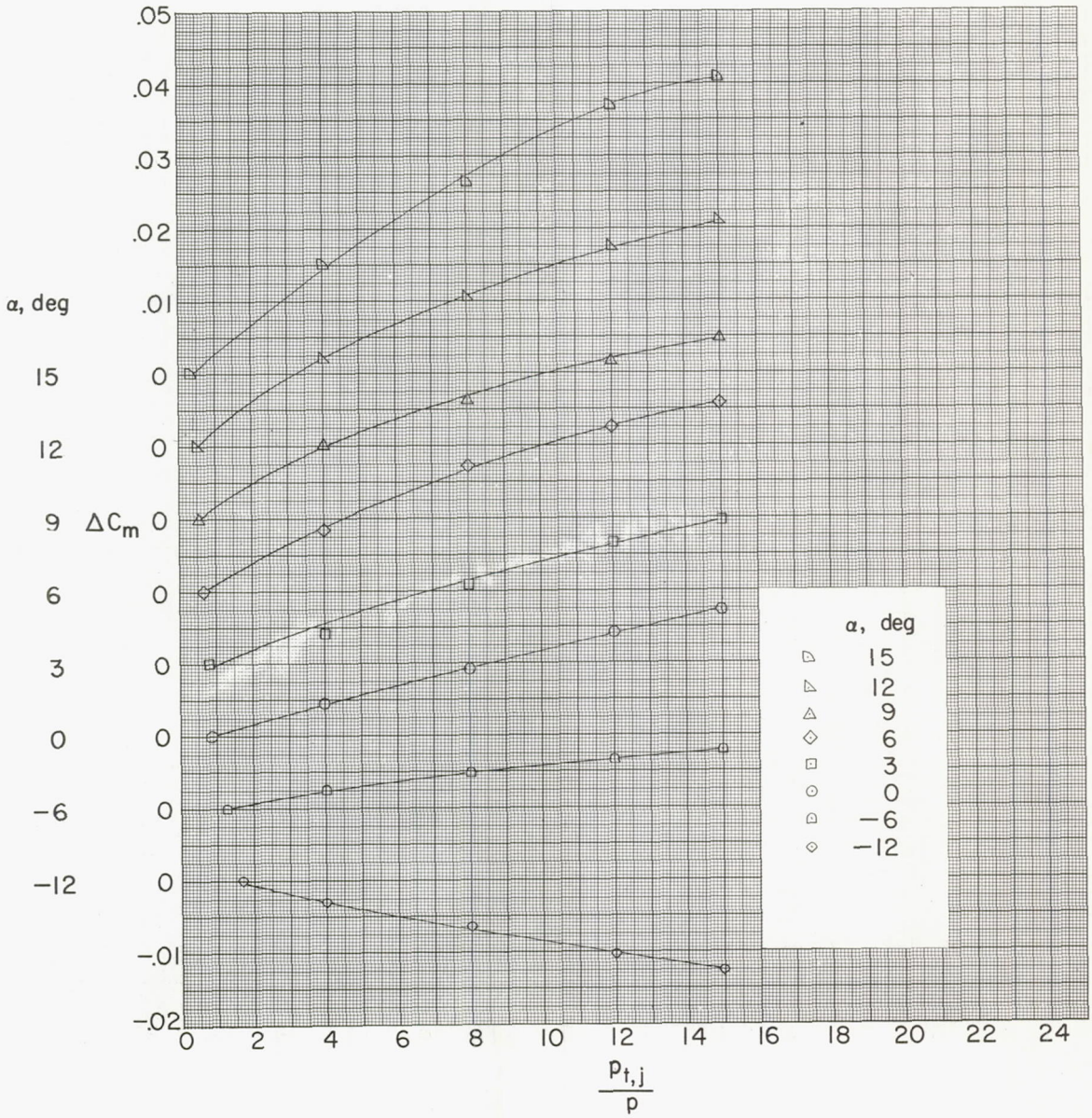

(a) Configuration 1; M = 1.61.

Figure 5.- Variation of incremental wing pitching-moment coefficient with jet pressure ratio.

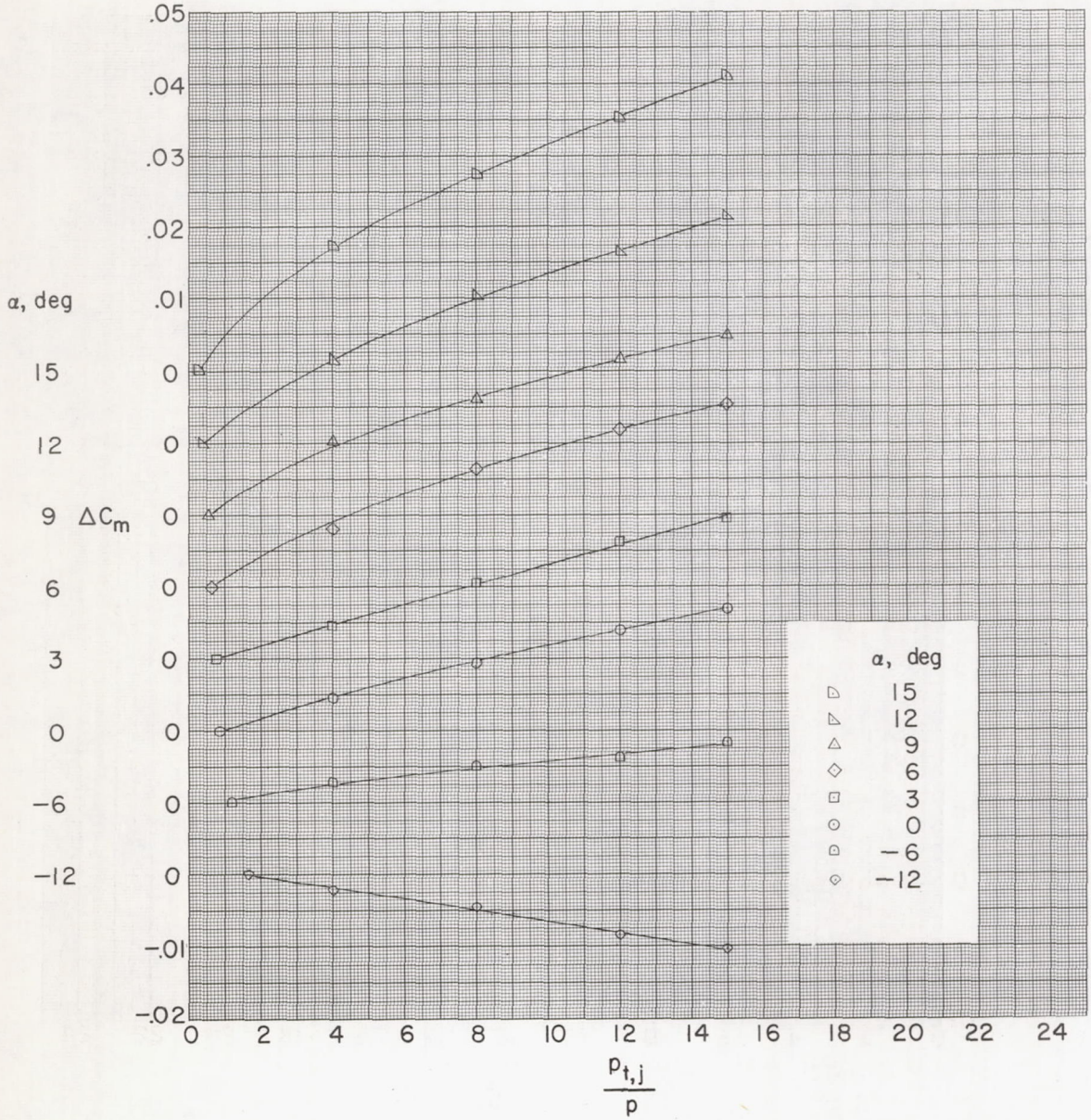

(b) Configuration 2; M = 1.61.

Figure 5.- Continued.

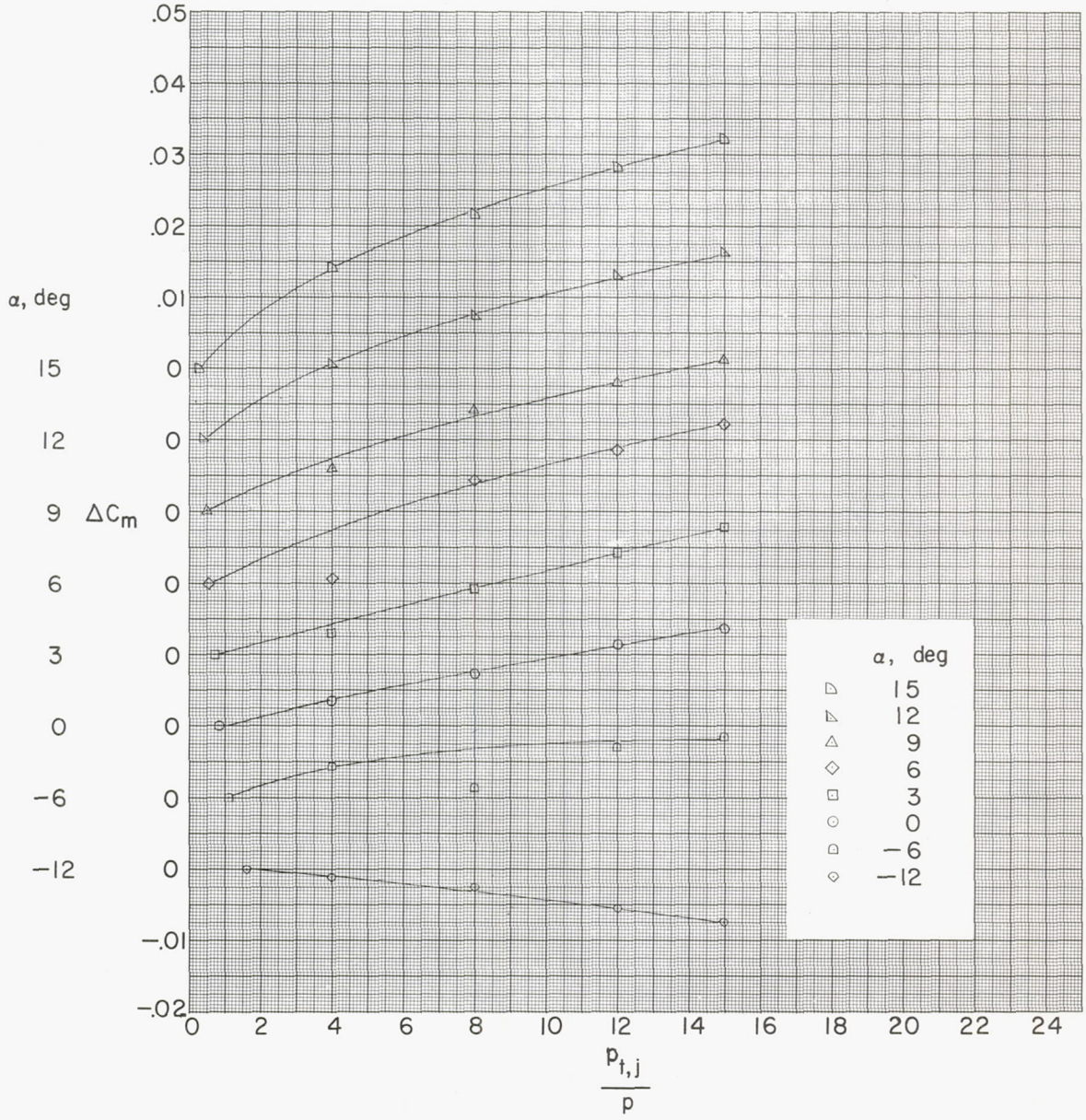

(c) Configuration 3; M = 1.61.

Figure 5.- Continued.

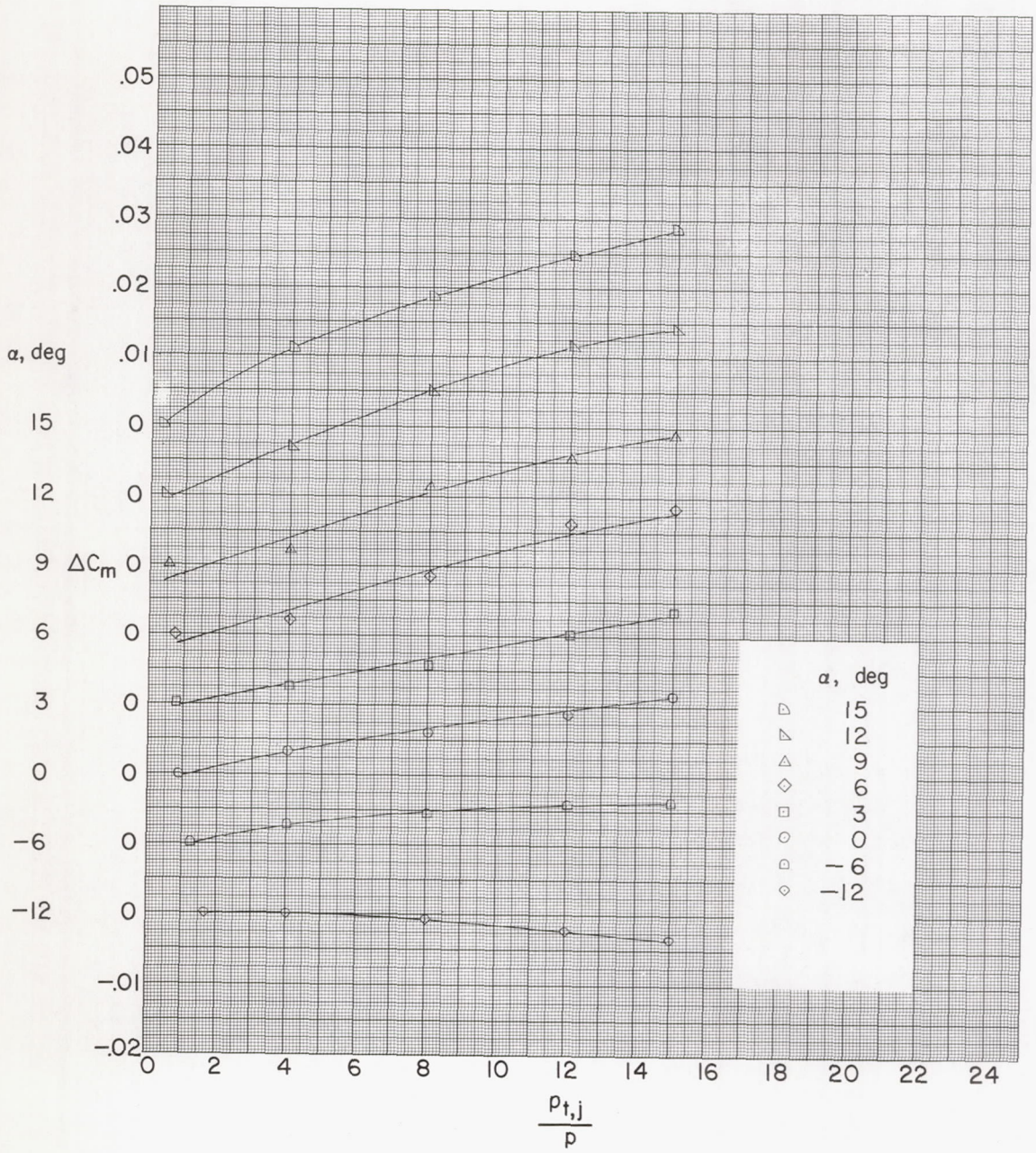

(d) Configuration 4; M = 1.61.

Figure 5.- Continued.

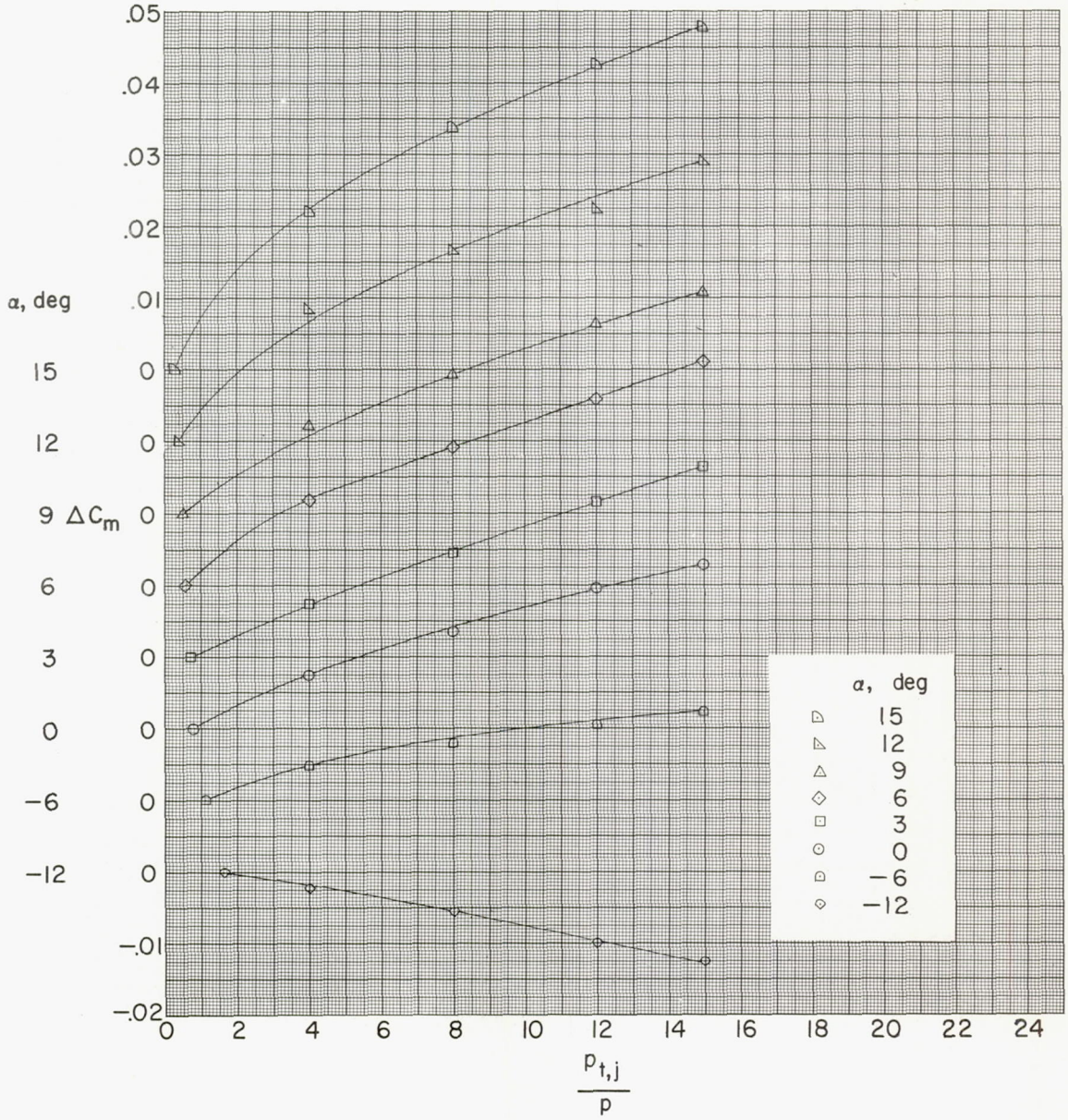

(e) Configuration 5; M = 1.61.

Figure 5.- Continued.

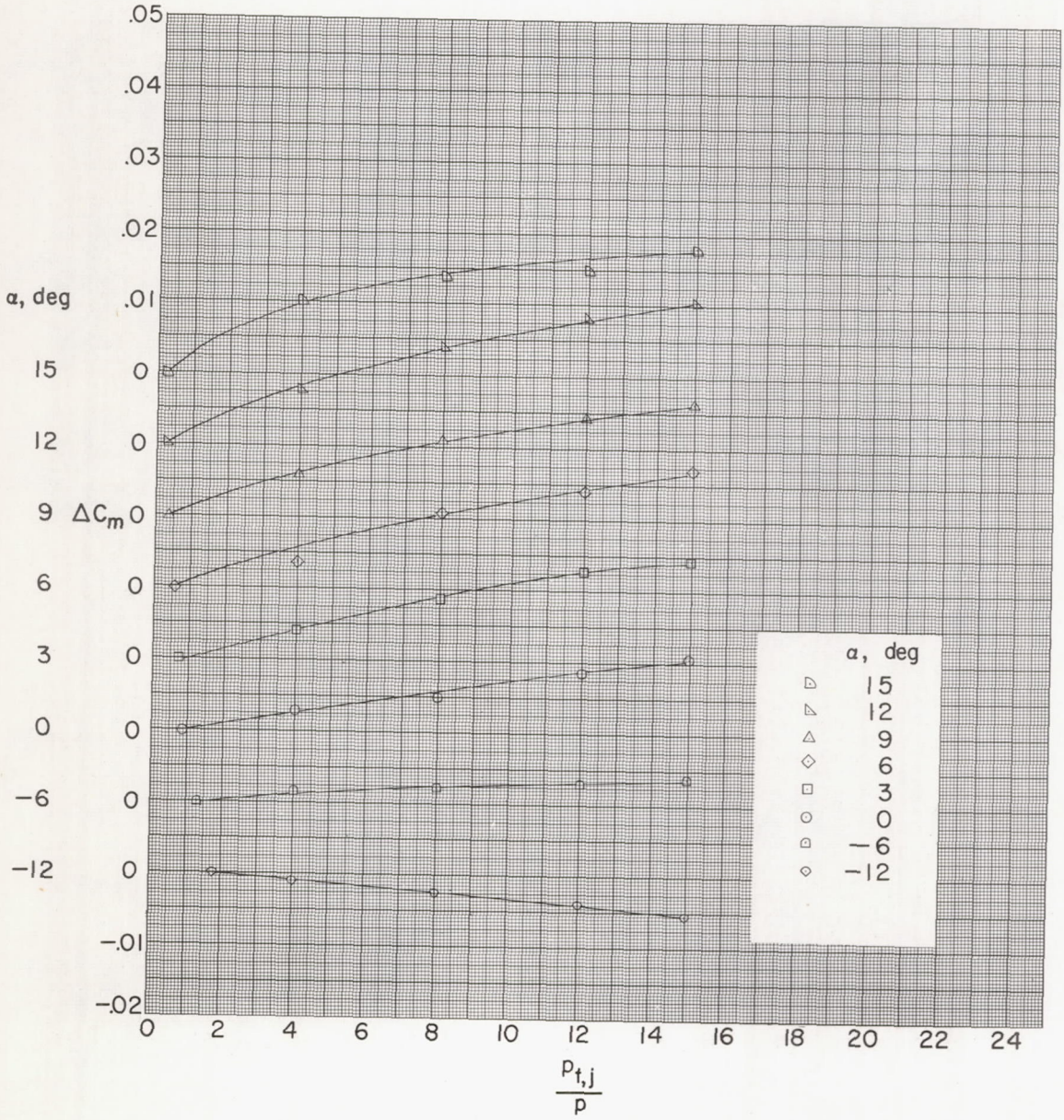

(f) Configuration 6; M = 1.61.

Figure 5.- Continued.

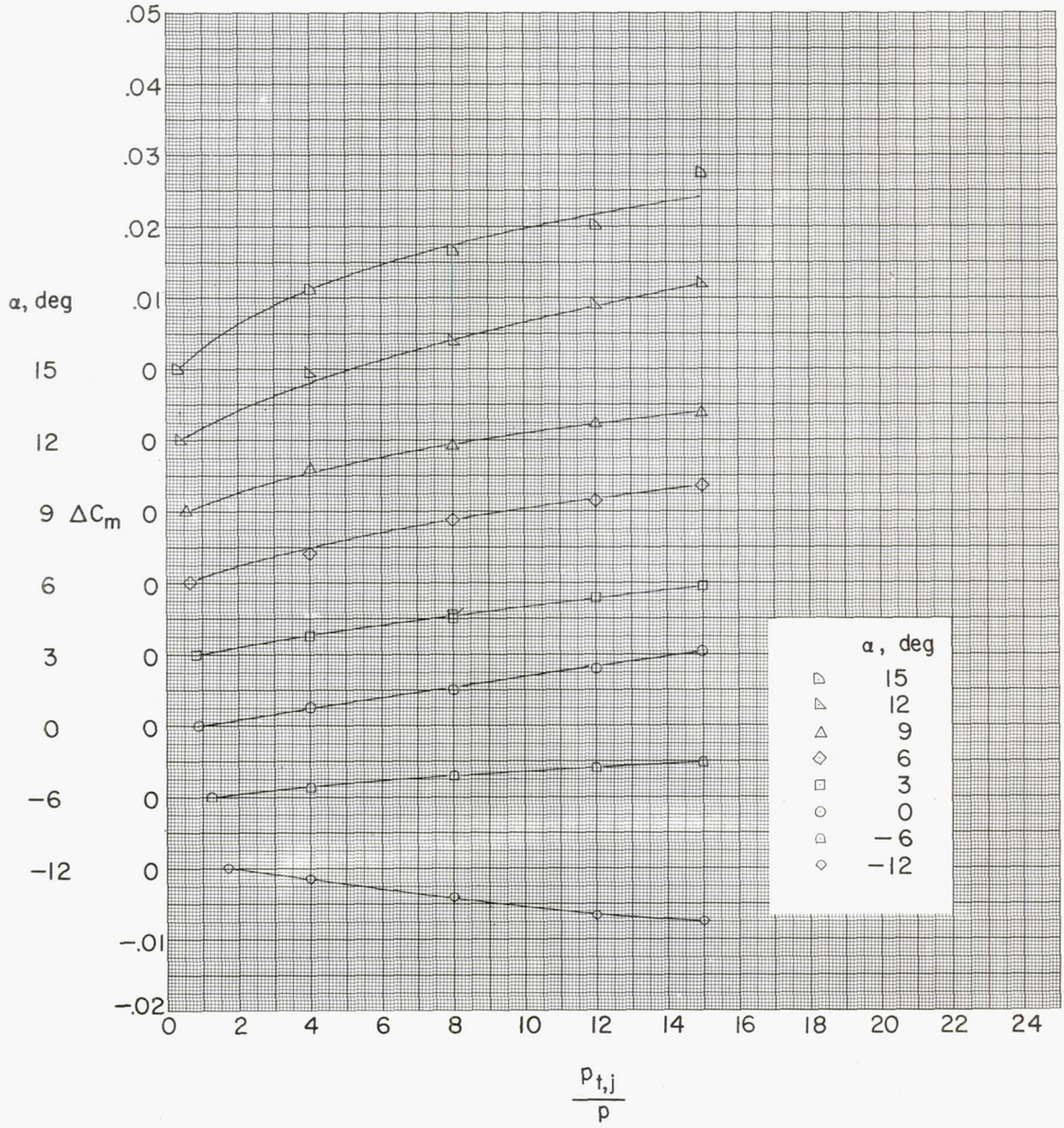

(g) Configuration 7; M = 1.61.

Figure 5.- Continued.

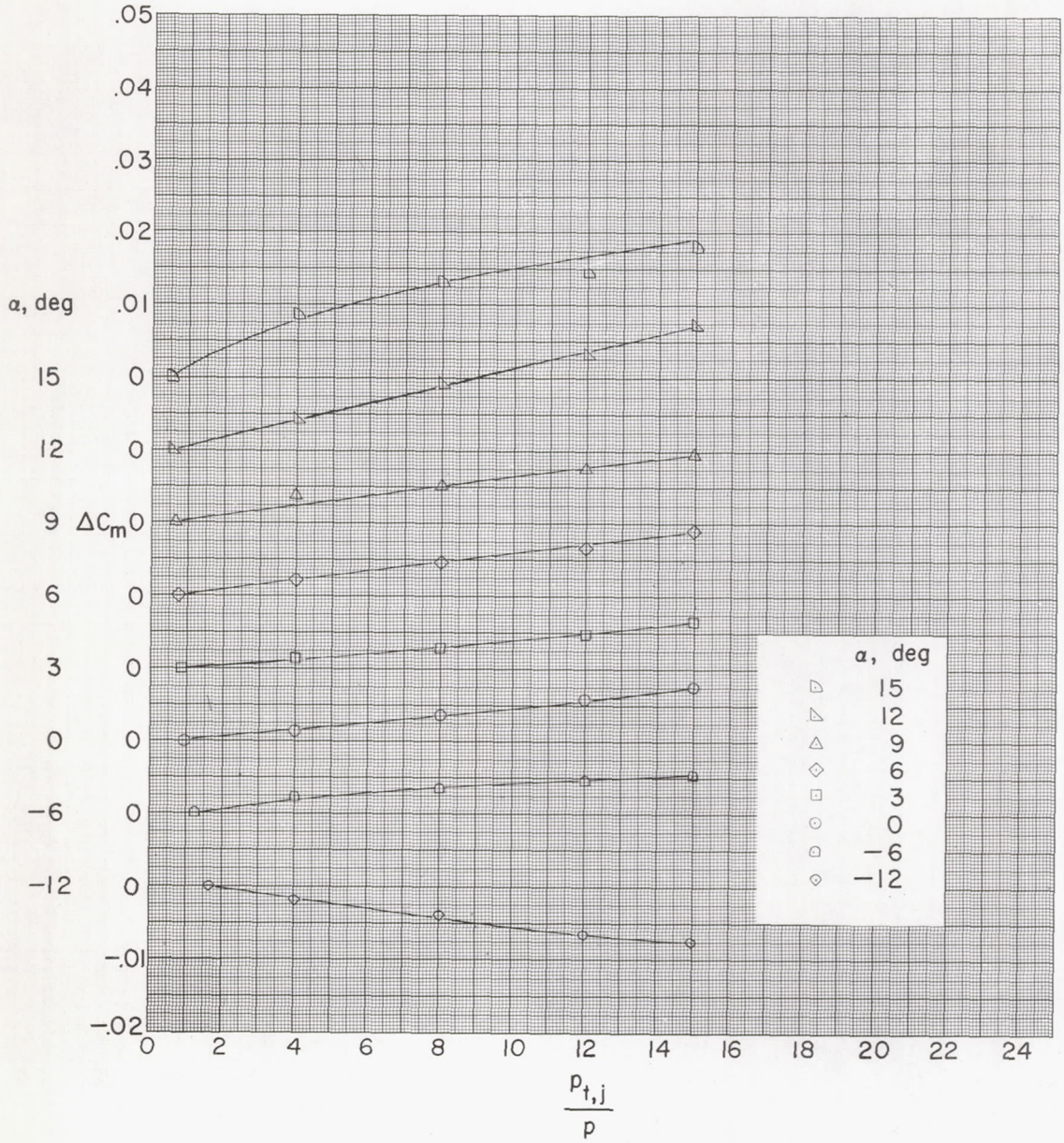

(h) Configuration 8; M = 1.61.

Figure 5.- Continued.

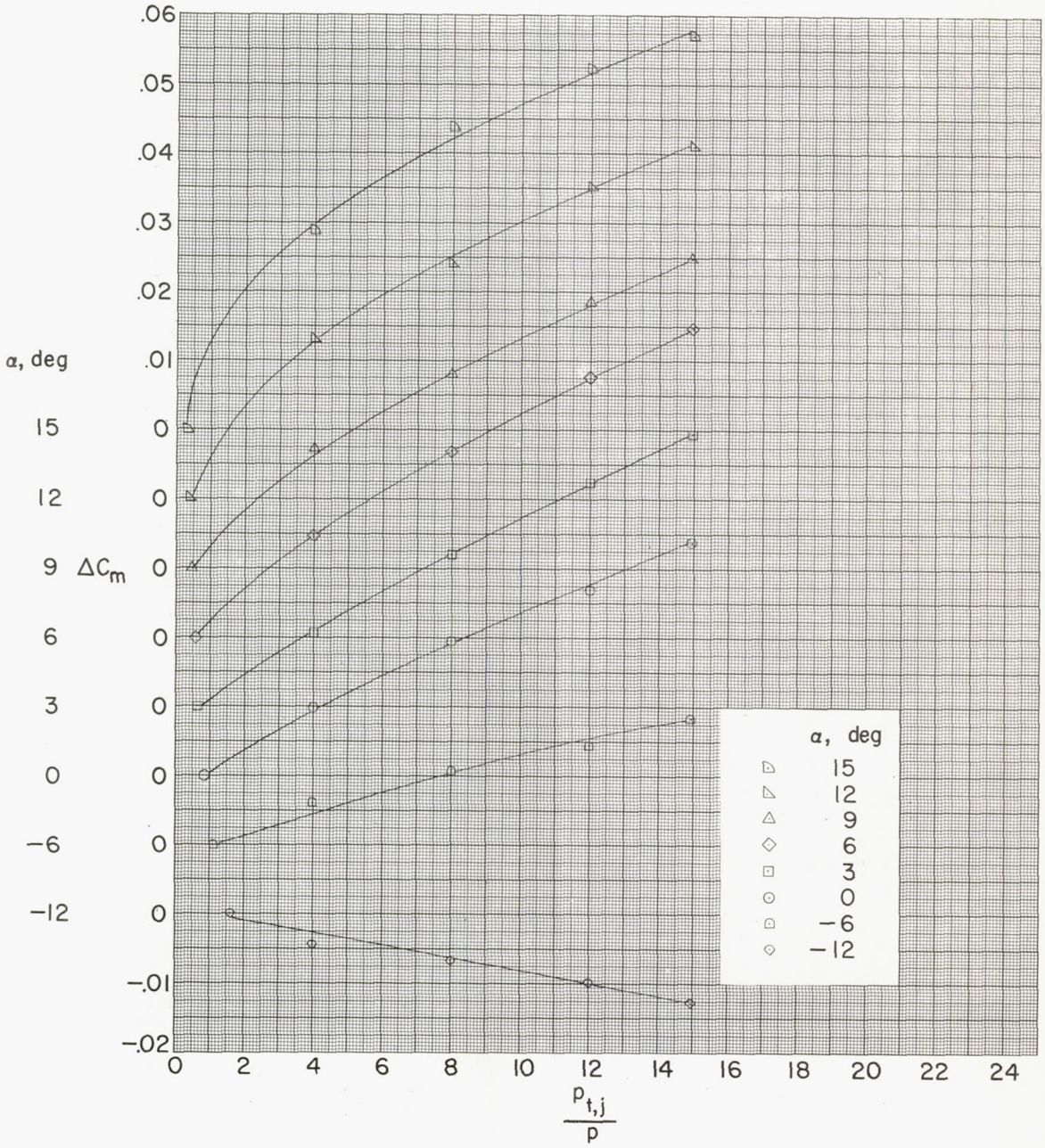

(i) Configuration 10; M = 1.61.

Figure 5.- Continued.

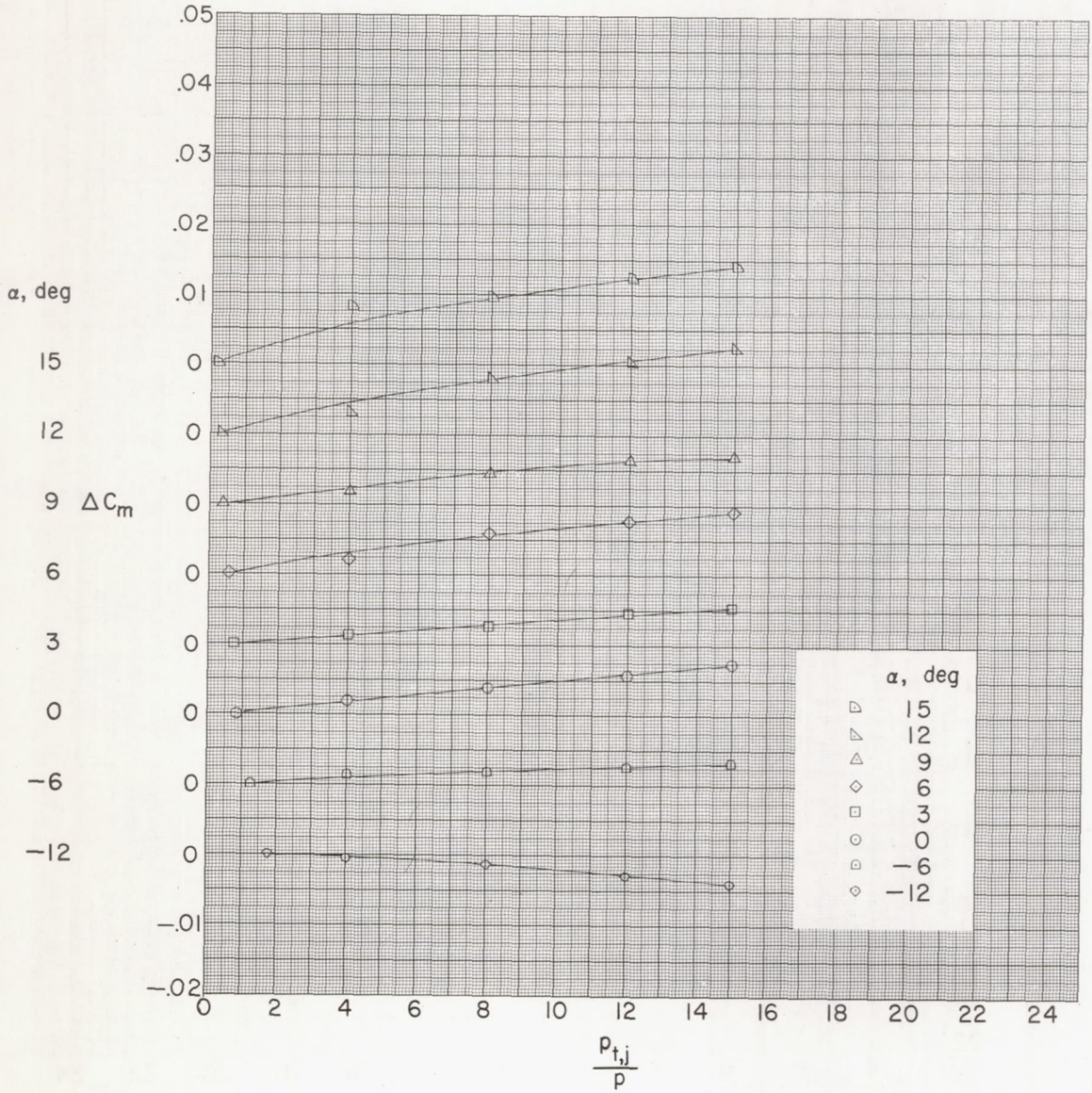

(j) Configuration 11; M = 1.61.

Figure 5.- Continued.

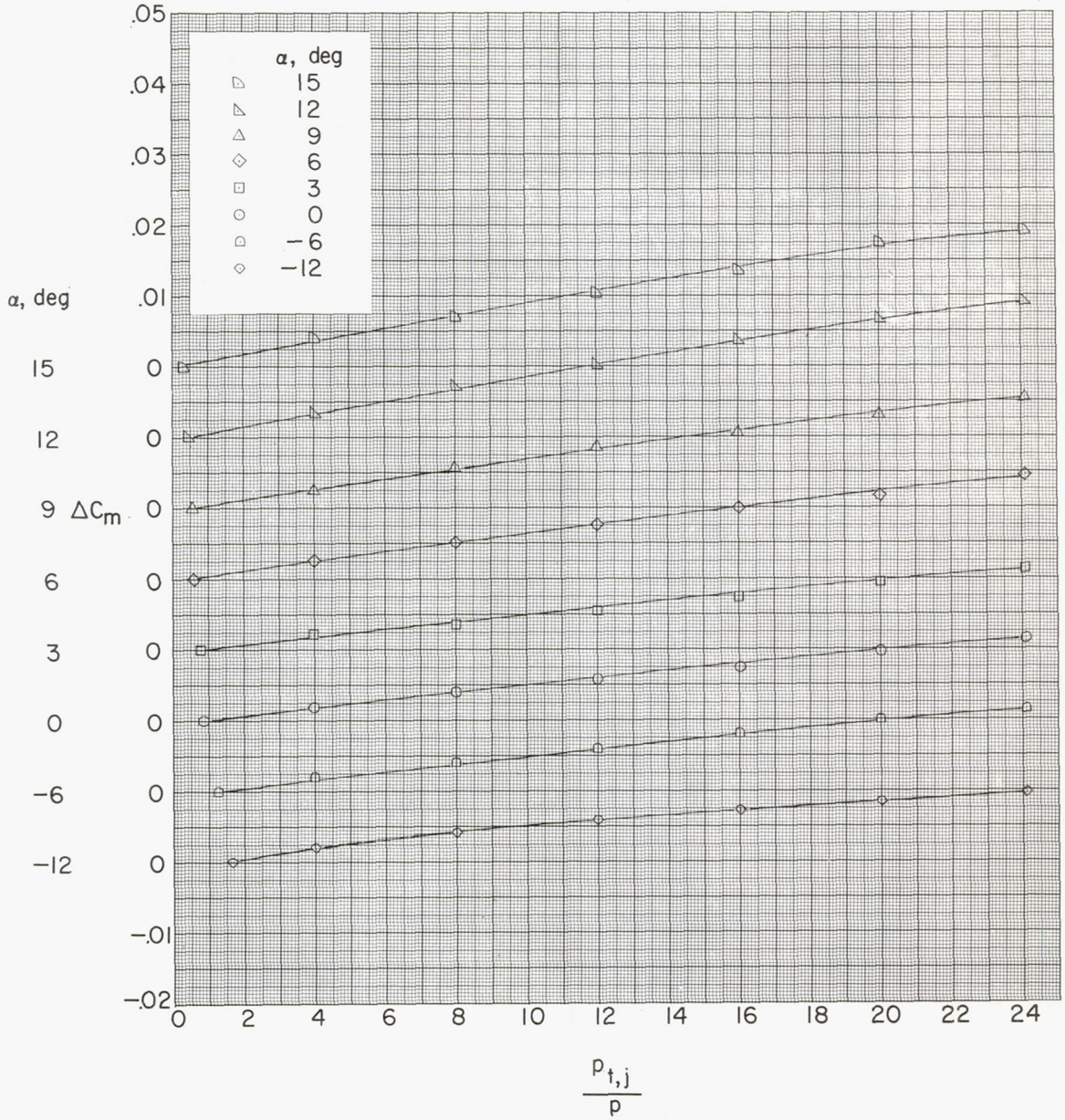

(k) Configuration 1; M = 2.01.

Figure 5.- Continued.

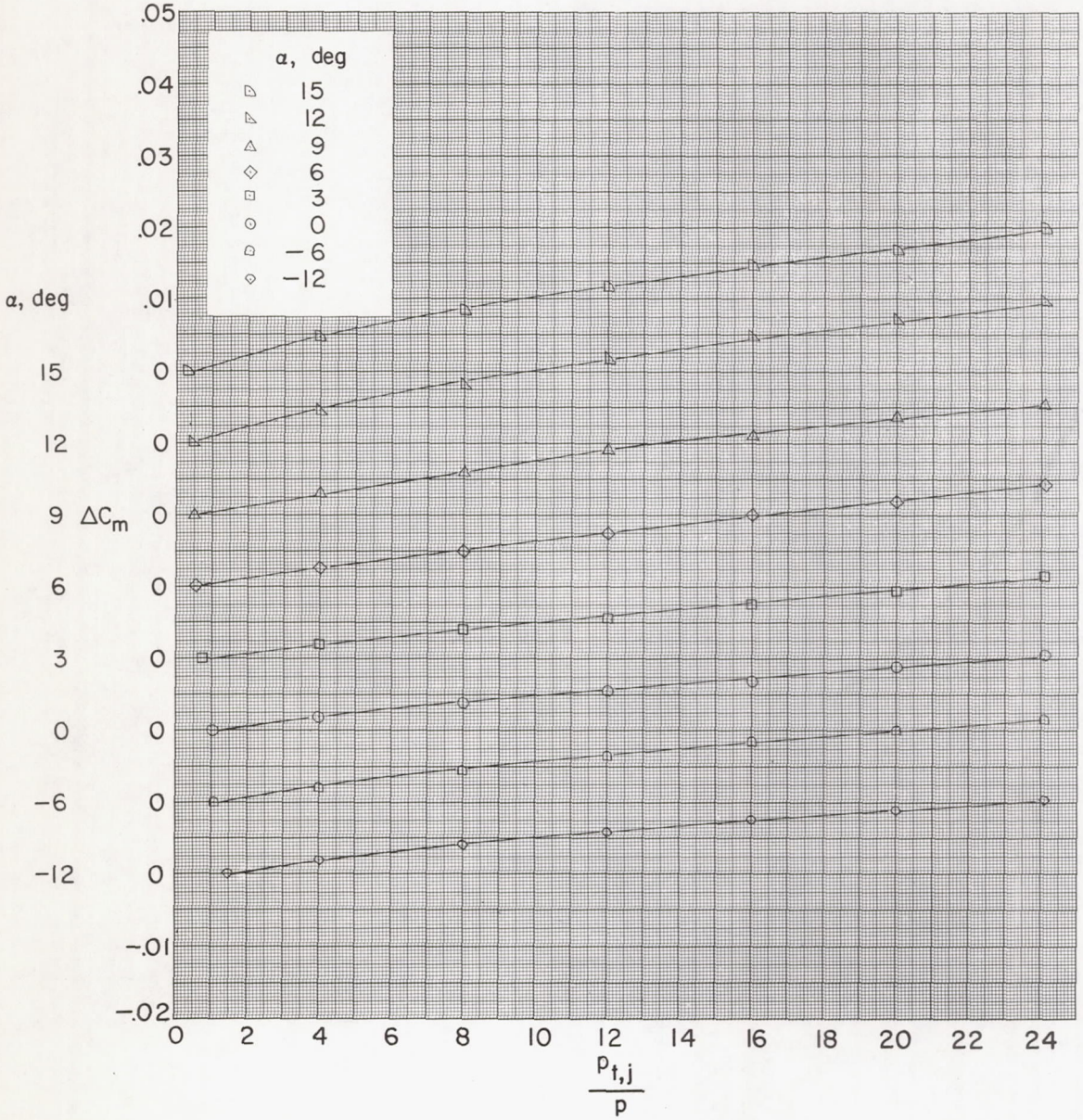

(l) Configuration 2; M = 2.01.

Figure 5.- Continued.

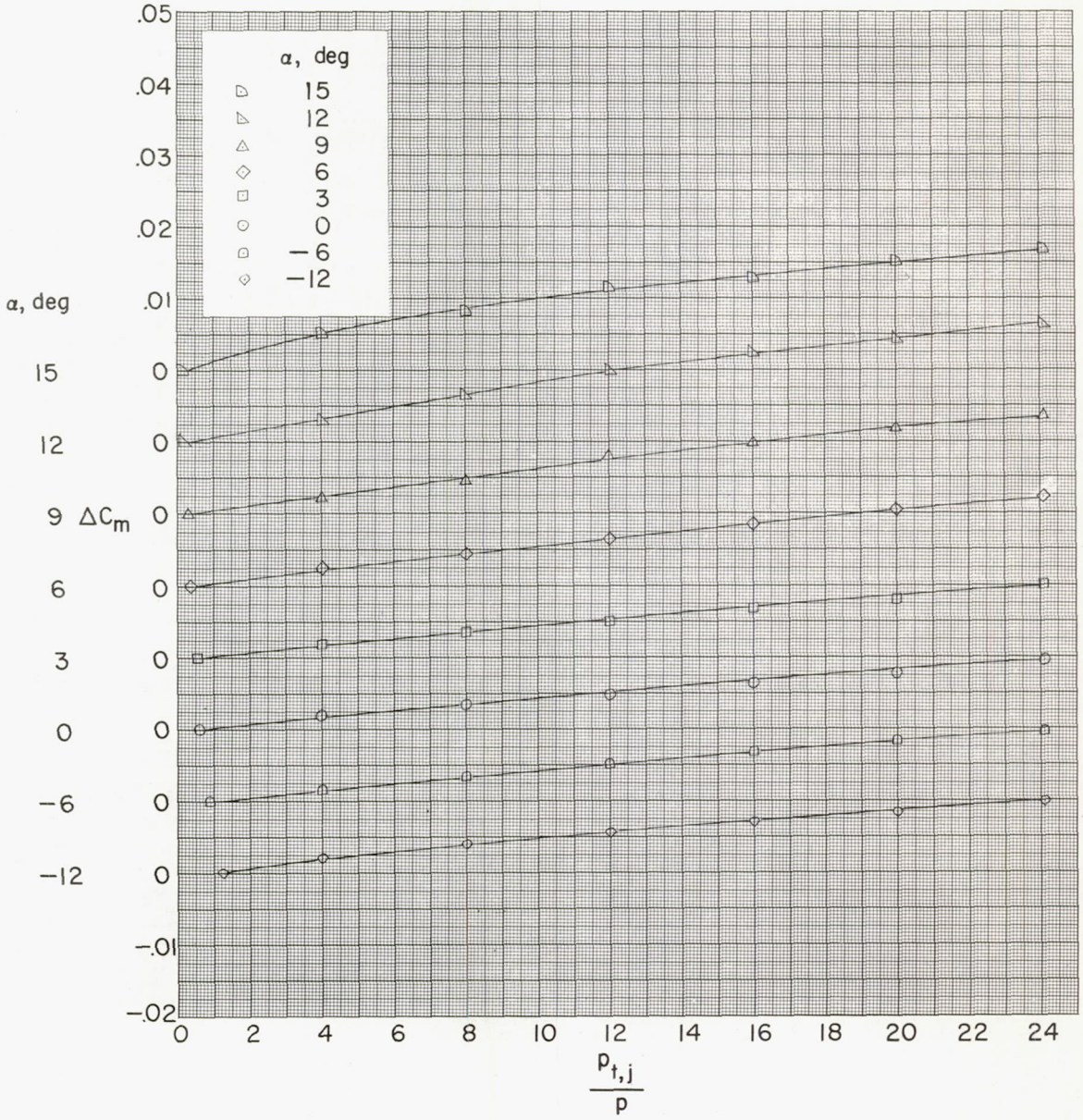

(m) Configuration 3; M = 2.01.

Figure 5.- Continued.

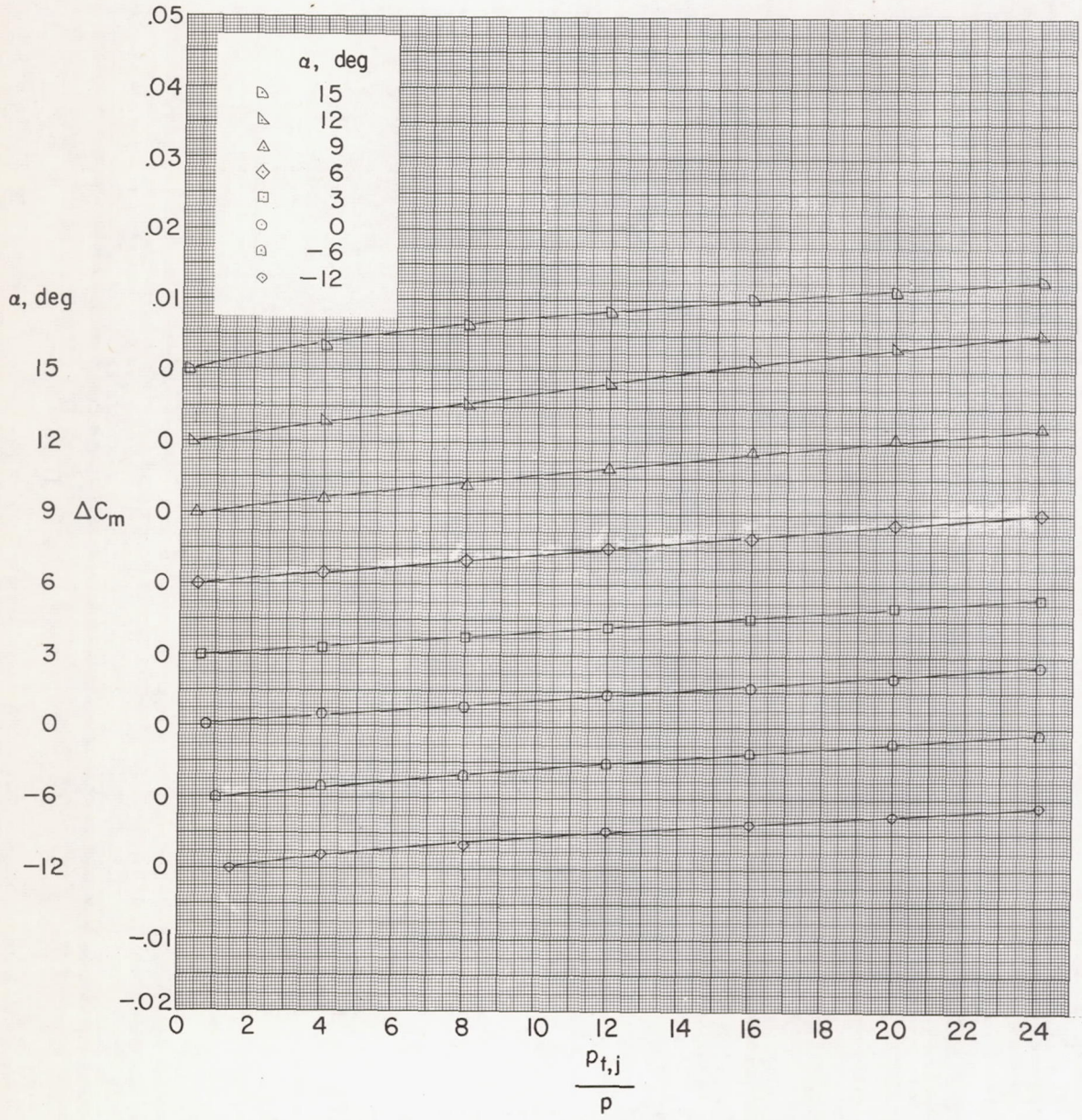

(n) Configuration 4; M = 2.01.

Figure 5.- Concluded.

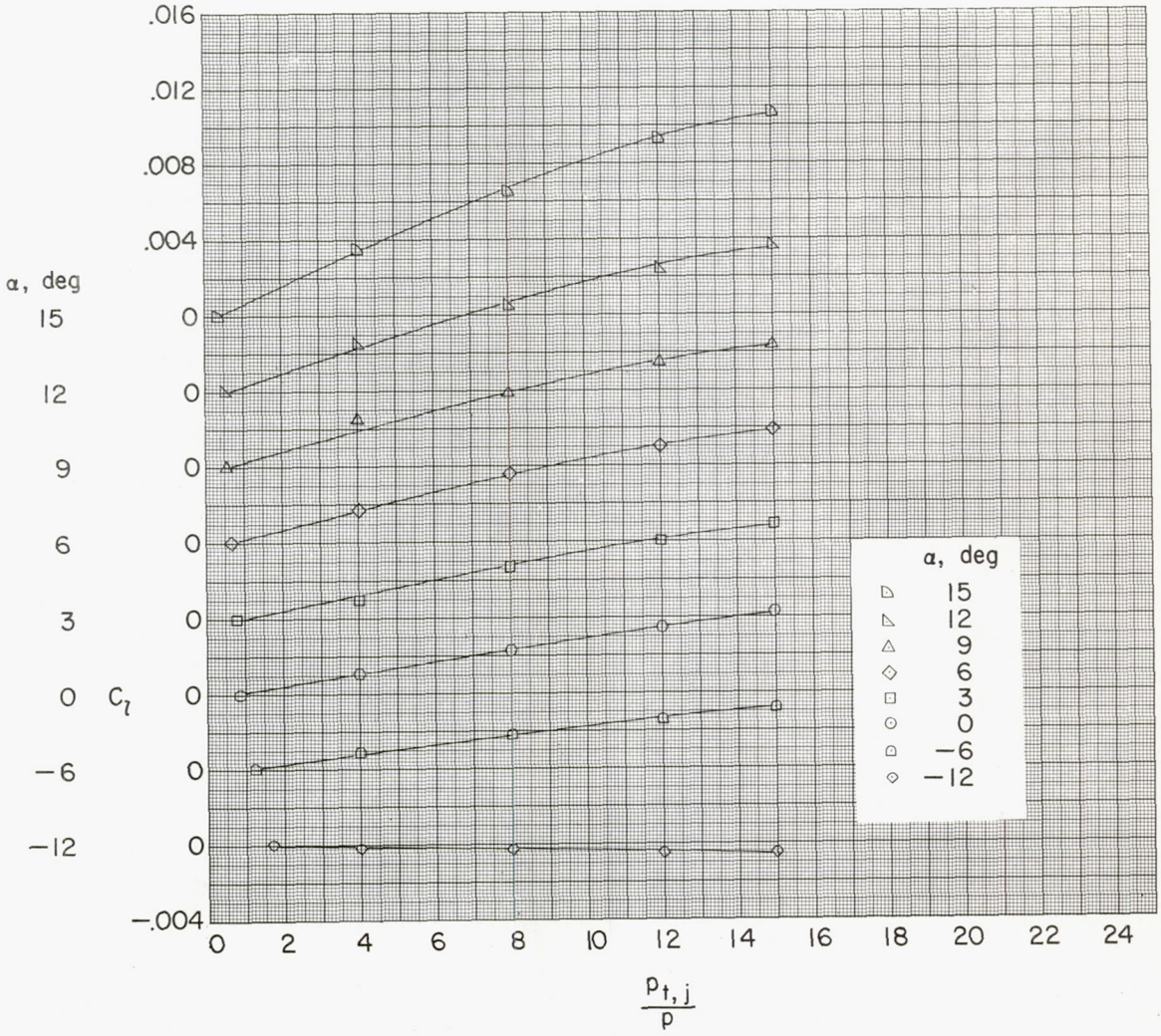

(a) Configuration 1; M = 1.61.

Figure 6.- Variation of incremental wing rolling-moment coefficient with jet pressure ratio.

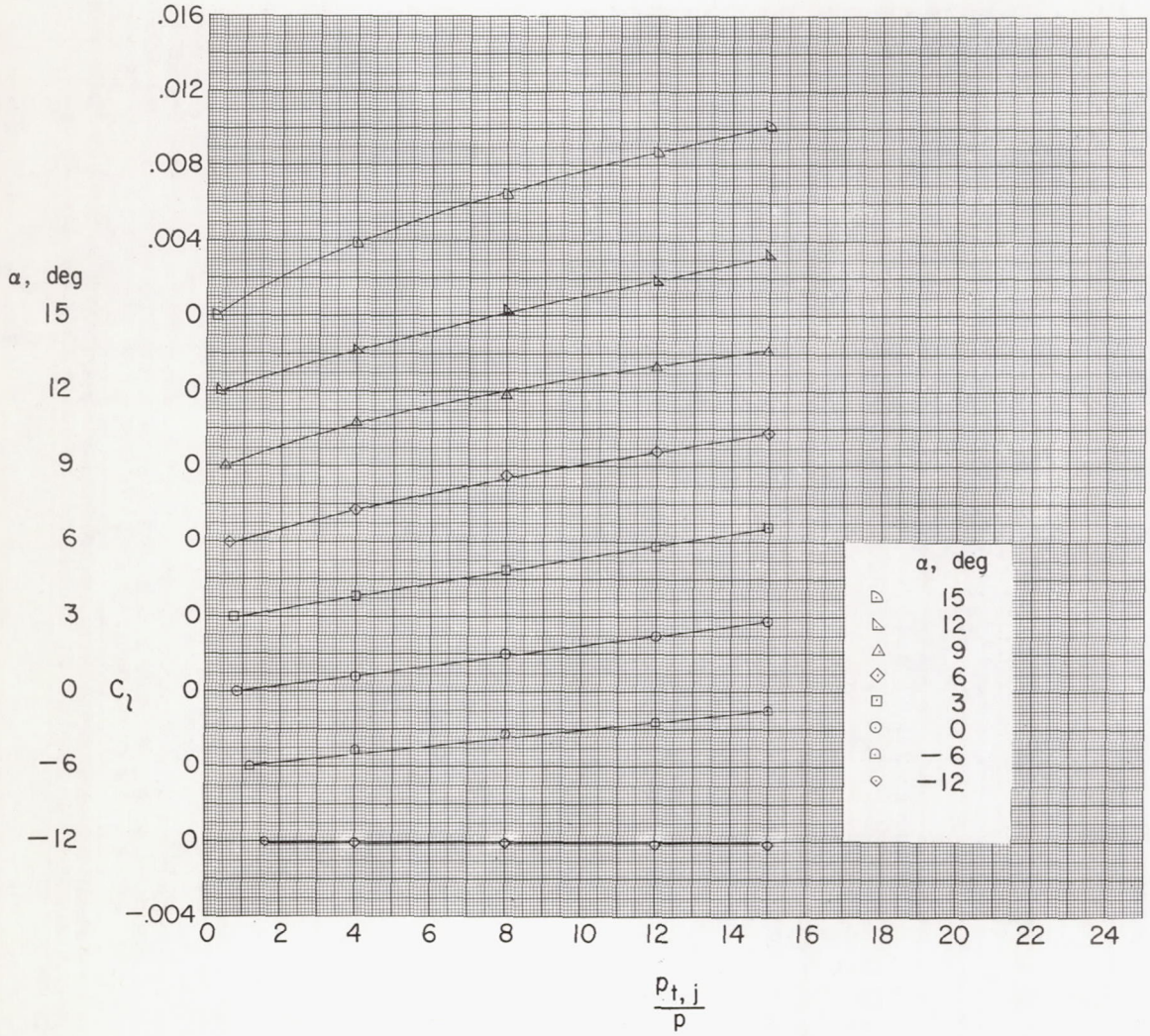

(b) Configuration 2; M = 1.61.

Figure 6.- Continued.

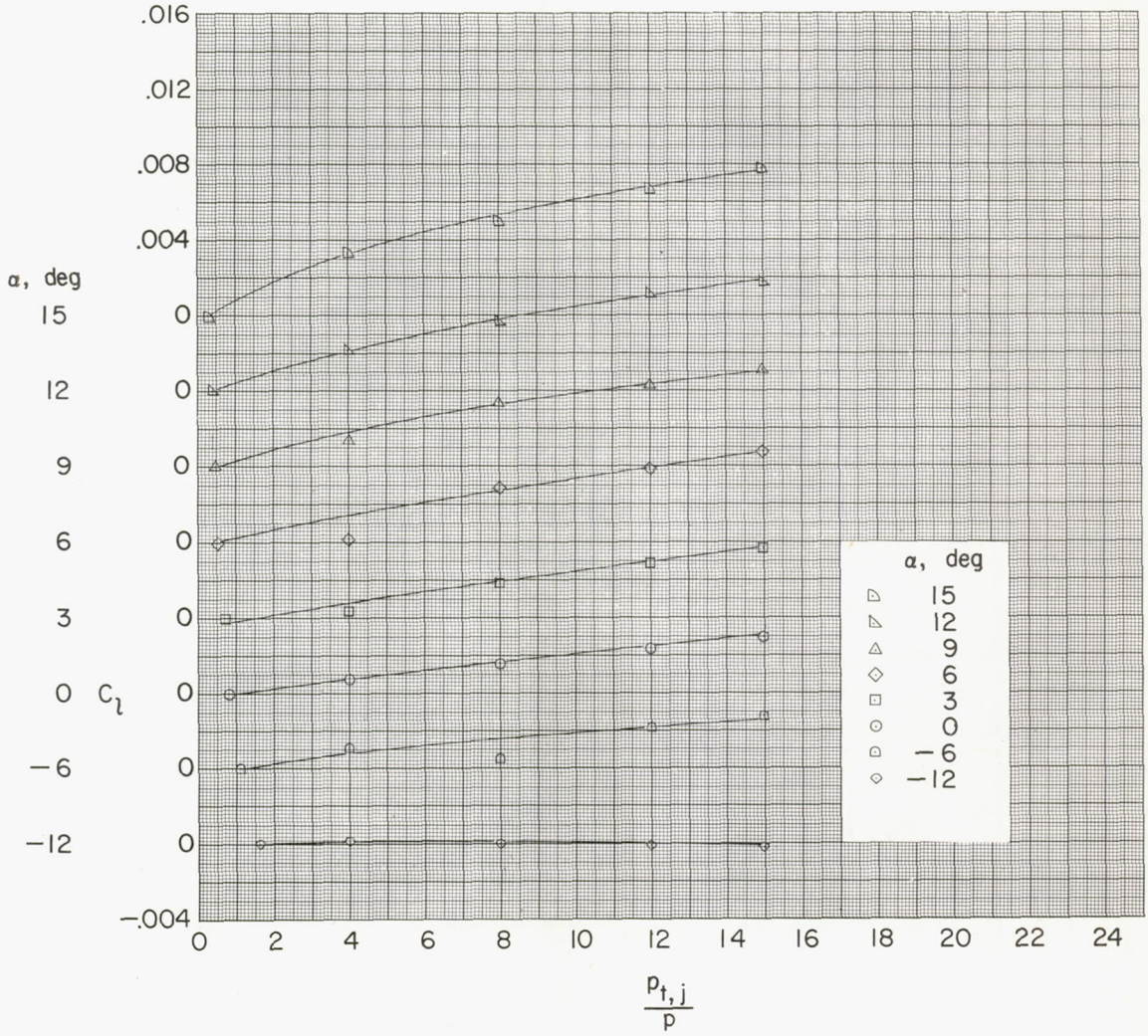

(c) Configuration 3; M = 1.61.

Figure 6.- Continued.

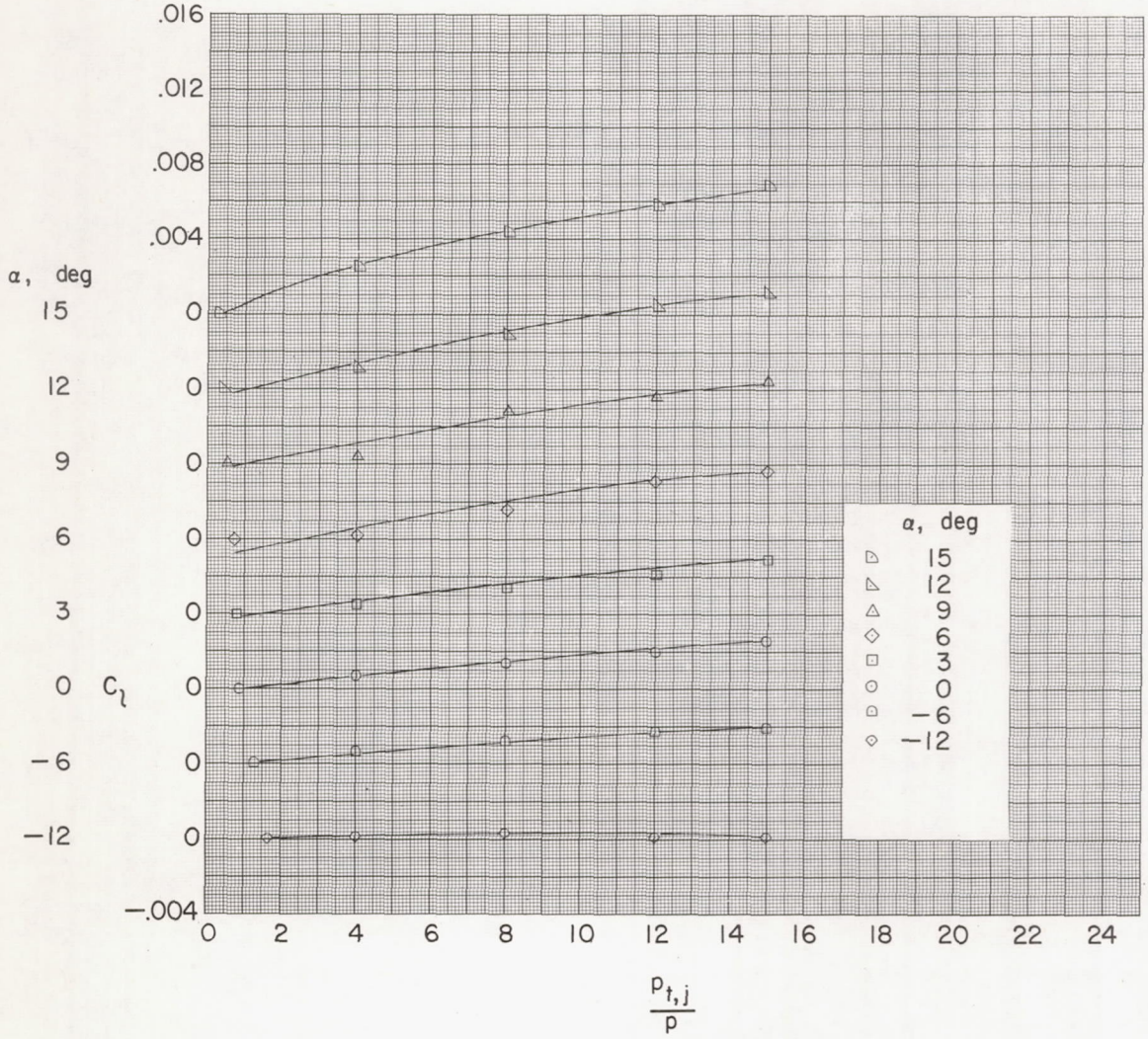

(d) Configuration 4; M = 1.61.

Figure 6.- Continued.

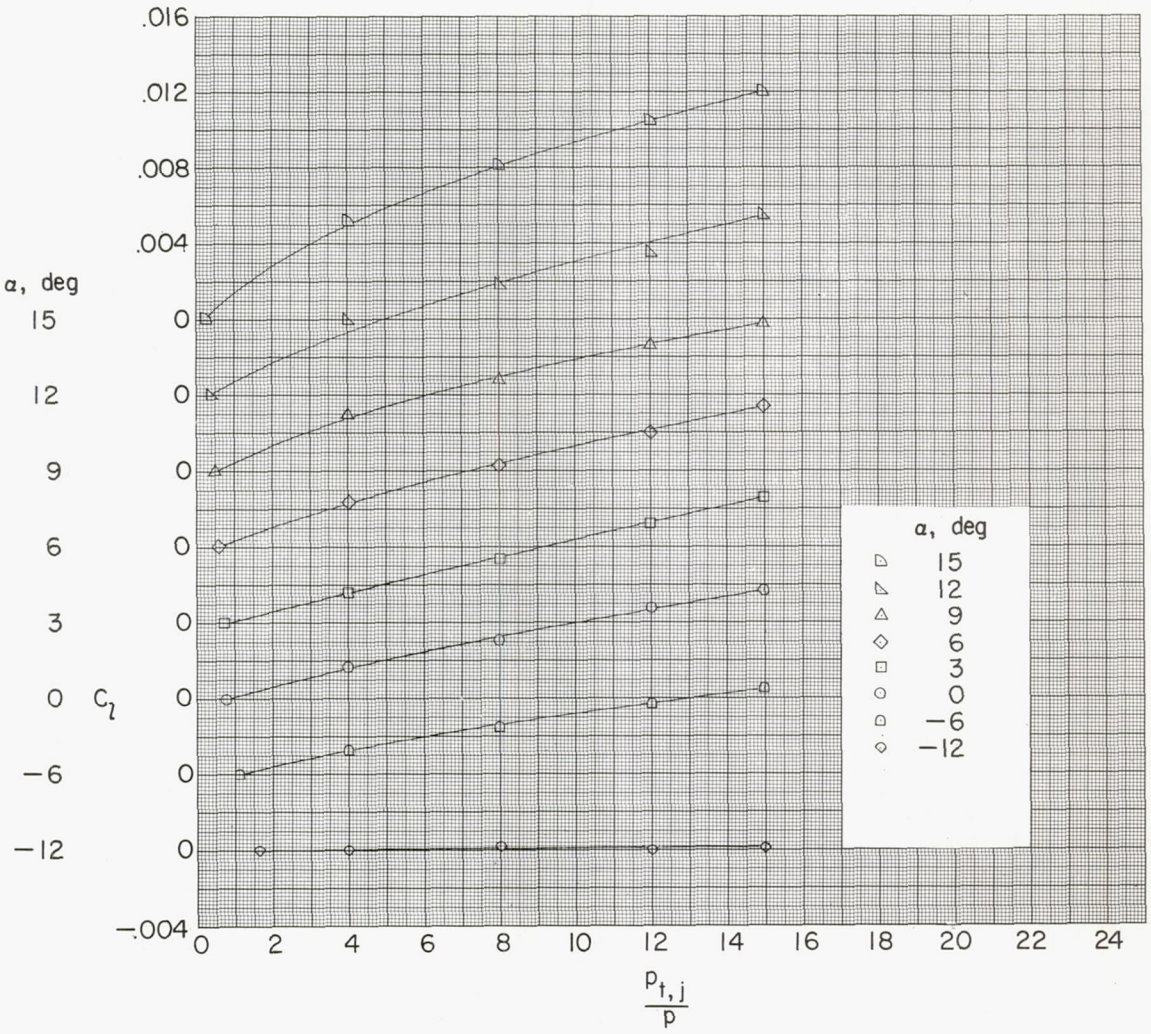

(e) Configuration 5; M = 1.61.

Figure 6.- Continued.

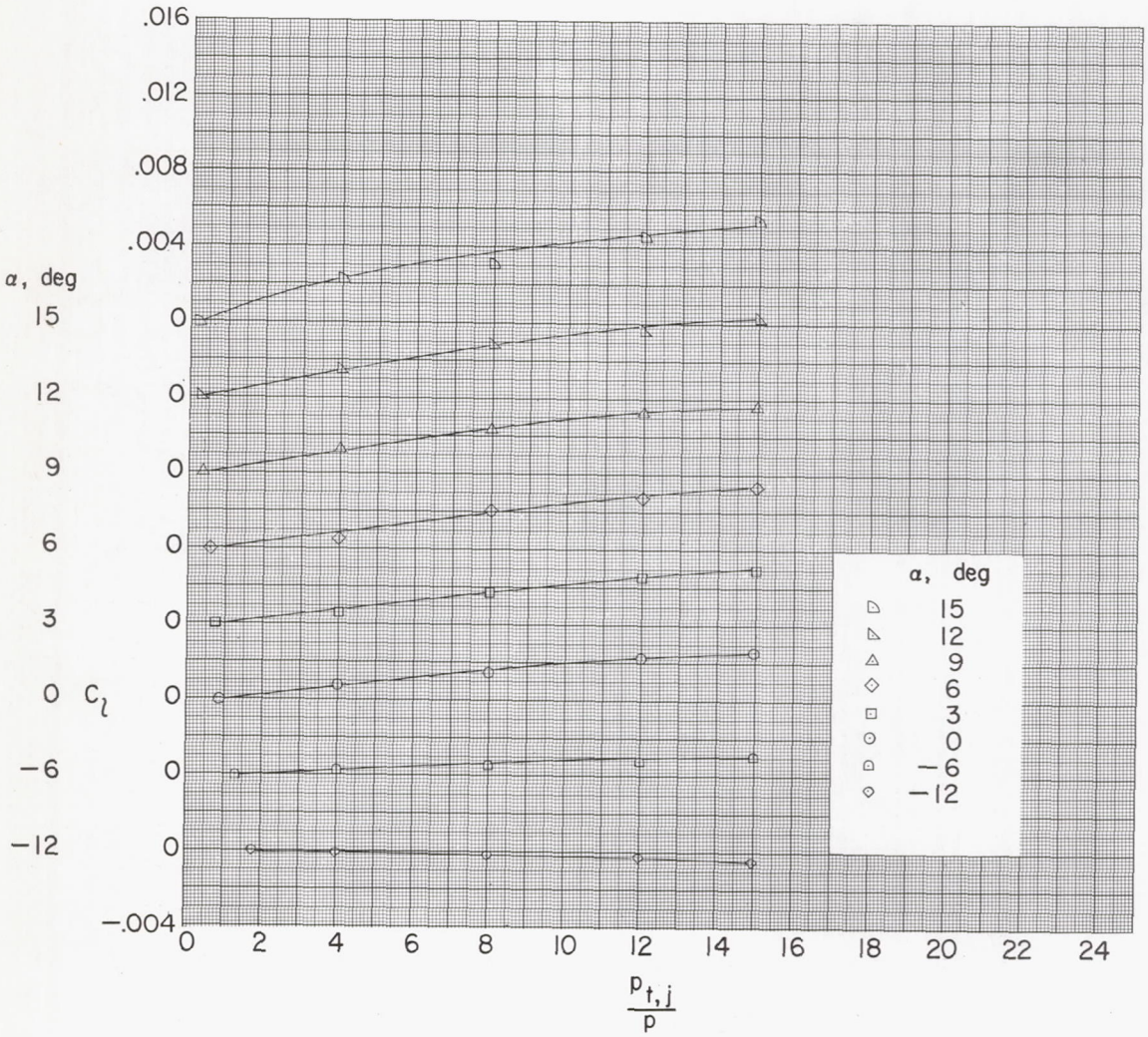

(f) Configuration 6; M = 1.61.

Figure 6.- Continued.

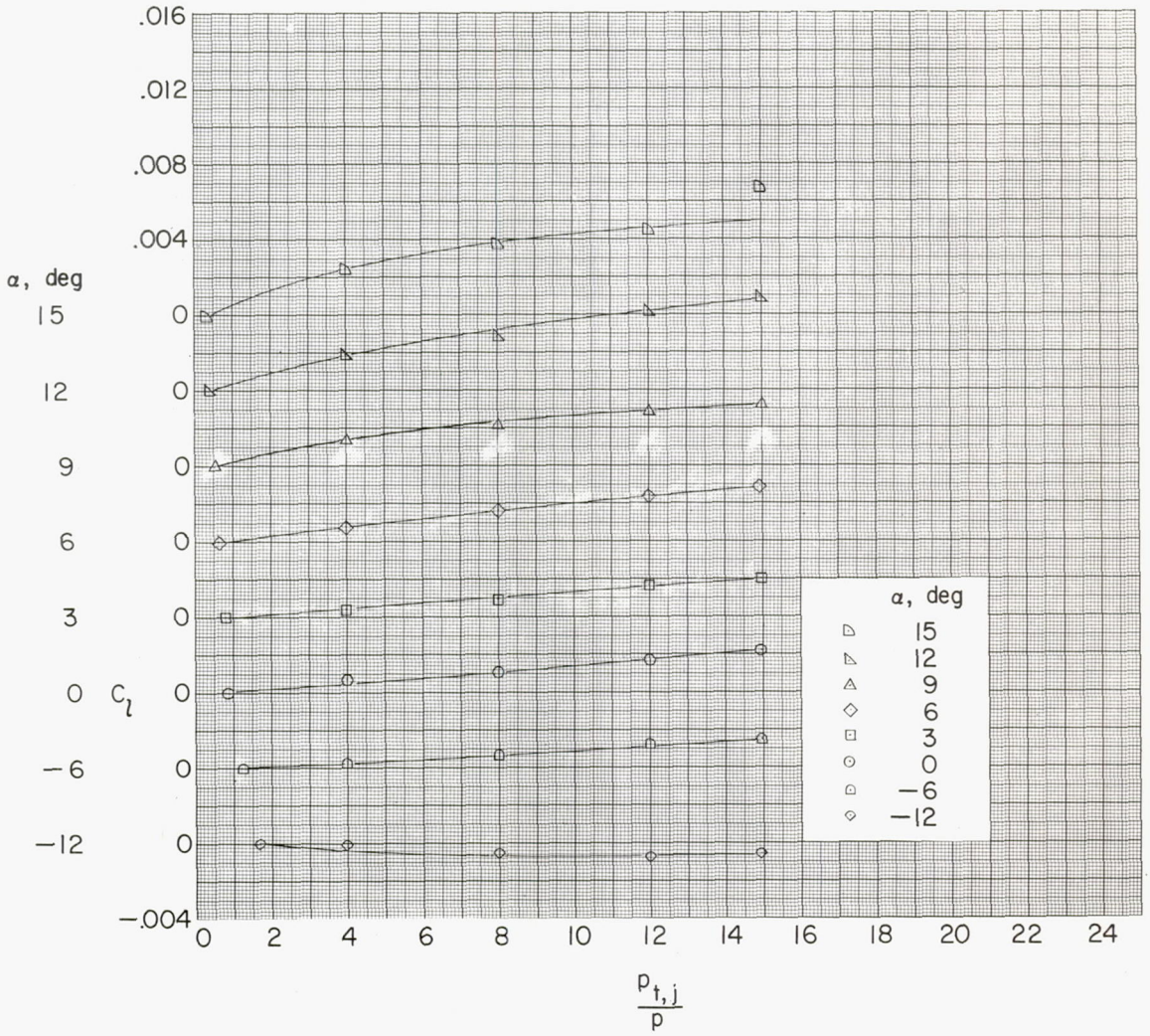

(g) Configuration 7; M = 1.61.

Figure 6.- Continued.

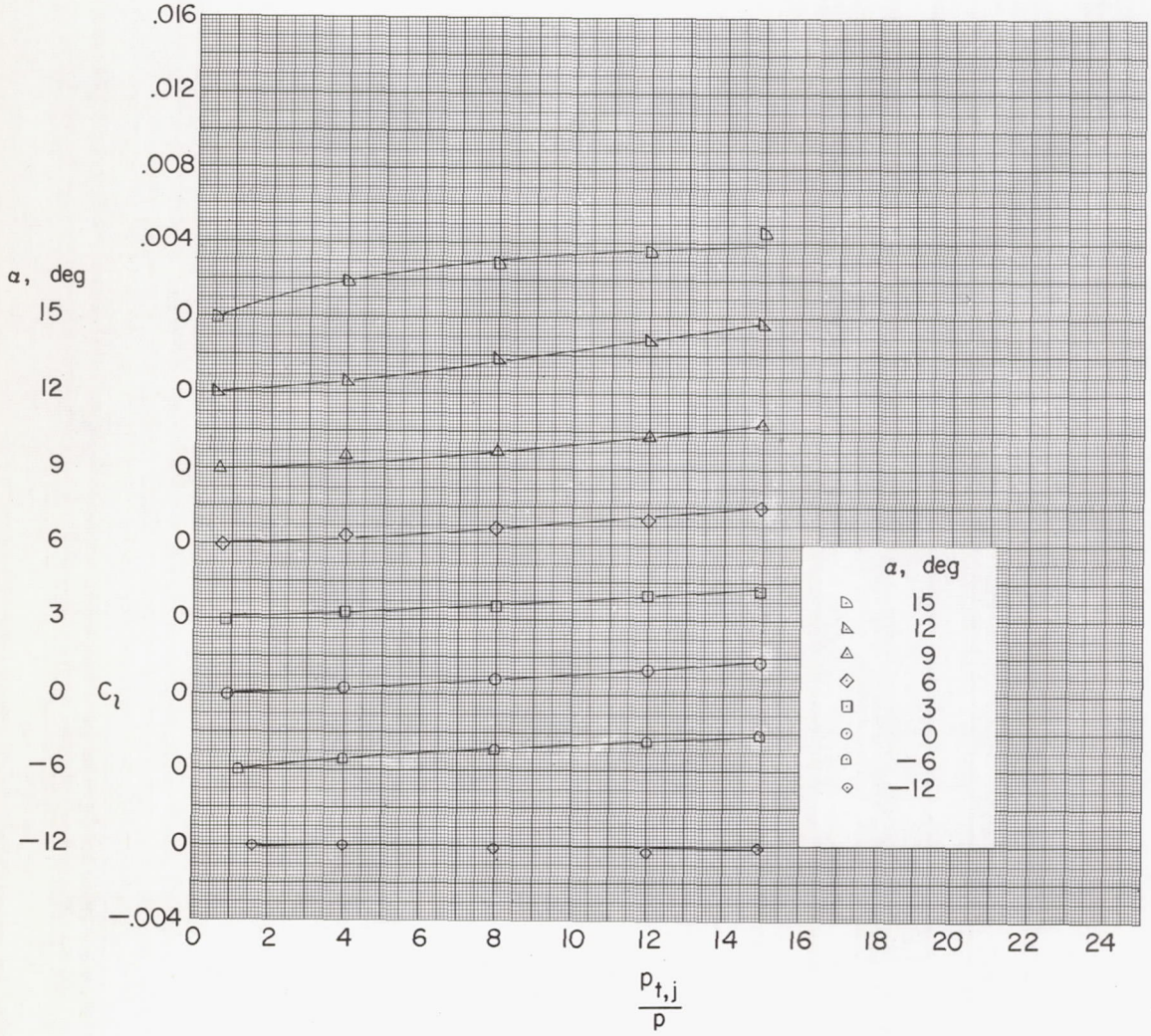

(h) Configuration 8; M = 1.61.

Figure 6.- Continued.

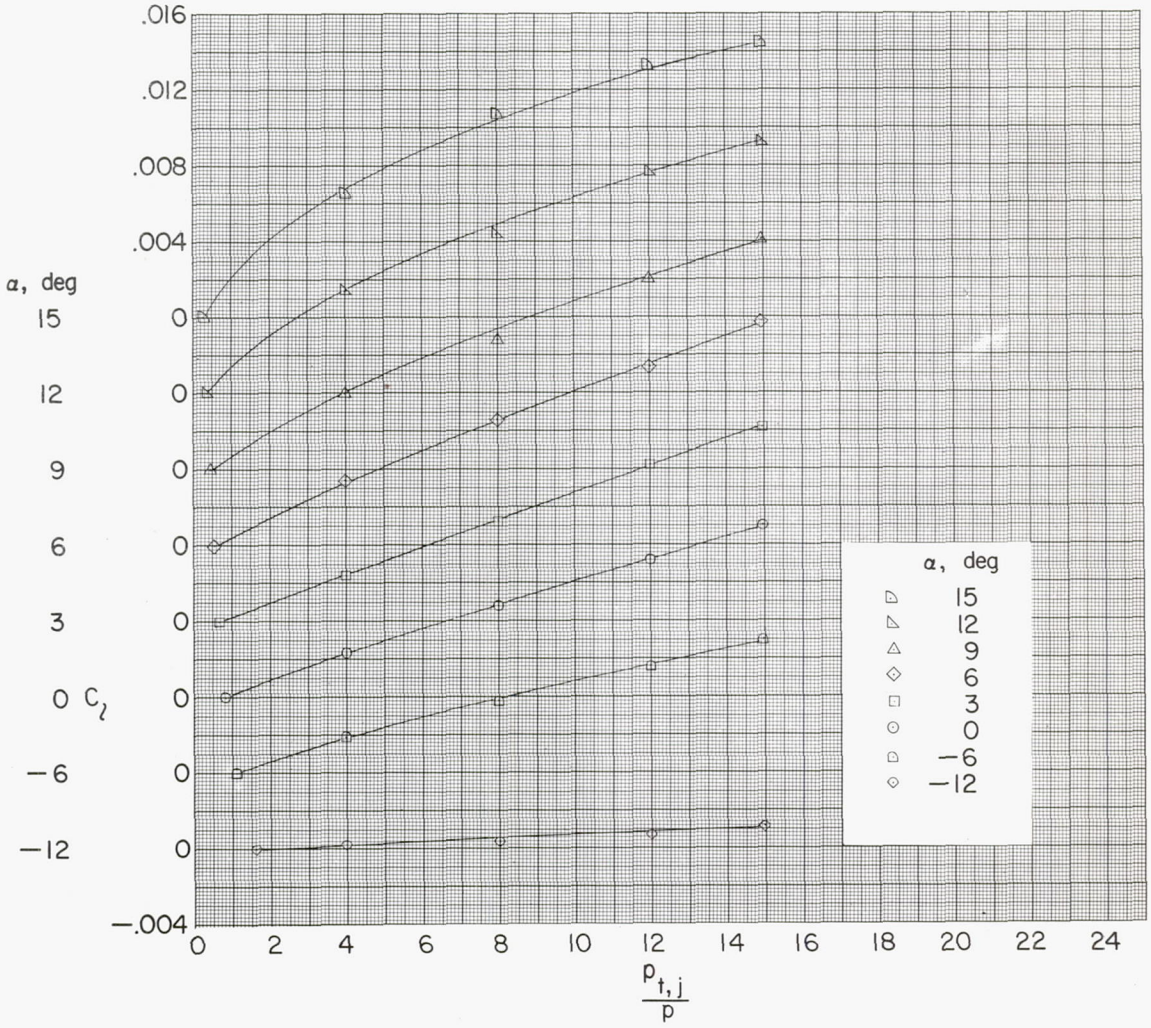

(i) Configuration 10; M = 1.61.

Figure 6.- Continued.

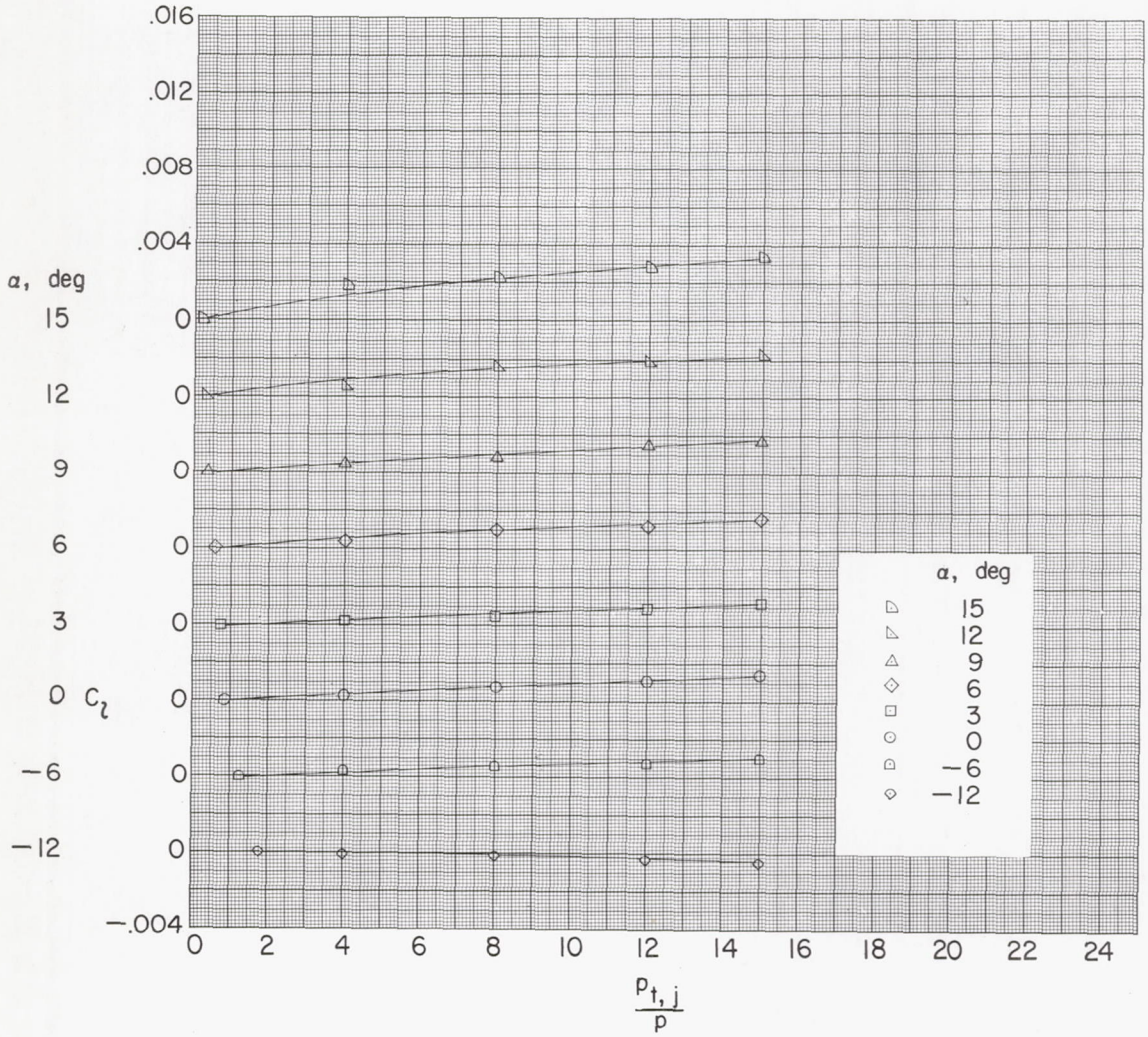

(j) Configuration 11; M = 1.61.

Figure 6.- Continued.

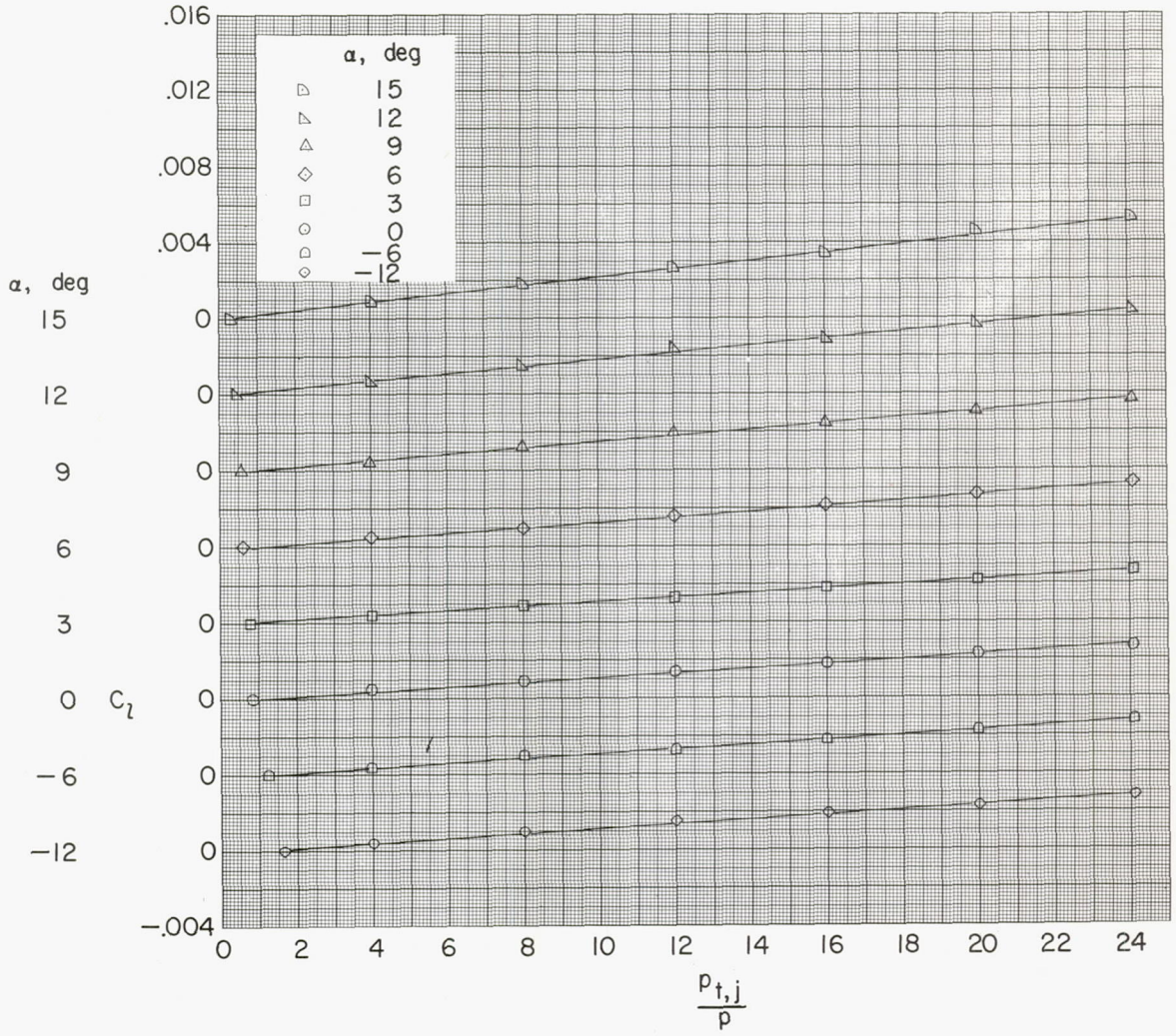

(k) Configuration 1; M = 2.01.

Figure 6.- Continued.

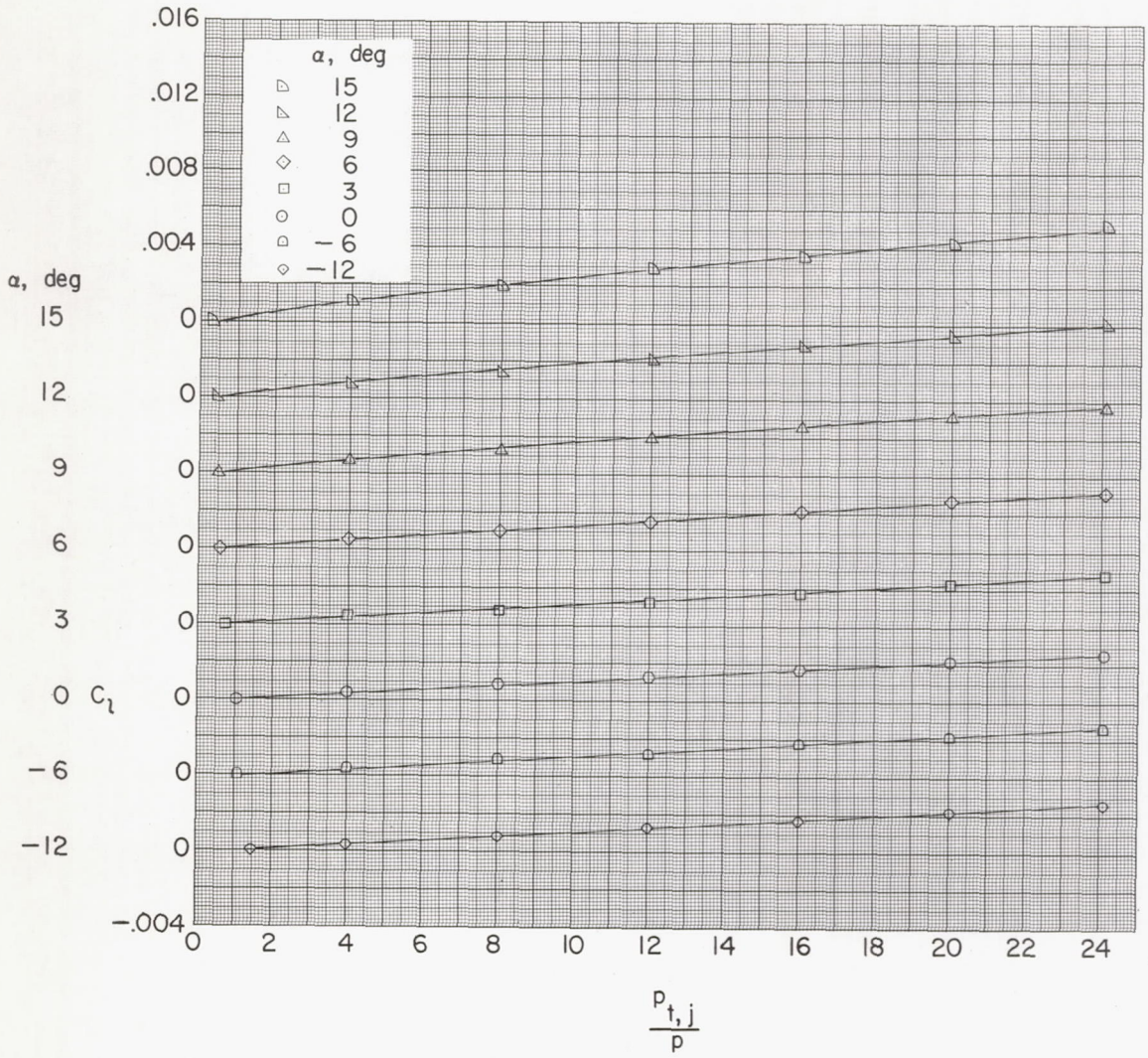

(*l*) Configuration 2; M = 2.01.

Figure 6.- Continued.

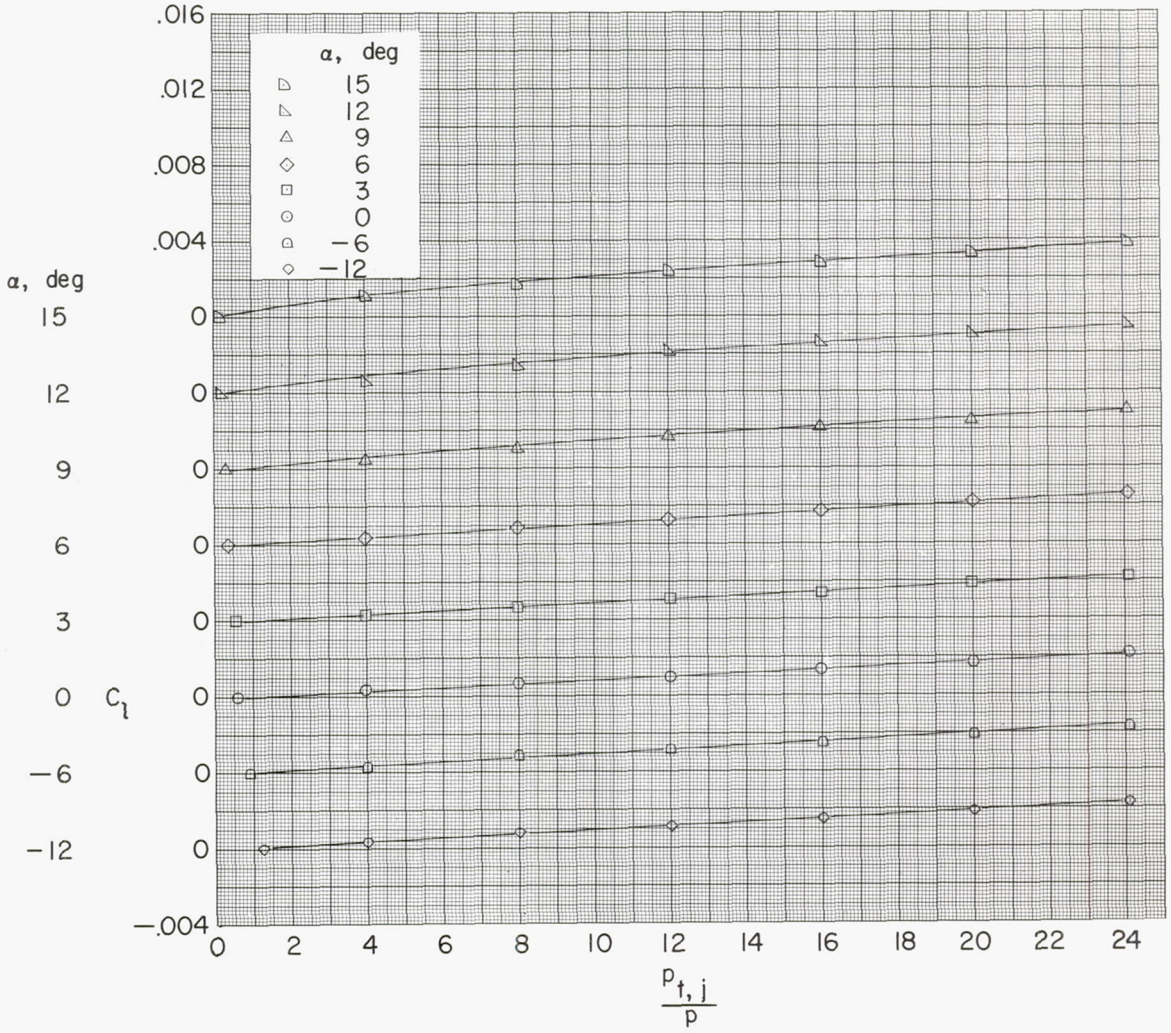

(m) Configuration 3; M = 2.01.

Figure 6.- Continued.

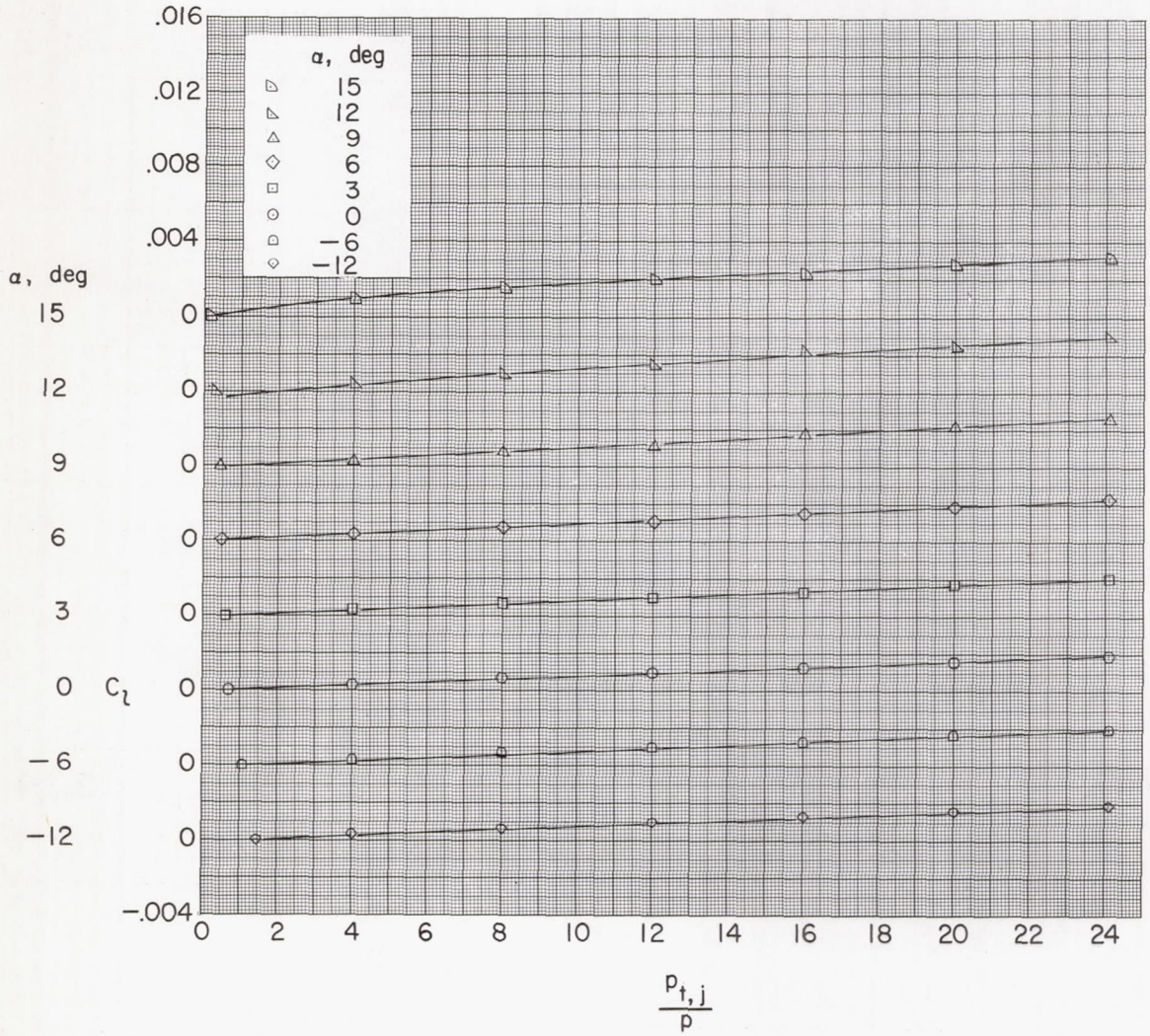

(n) Configuration 4; M = 2.01.

Figure 6.- Concluded.

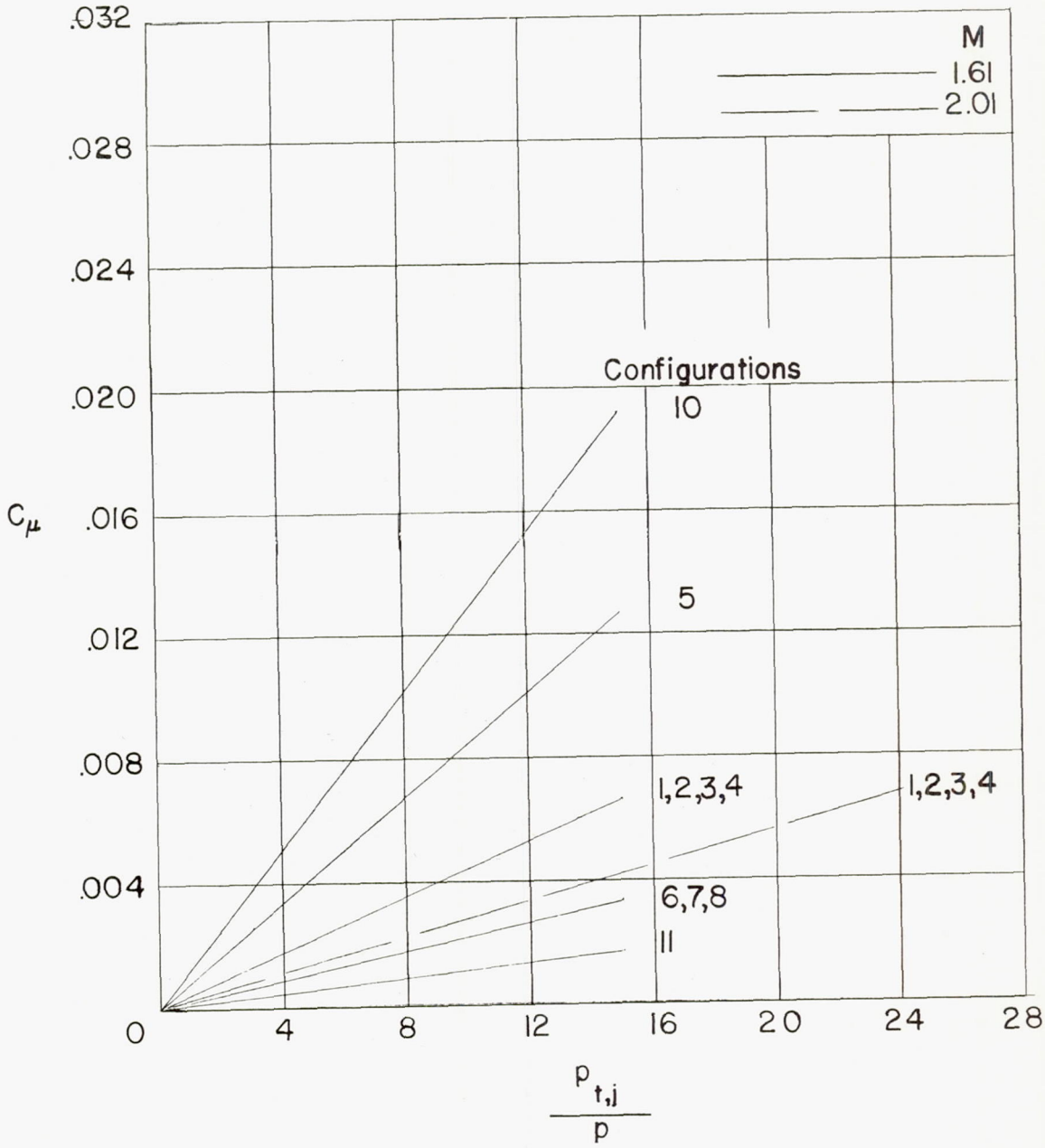

Figure 7.- Variation of computed momentum coefficient with jet pressure ratio for the 10 jet-spoiler configurations.

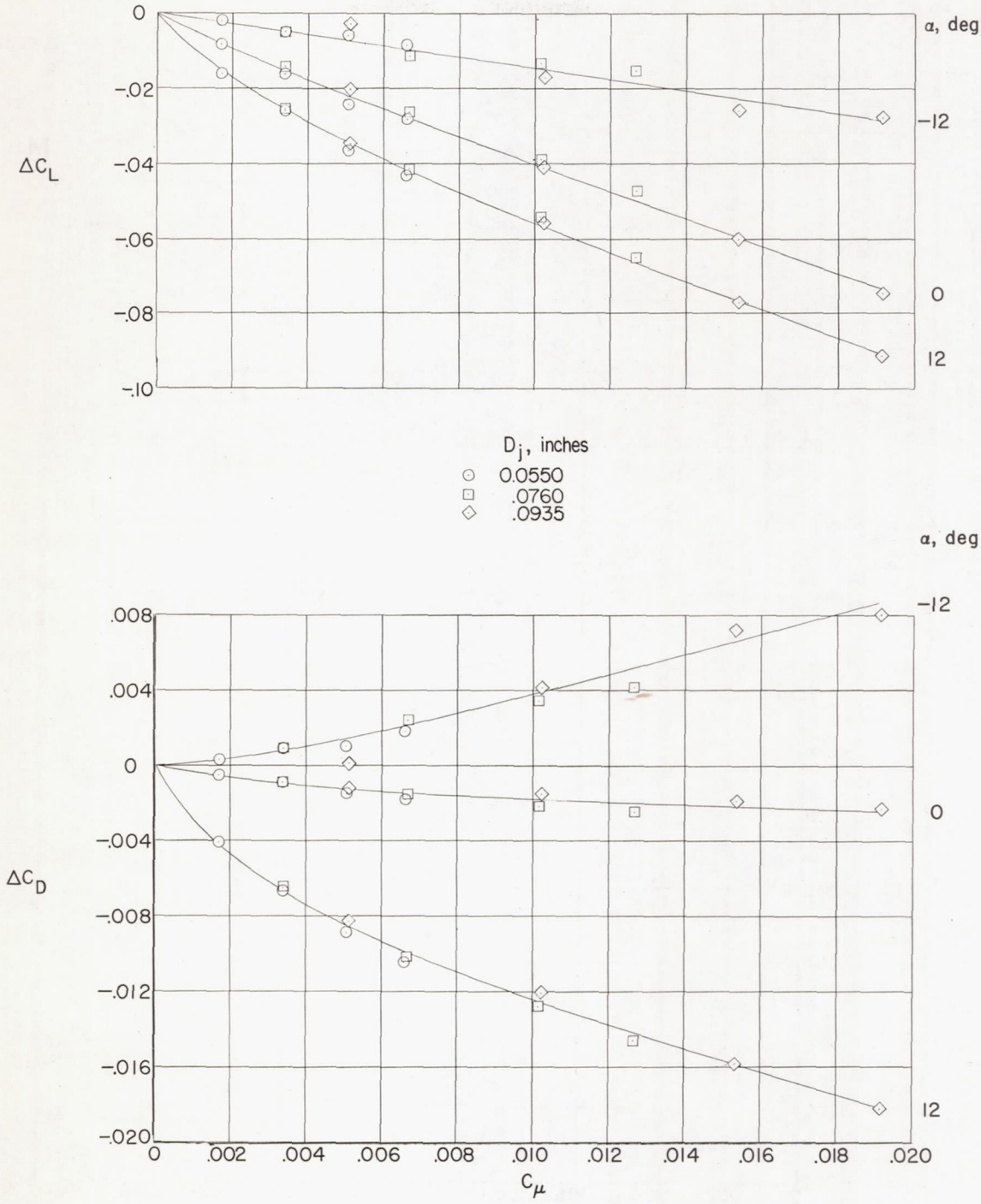

(a) ΔC_L and ΔC_D.

Figure 8.- Correlation of incremental wing coefficients with jet momentum coefficient. $M = 1.61$; $\delta_j = 90^\circ$; $\frac{2b_j}{b} = 0.65$.

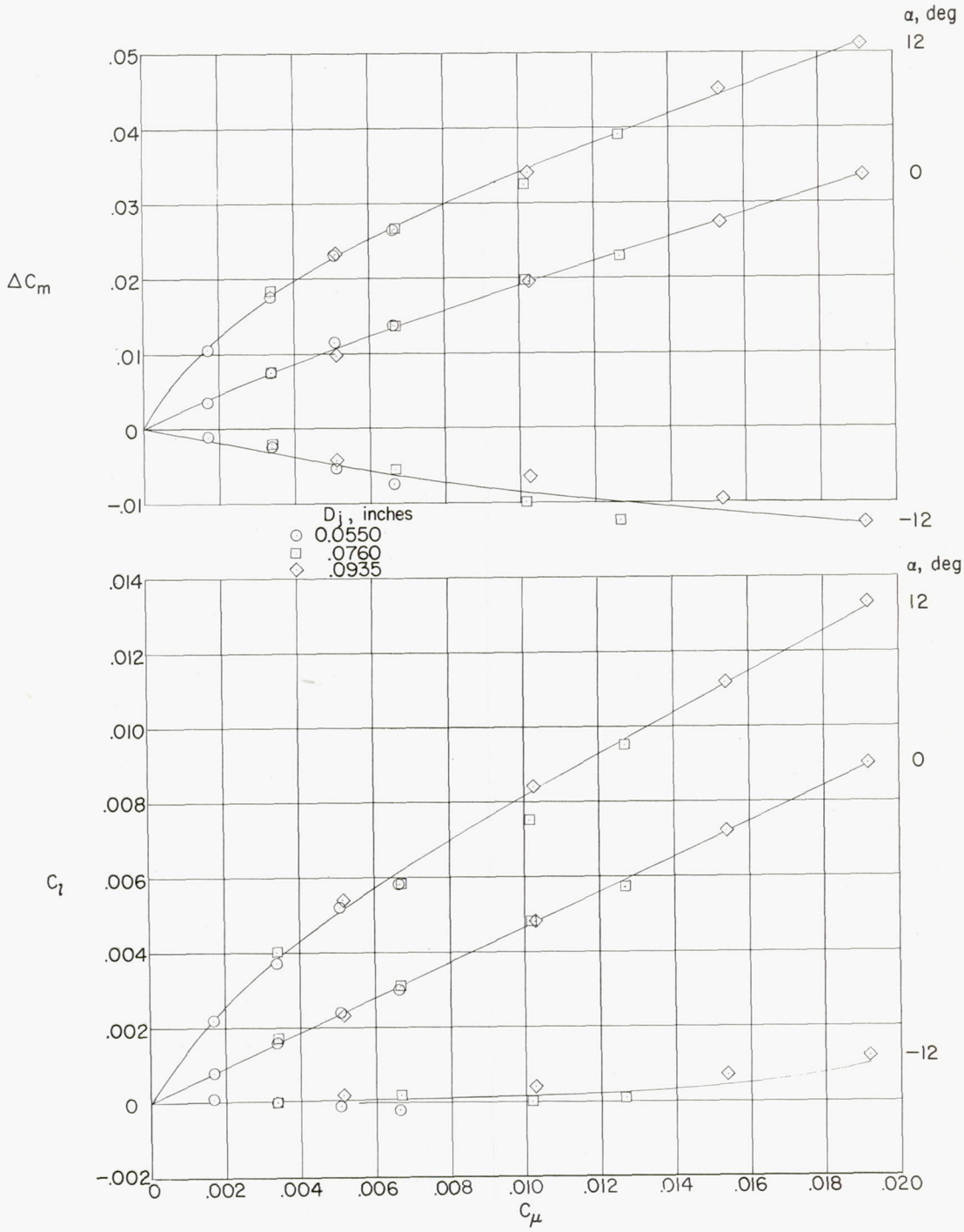

(b) ΔC_m and C_l.

Figure 8.- Concluded.

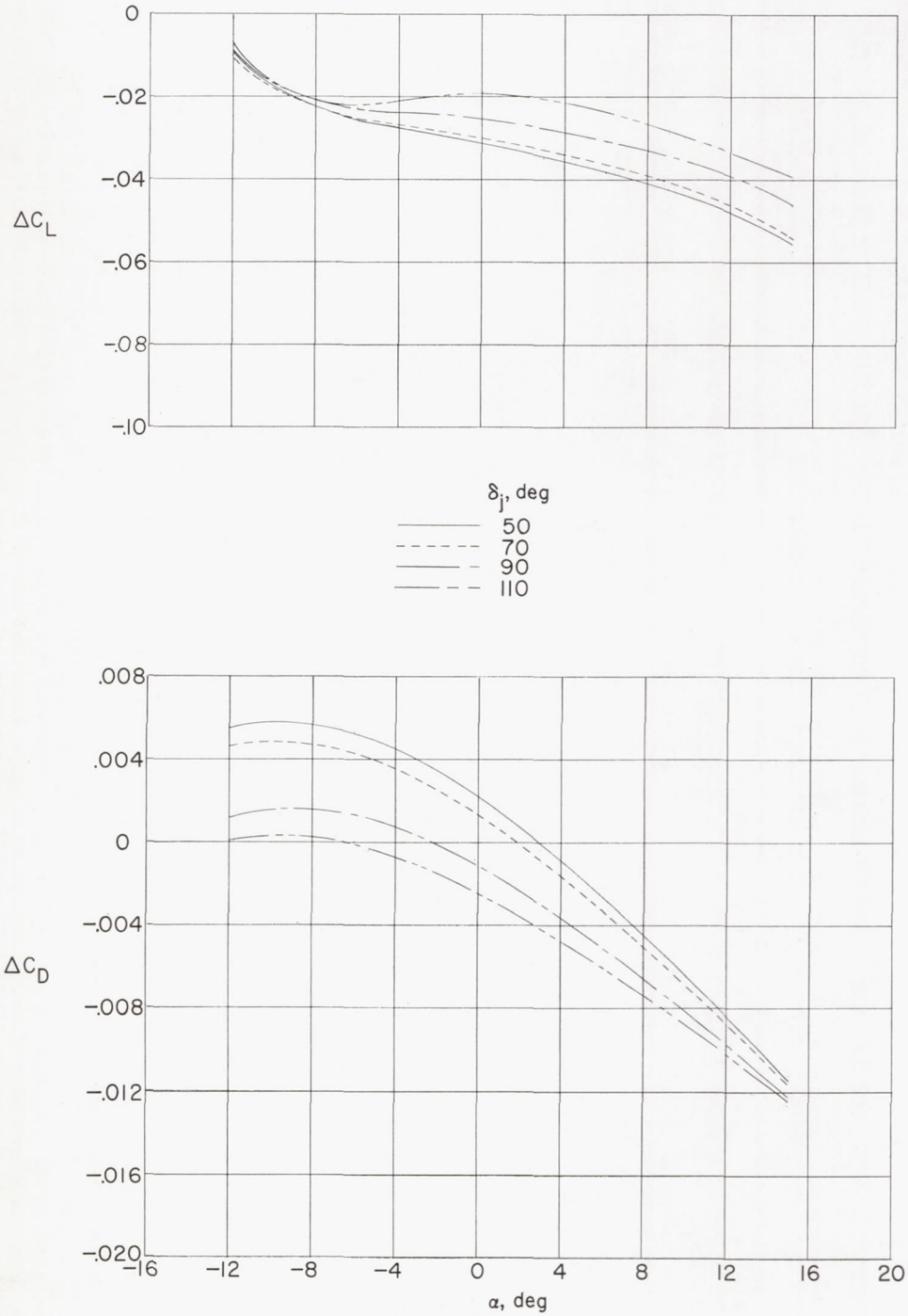

(a) ΔC_L and ΔC_D.

Figure 9.- Effect of jet hole angle on the variation of incremental wing coefficients with angle of attack. $M = 1.61$; $D_j = 0.0550$ in.; $\frac{p_{t,j}}{p} = 12.0$.

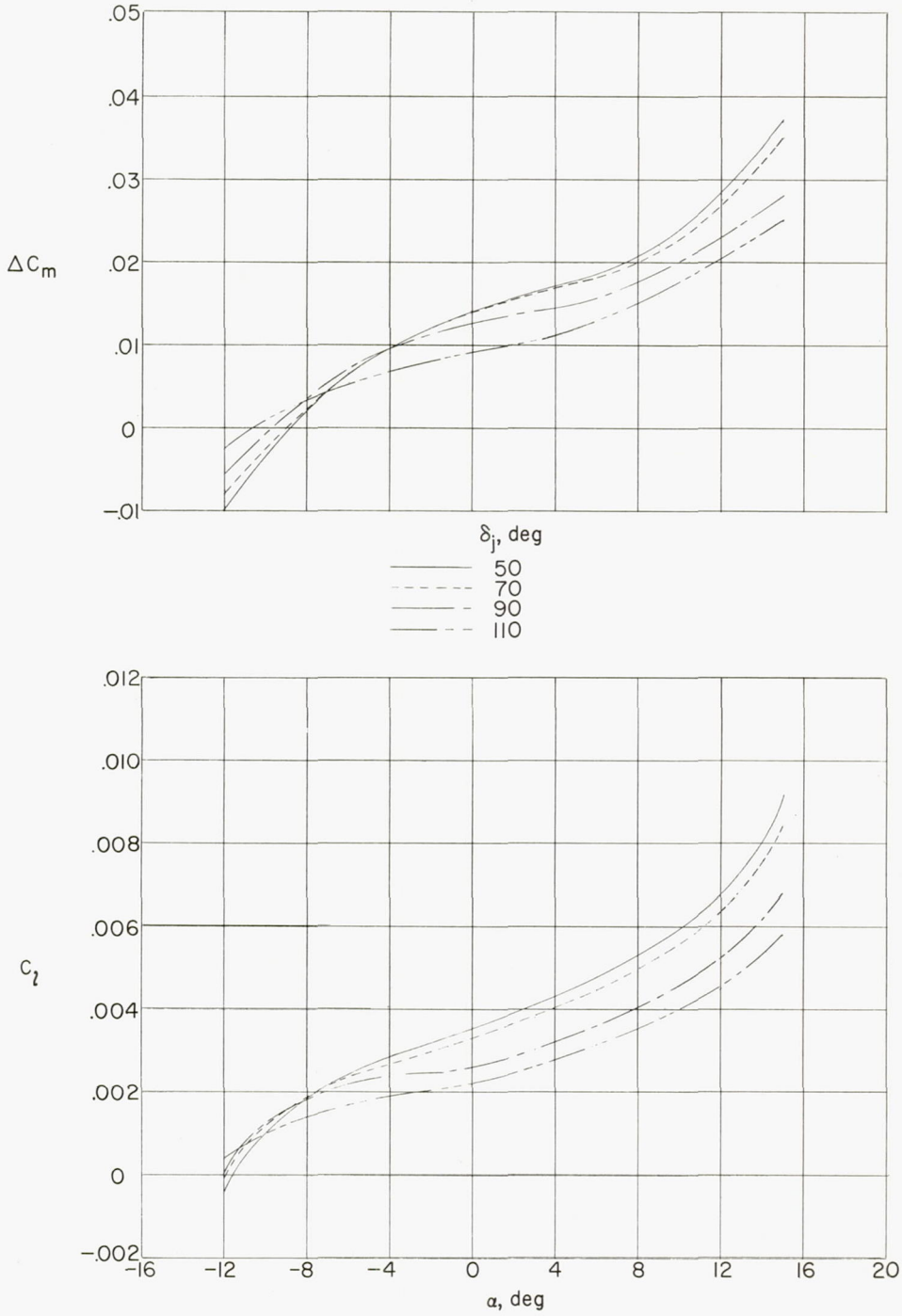

(b) ΔC_m and C_l.

Figure 9.- Concluded.

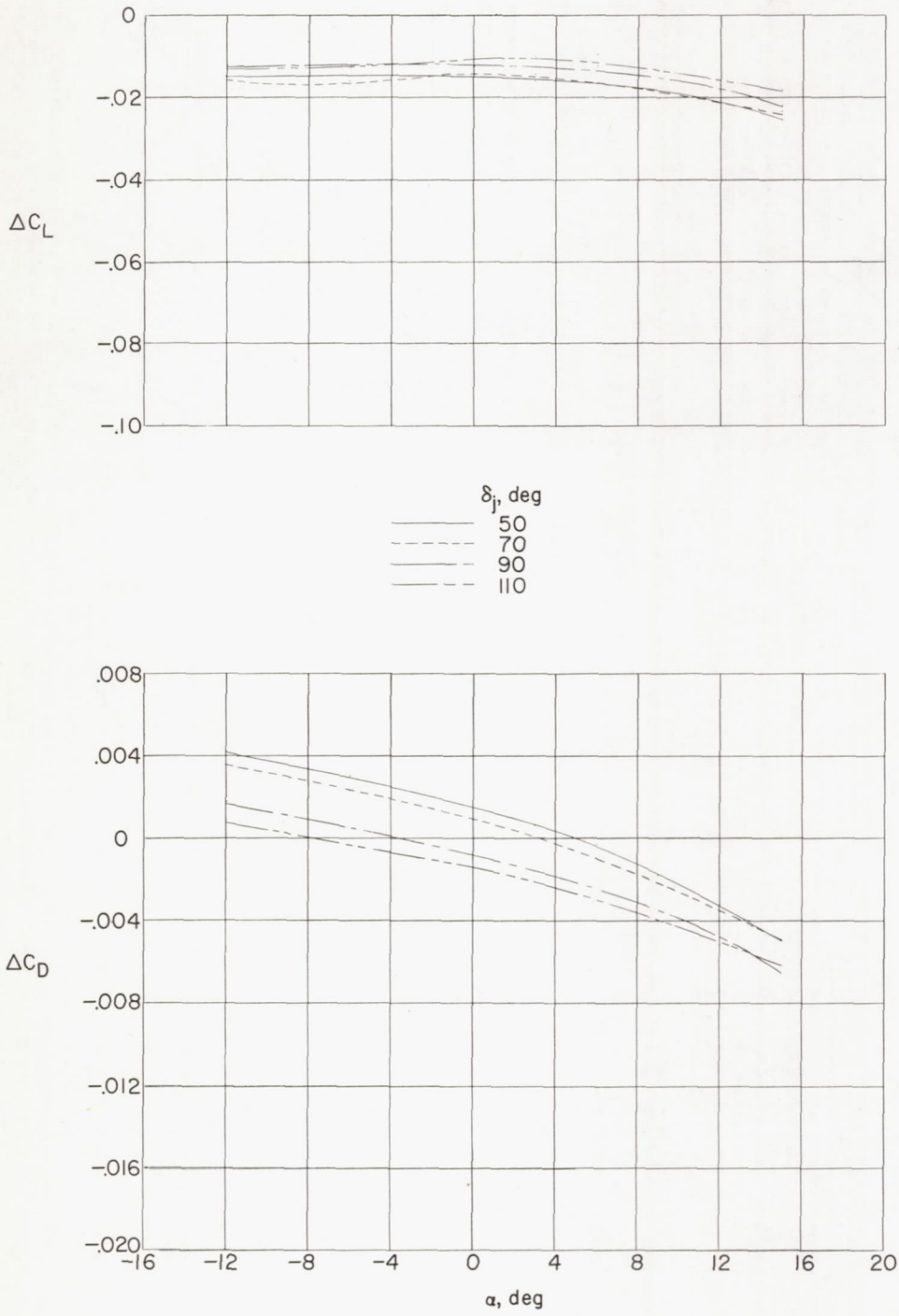

(a) ΔC_L and ΔC_D.

Figure 10.- Effect of jet hole angle on the variation of incremental wing coefficients with angle of attack. M = 2.01; D_j = 0.0550 in.; $\frac{p_{t,j}}{p}$ = 12.0.

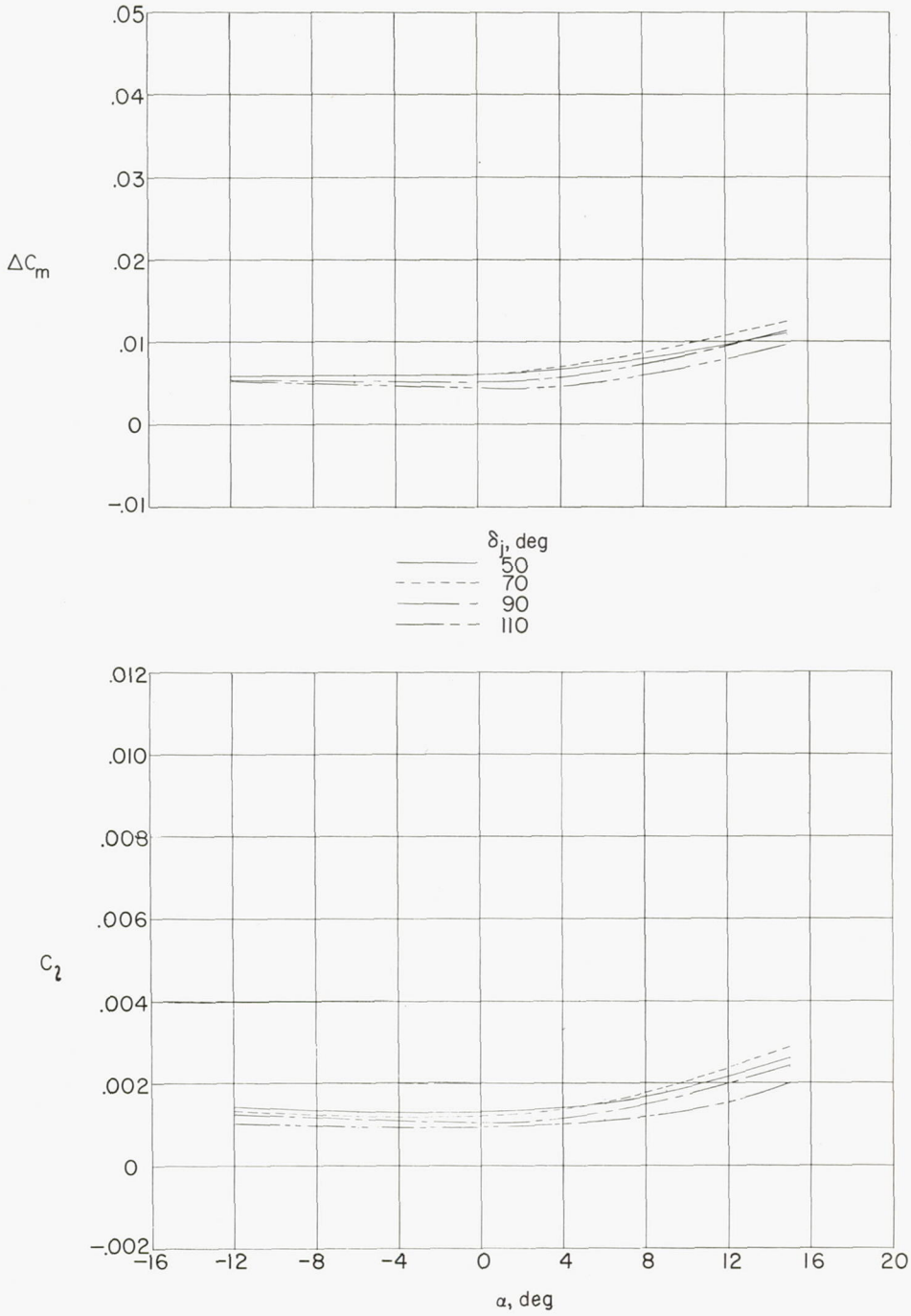

(b) ΔC_m and C_l.

Figure 10.- Concluded.

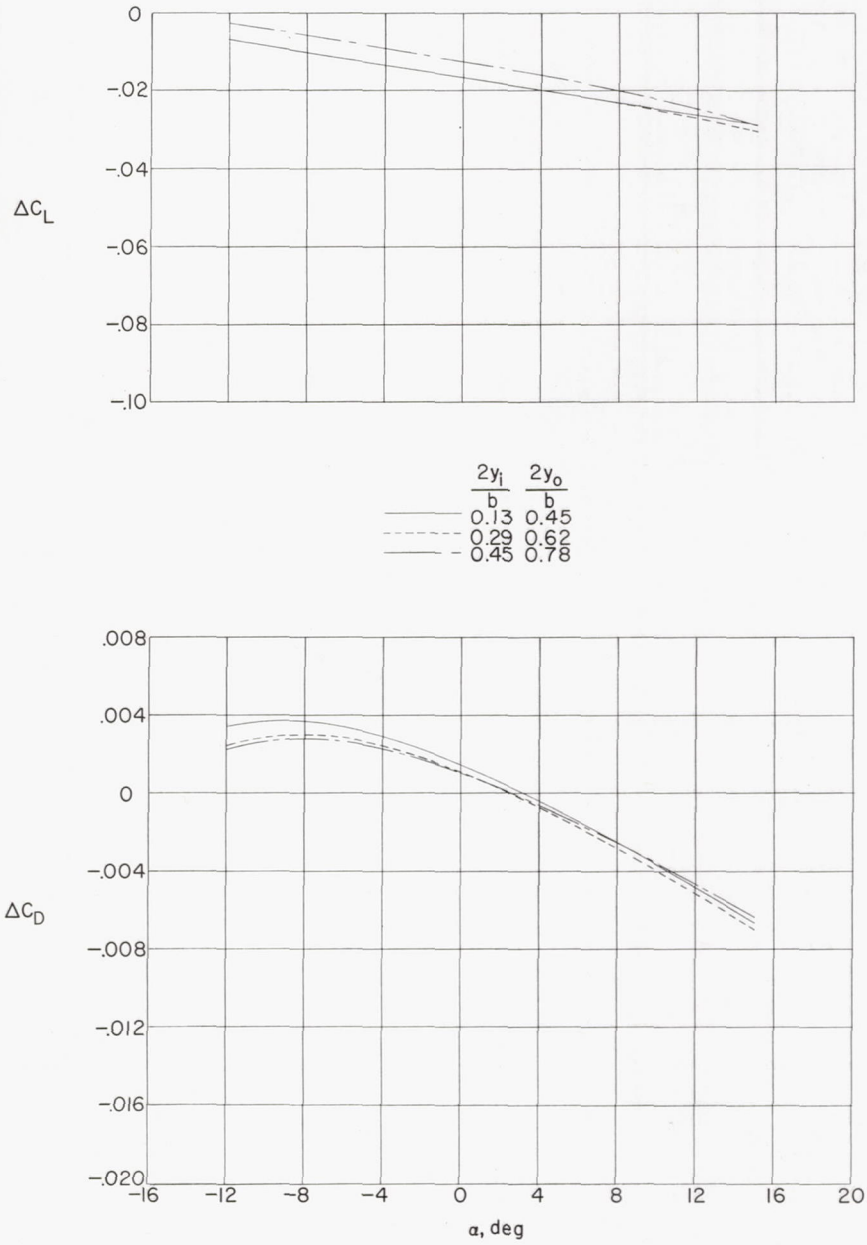

(a) ΔC_L and ΔC_D.

Figure 11.- Effect of spanwise location on the variation of incremental wing coefficient with angle of attack. $M = 1.61$; $\delta_j = 50^{\circ}$; $D_j = 0.0550$ in.; $\frac{p_{t,j}}{p} = 12.0$.

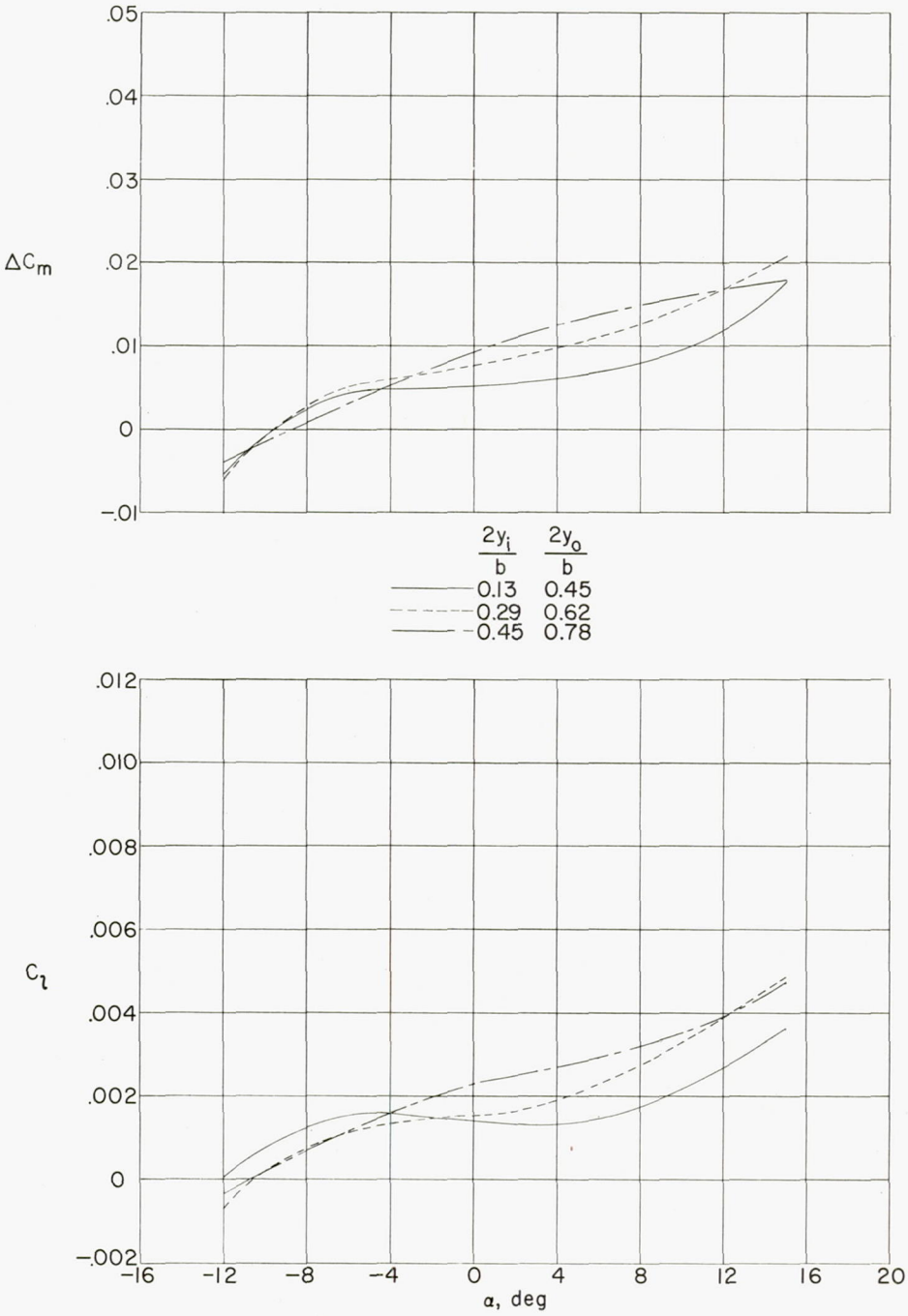

(b) ΔC_m and C_l.

Figure 11.- Concluded.

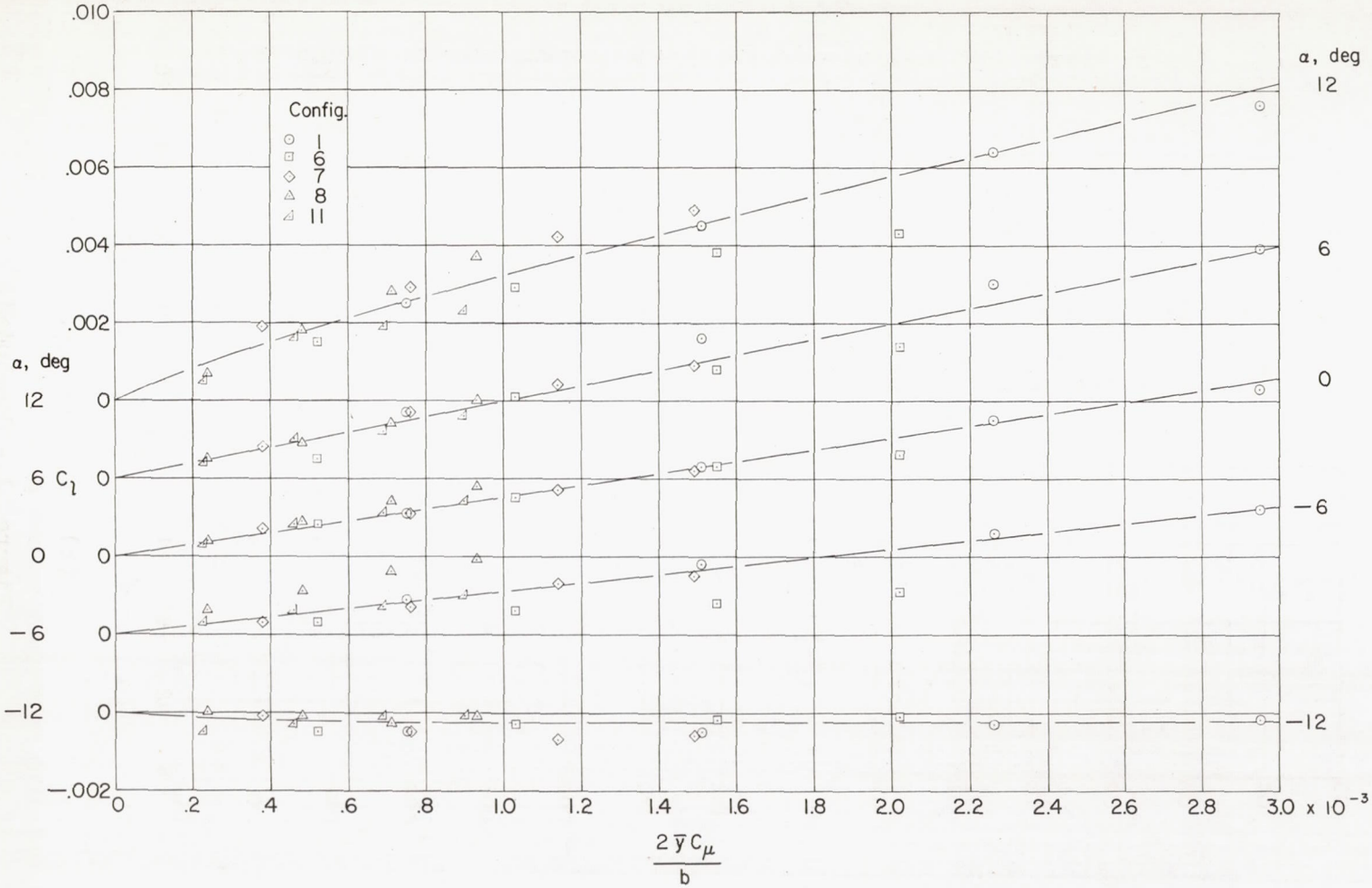

Figure 12.- Correlation of rolling-moment coefficient with span times momentum factor. $M = 1.61$; $\delta_j = 50^\circ$; $D_j = 0.0550$ in.

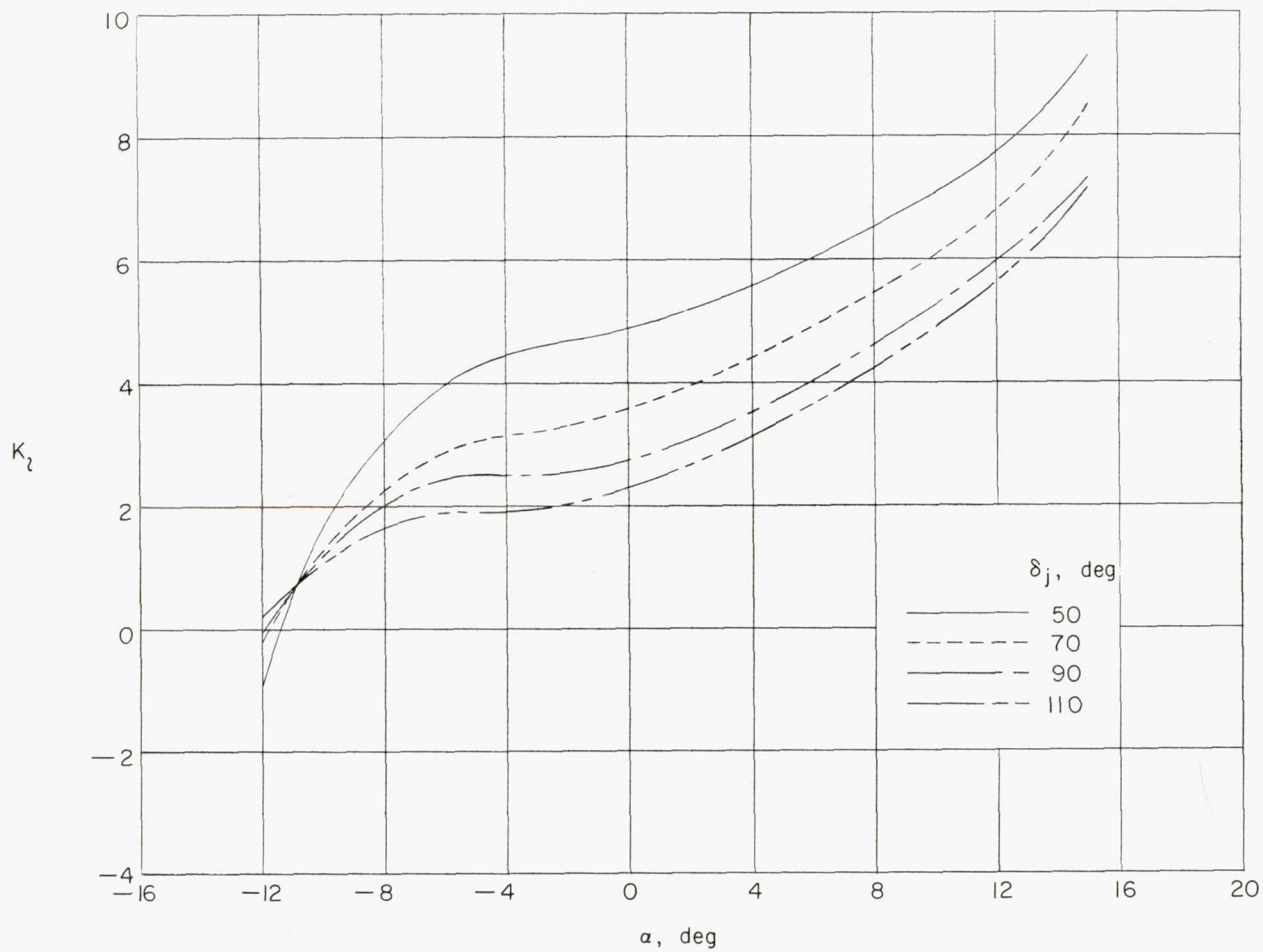

(a) Effect of hole angle. $M = 1.61$; $D_j = 0.0550$ in.; $\frac{p_{t,j}}{p} = 12.0$.

Figure 13.- Variation of roll magnification factor with angle of attack.

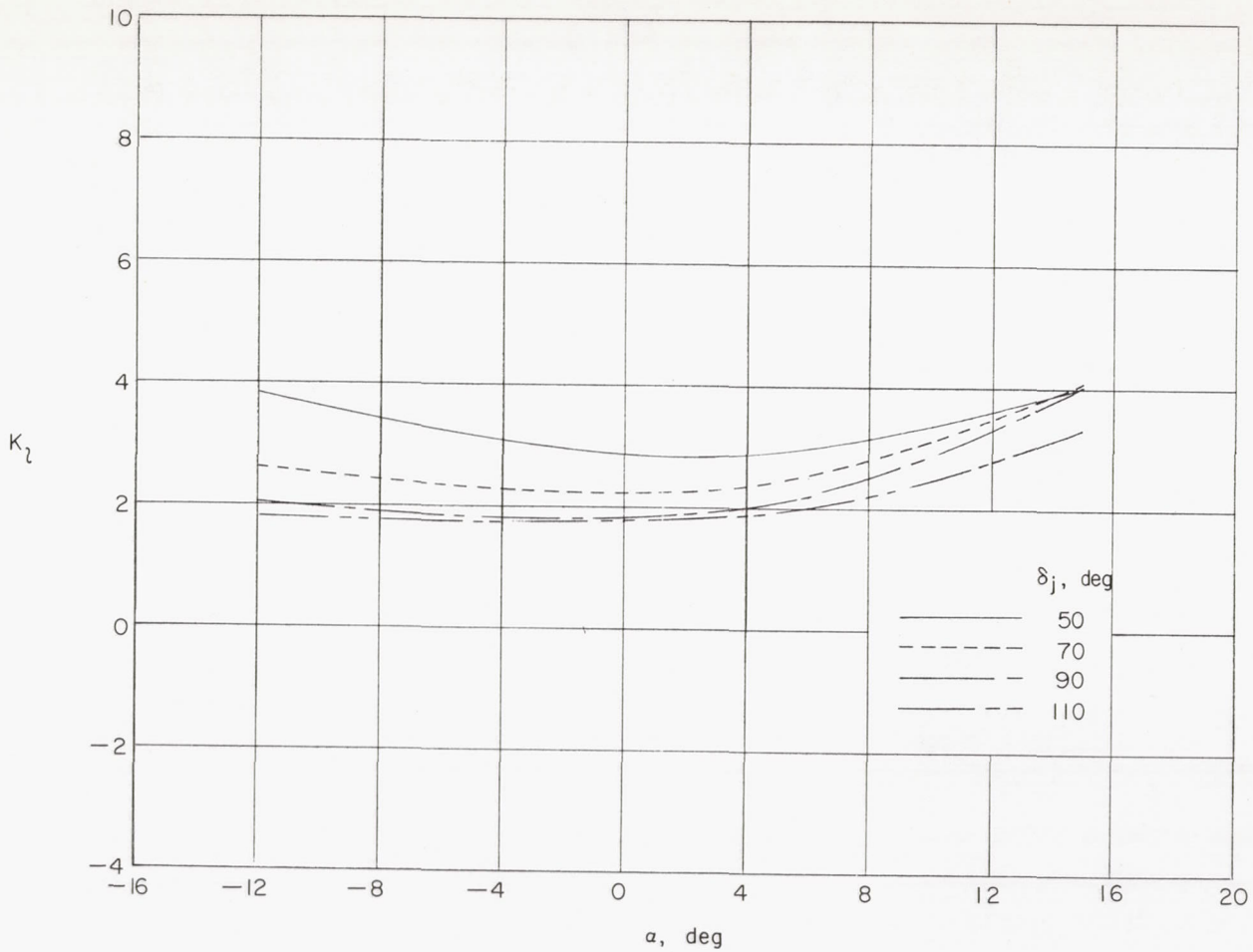

(b) Effect of hole angle. $M = 2.01$; $D_j = 0.0550$ in.; $\frac{p_{t,j}}{p} = 12.0$.

Figure 13.- Continued.

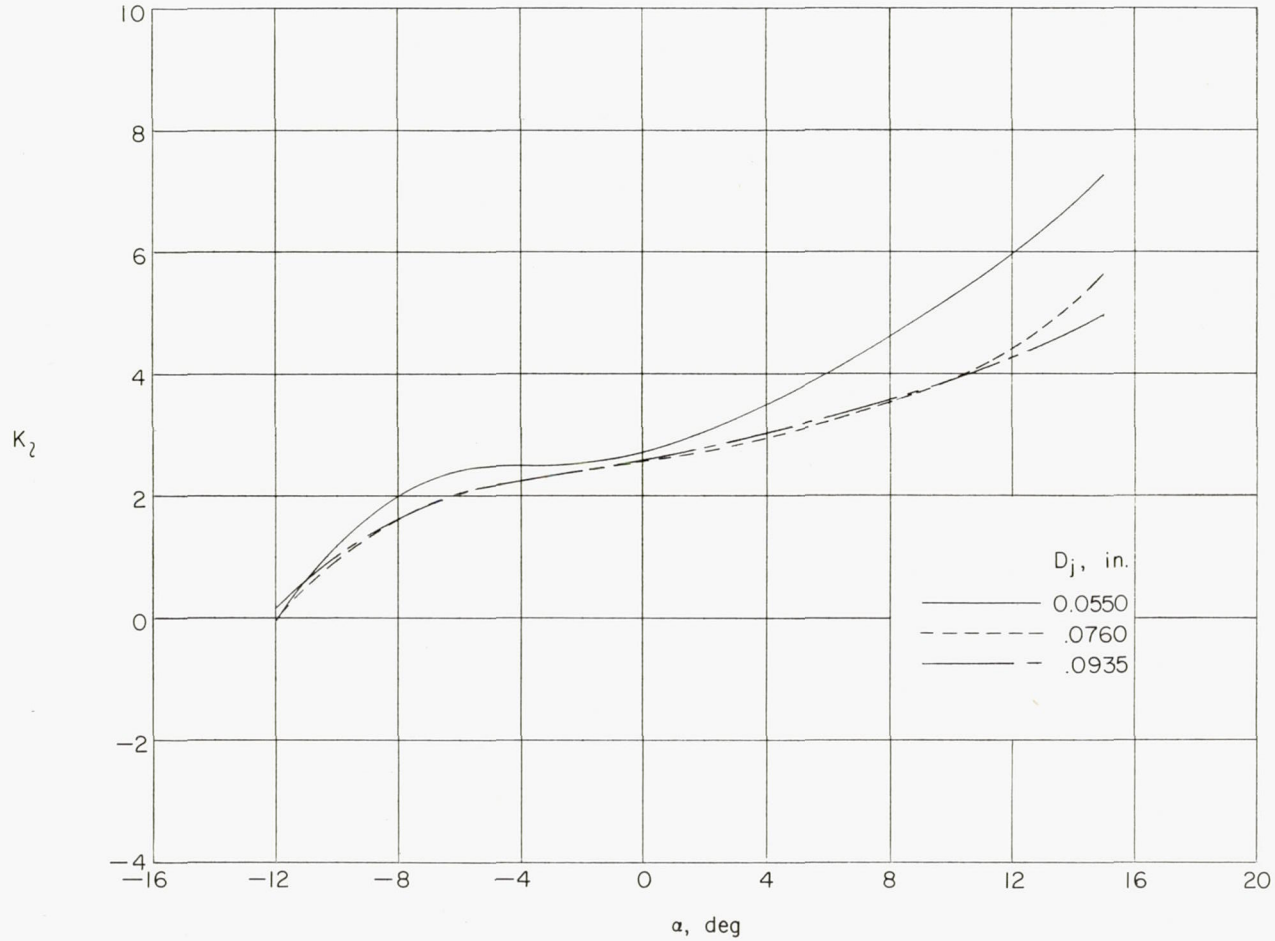

(c) Effect of hole size. $M = 1.61$; $\delta_j = 90^\circ$; $\frac{p_{t,j}}{p} = 12.0$.

Figure 13.- Continued.

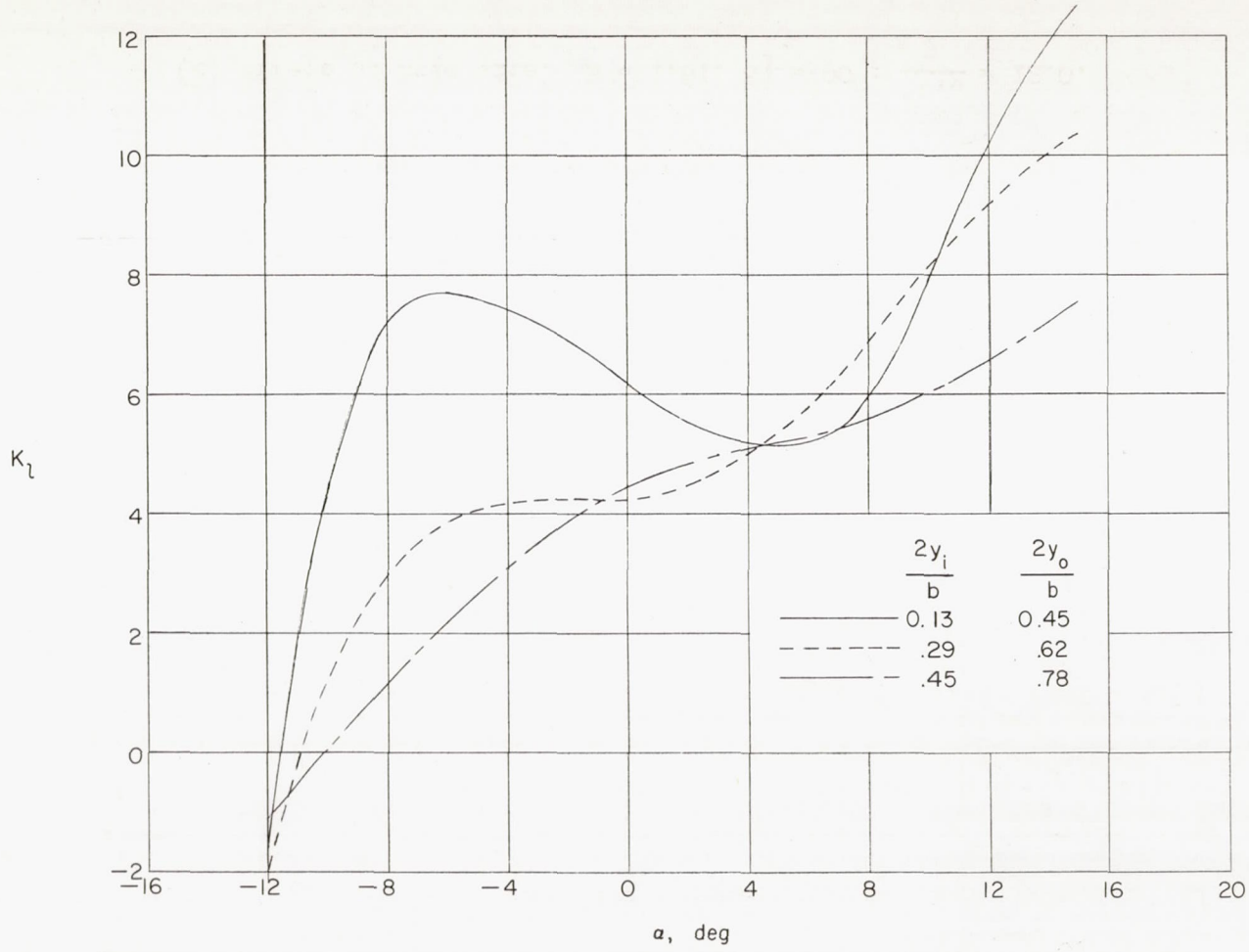

(d) Effect of spanwise location. $M = 1.61$; $\delta_j = 50^\circ$; $\frac{p_{t,j}}{p} = 12.0$.

Figure 13.- Concluded.

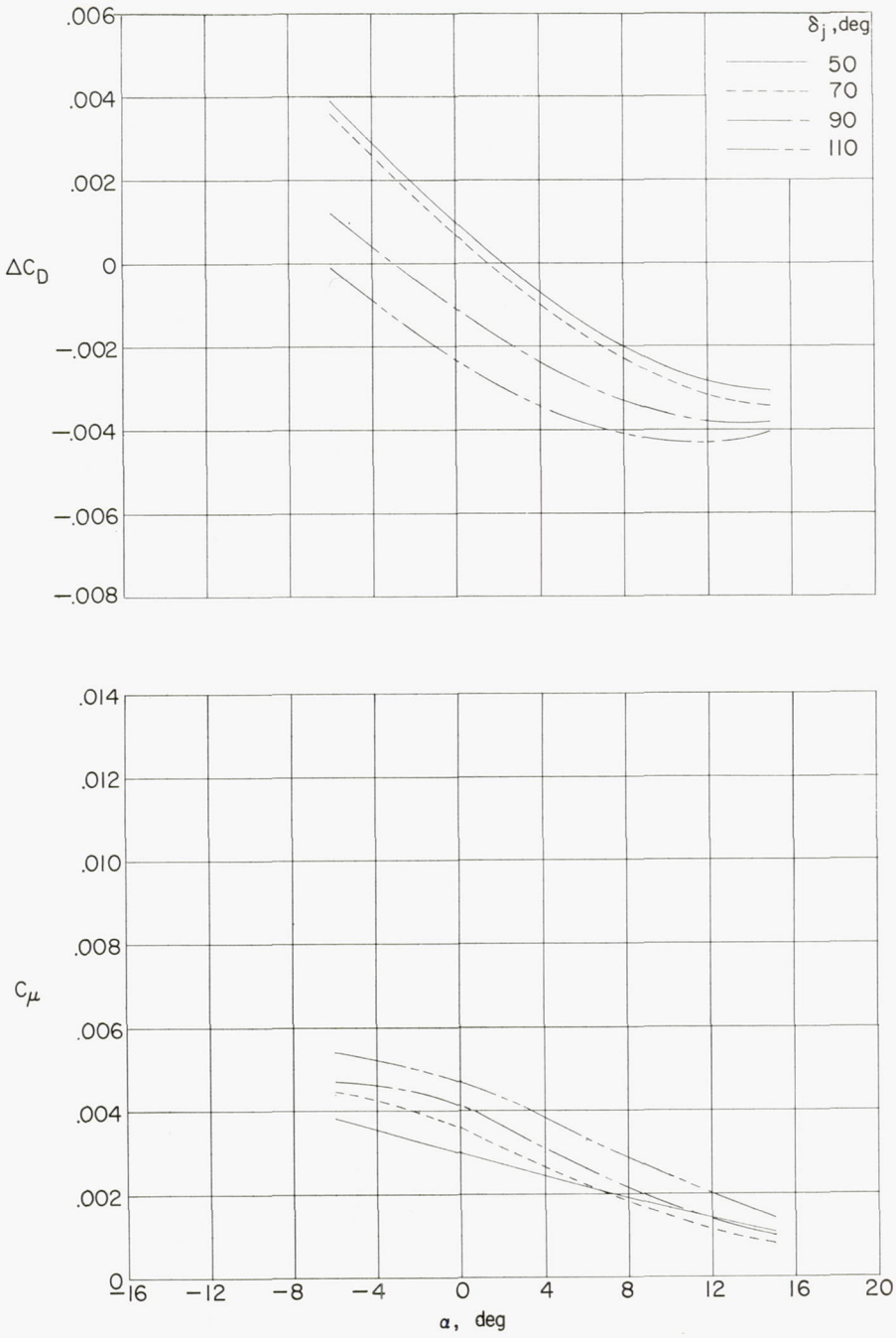

(a) M = 1.61; C_l = 0.002; D_j = 0.0550 in.

Figure 14.- Incremental drag coefficient and momentum coefficient for a given rolling-moment coefficient.

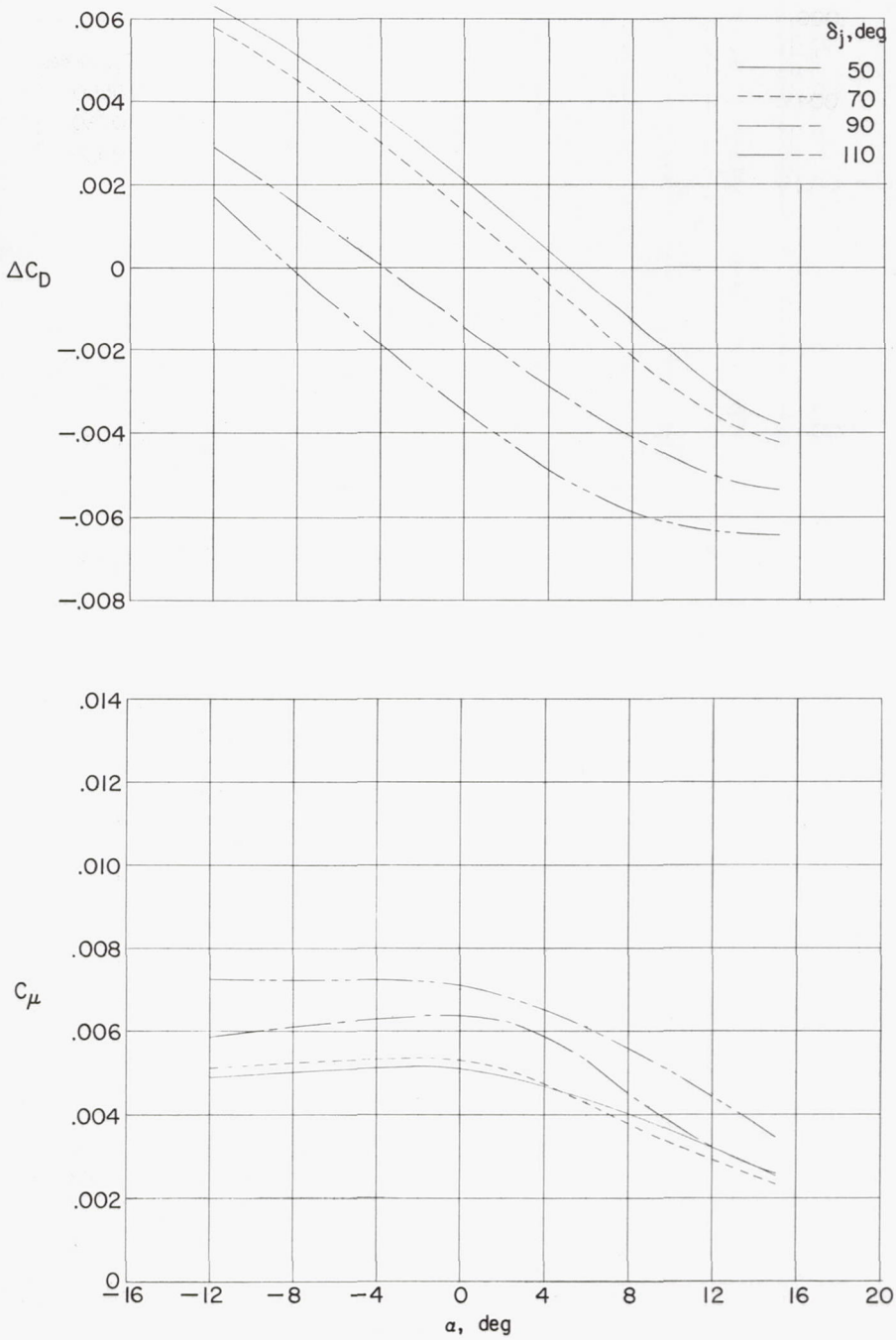

(b) M = 2.01; C_l = 0.002; D_j = 0.0550 in.

Figure 14.- Continued.

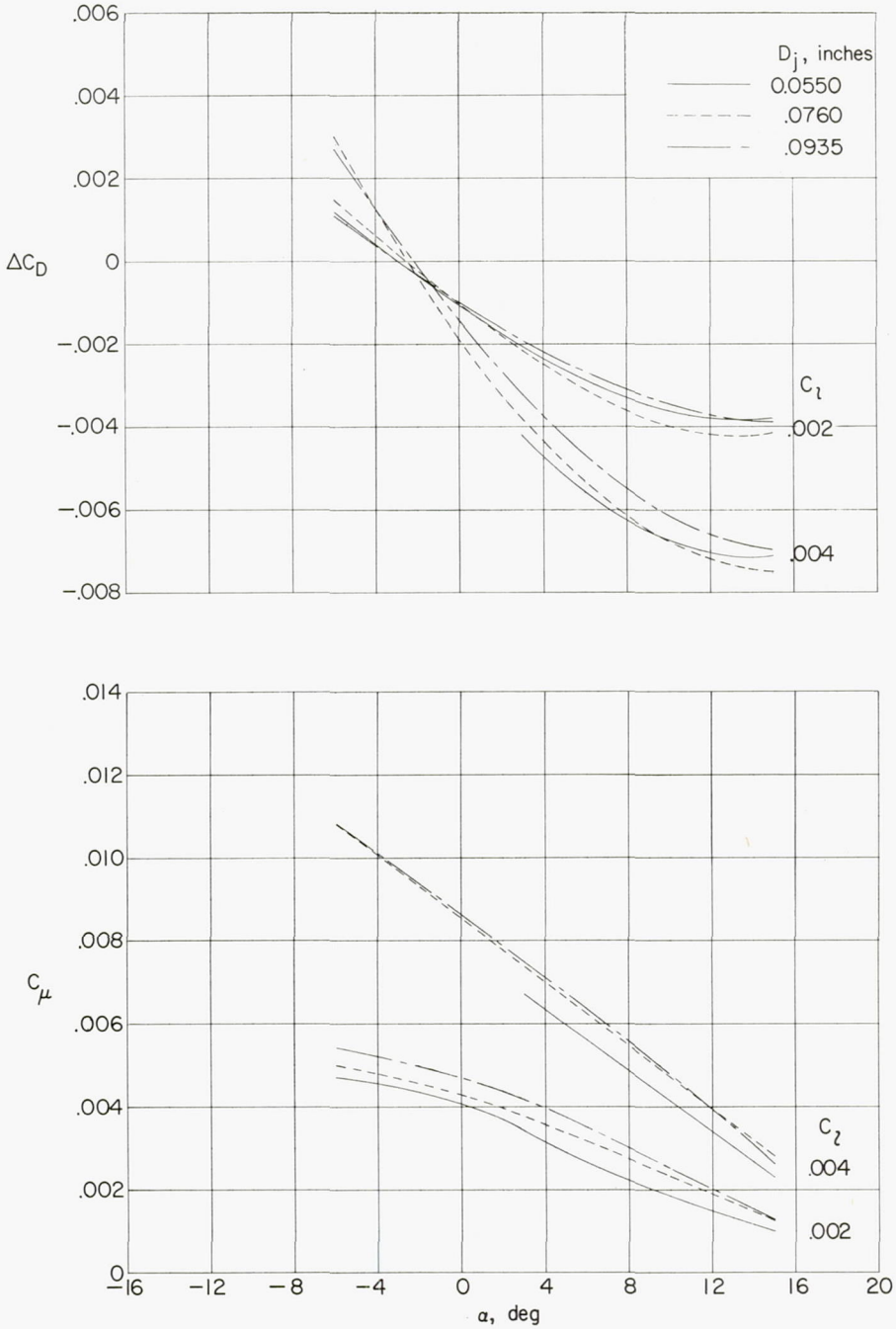

(c) $M = 1.61$; $\delta_j = 90^\circ$.

Figure 14.- Concluded.

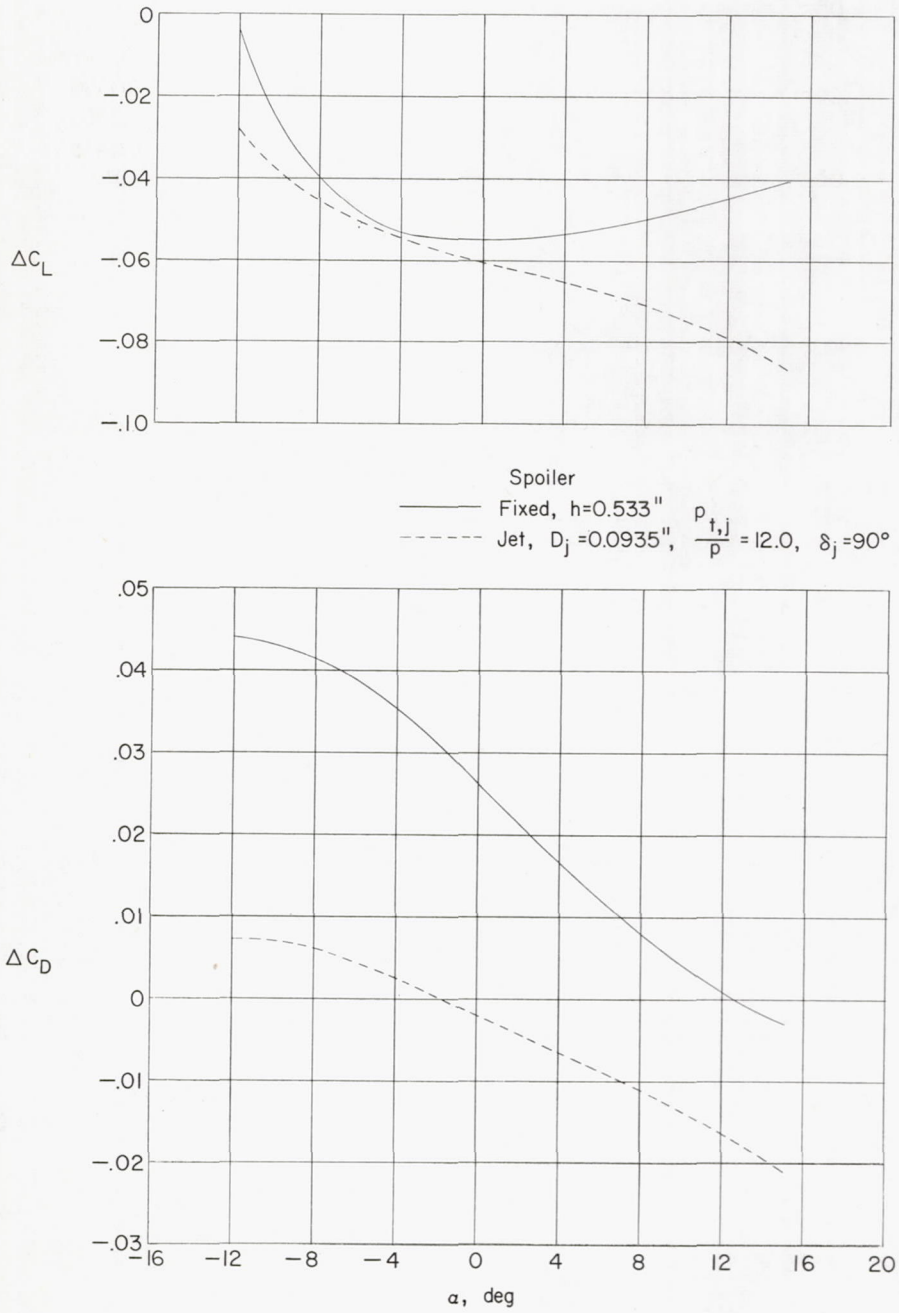

(a) ΔC_L and ΔC_D.

Figure 15.- Comparison of the variation in incremental wing coefficient with angle of attack for the fixed spoiler and the large jet spoiler. M = 1.61.

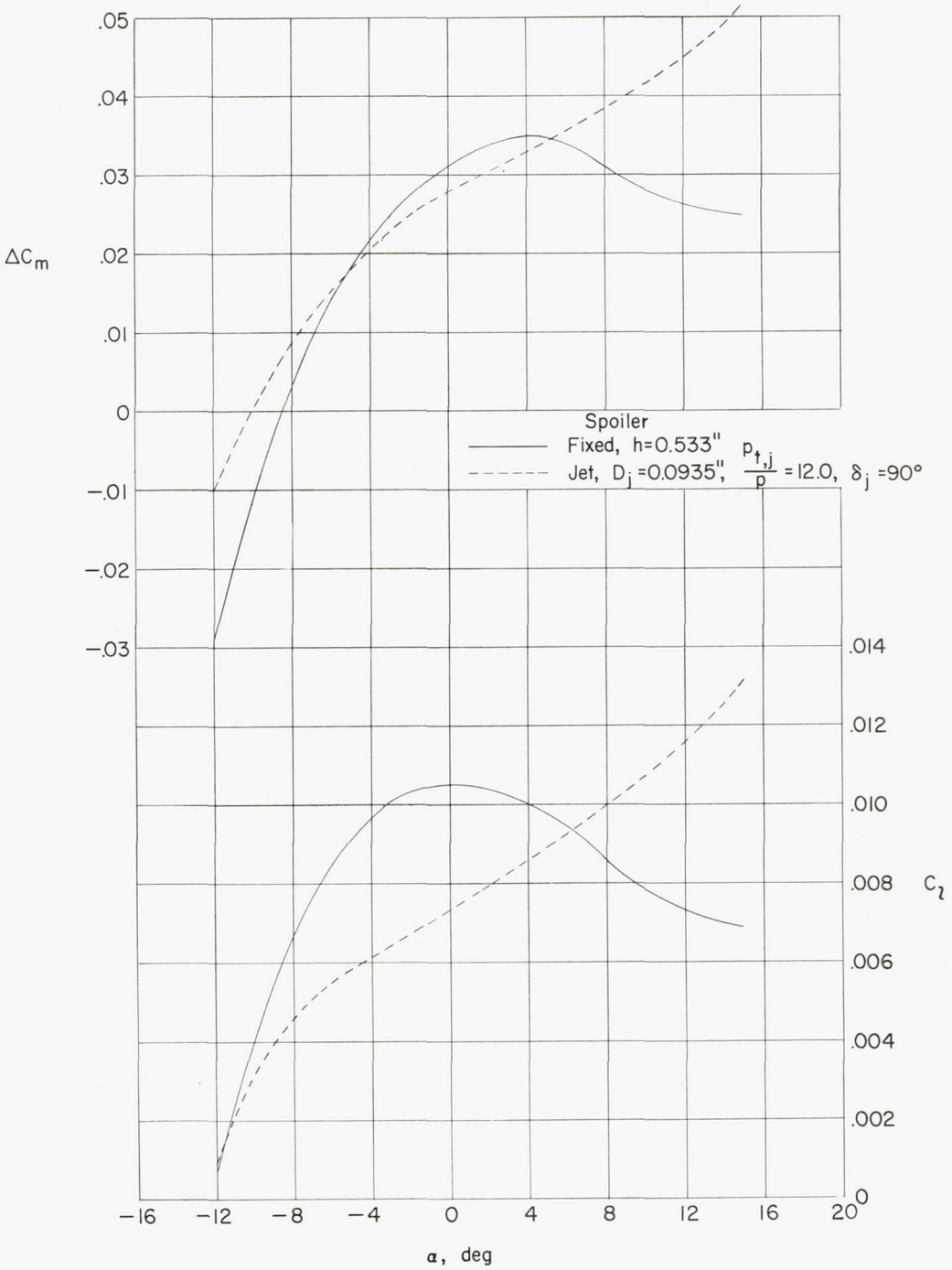

(b) ΔC_m and C_l.

Figure 15.- Concluded.

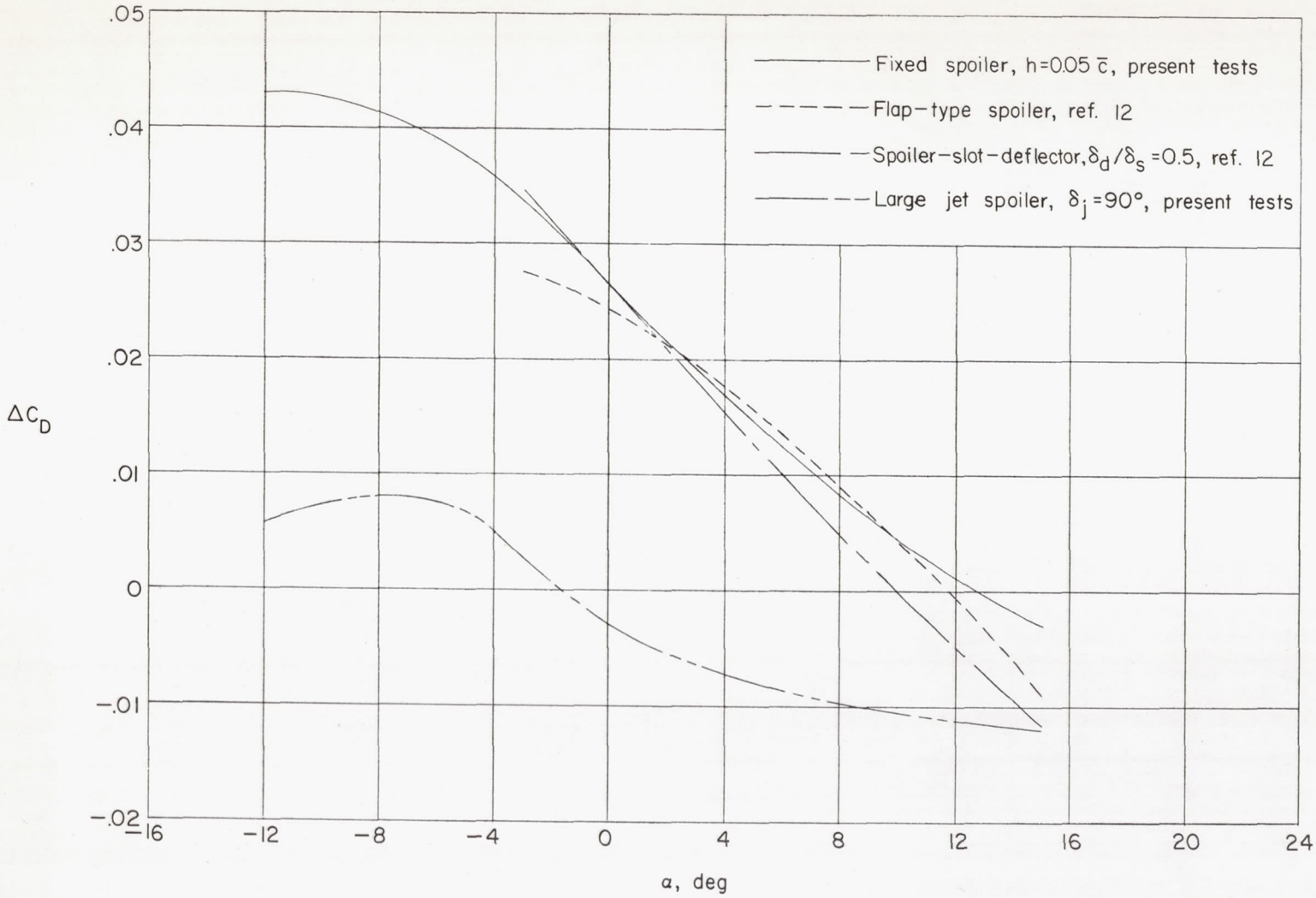

Figure 16.- Incremental drag coefficients for several spoilers, with each of the variable spoilers deflected to produce the same rolling-moment coefficient as obtained with the fixed spoiler. M = 1.61.

CONFIDENTIAL

CONFIDENTIAL